

University of Mississippi

eGrove

Electronic Theses and Dissertations

Graduate School

2011

Improving Sample Collection Of Trace Particles Of Mock Explosive On Nano Coated Sensor

Daniel Woldemichael Yebo
University of Mississippi

Follow this and additional works at: <https://egrove.olemiss.edu/etd>



Part of the [Mechanical Engineering Commons](#)

Recommended Citation

Yebo, Daniel Woldemichael, "Improving Sample Collection Of Trace Particles Of Mock Explosive On Nano Coated Sensor" (2011). *Electronic Theses and Dissertations*. 684.
<https://egrove.olemiss.edu/etd/684>

This Dissertation is brought to you for free and open access by the Graduate School at eGrove. It has been accepted for inclusion in Electronic Theses and Dissertations by an authorized administrator of eGrove. For more information, please contact egrove@olemiss.edu.

IMPROVING SAMPLE COLLECTION OF TRACE PARTICLES OF MOCK EXPLOSIVE
ON NANO COATED SENSOR

A Thesis
presented for the
Master of Science
Degree
in
Engineering Science
The University of Mississippi

DANIEL W. YEBO

May 2011

ABSTRACT

In protection against explosive-based terrorism, development and mass deployment of miniature sensors can play a tremendous role. In trace explosive detection, one of the challenges is bringing explosive vapor samples from the environment to the sensor element. Such collection of a selective and sufficient amount of air sample will enable the device detect the explosive at lower concentration.

This can be done by adsorption of the explosive vapor on a substrate. This research implements the idea by developing a nano coated sensor on a lead zirconate titanate (PZT) substrate. The effects of varying the amount of polyethyleneimine in the nano coating solution of the sensor to adsorb trace particles of a mock explosive are studied.

A nano coating mixture of ferrofluid, polyethyleneimine and epoxy are coated on the surface of PZT substrate, and exposed to a magnetic field to create a pattern of cones. Then it is exposed to ultraviolet rays for curing during a 24 hours period. Finally, adsorption tests are conducted on the newly created sensor. In the adsorption test, nitrogen gas is used as carrier and 2-nitrotoluene is used as the mock explosive. The carrier gas is routed to the 2-nitrotoluene in a bubbler. Then the vapor mixture of 2-nitrotoluene and nitrogen is routed to the sensor box. Next the sensor is scanned with a Raman spectrometer for spectral identification. This procedure is conducted on different sensors which are made by varying the amount of polyethyleneimine, and tested before and after plasma etching using argon gas.

The results showed that increasing the amount of polyethyleneimine by mass yields an increase in the adsorption rate and also leads to the adsorption of a smaller concentration of the mock explosive. In addition, plasma etching of the sensor further improved these results. It enabled adsorption at a less concentration up to 19 ppm. This research showed that the best composition for consistent and reliable adsorption is 80% ferrofluid, 15% polyethyleneimine and 5% epoxy.

The trends in this work indicate further research can lead to this sensor concept being able to capture trace explosive particles on a much lower level.

ACKNOWLEDGMENTS

I would like to express my gratitude to my advisor and thesis director, Dr. Tyrus A. McCarty, who was abundantly helpful and offered invaluable assistance, support and guidance through the past two years. I am grateful to my co-advisor Dr. J.P. Sharma, without whose knowledge and assistance this study would not have been successful. I also would like to express my deepest appreciation to Dr. Arunachalam M. Rajendran, Professor and Chair, Mechanical Engineering Department, for his kind financial support. I would also like to convey my appreciation to all other project team members for their effort to come up with this research direction. Finally, I would especially like to express my gratitude to my families and friends for their constant love and support both morally and materially.

TABLE OF CONTENTS

	PAGE
ABSTRACT.....	ii
ACKNOWLEDGMENTS	iv
LIST OF TABLES	viii
LIST OF FIGURES	ix
 CHAPTER	
1. INTRODUCTION	1
1.1. Raman Spectrometry	2
1.2. Microcantilever Sensor	4
1.3. Surface Acoustic Wave (SAW) Sensors	6
1.4. Surface Enhanced Raman Spectroscopy (SERS)	8
1.5. Amplifying Fluorescent Polymer	8
1.6. Ion Mobility Spectrometer (IMS) , Differential Mobility Spectrometer (DMS), and Ion Trap Mobility Spectrometer (ITMS)	8
1.7. Mass Spectrometry	13
1.8. Chemiluminescence (CL)	13
1.9. Electron Capture Detector	14

1.10. Micro Analyzer	16
1.11. Thermo-Redox	16
1.12. More Research	16
2. STATEMENT OF PROBLEM.....	19
3. EXPERIMENTAL SETUP.....	24
3.1. Sensor Preparation	24
3.2. Adsorption Test for Trace Particles	29
3.3. Concentration of Mock Explosive in Carrier Gas	32
3.4. Plasma Etching of Sensors	35
4. RESULTS AND DISCUSSION	38
4.1. Spectra of 2-Nitrotoluene	38
4.2. Effect of Polyethyleneimine on Adsorption of Mock Explosive	41
4.2.1. Results of Adsorption Test with Mixture Concentration of 43 ppm	41
4.2.2. Results of Adsorption Test with Mixture Concentration of 23 ppm	56
4.2.3. Results of Adsorption Test with Mixture Concentration of 19 ppm	64
4.3. Effect of Plasma Etching of the Sensor	64
4.3.1. Adsorption of 43 ppm Mixture Concentration on Plasma Etched Sensor	64
4.3.2. Adsorption of 23 ppm Mixture Concentration on Plasma Etched Sensor	73
4.3.3. Adsorption of 19 ppm Mixture Concentration on Plasma Etched Sensor	84

5. CONCLUSION.....	91
REFERENCES	93
VITA.....	97

LIST OF TABLES

TABLE	PAGE
1. Table 1-1 Different polymers for Different Explosives.....	7
2. Table 3-1 Magnetic Strength at distance from top of the lower magnetic source	27
3. Table 3-2 Evaporation rate of 2-nitrotoluene at different flow rates of N ₂ carrier gas	33
4. Table 3-3 Concentration of 2-nitrotoluene at different flow rates of N ₂ carrier gas	35
5. Table 4-1 Composition of different sensor samples	41
6. Table 4-2 Adsorption test results at 43 ppm concentration	42
7. Table 4-3 Adsorption test results at 23 ppm concentration	56
8. Table 4-4 Adsorption test results of plasma etched sensor at 43 ppm concentration	66
9. Table 4-5 Adsorption test results of plasma etched sensor M2 at 23 ppm concentration	74
10. Table 4-6 Adsorption test results of plasma etched sensors M3 and M4 at 23 ppm concentration.....	75
11. Table 4-7 Adsorption test results of plasma etched sensor at 19 ppm concentration	86

LIST OF FIGURES

FIGURE	PAGE
1. Figure 1-1 Principle of Rama Spectroscopy	3
2. Figure 1-2 Schematic diagram of Microcantilever bending due to adsorption	4
3. Figure 1-3 Microcantilever sensor	5
4. Figure 1-4 SAW system.....	7
5. Figure 1-5 Principle of Ion Mobility Spectrometer (IMS).....	10
6. Figure 1-6 Plot of IMS signal Vs drift time.....	10
7. Figure 1-7 Principle of Differential Mobility Spectrometer (DMS).....	11
8. Figure 1-8 Schematic diagram of operation Electron capture detector	15
9. Figure 2-1 Structure of Nano-coated sensor	22
10. Figure 3-1a Experimental set up for coating of nano particles	25
11. Figure 3-1b Experimental set up for coating of nano particles.....	26
12. Figure 3-2 Magnetic field strength at a distance from top of magnet.....	27
13. Figure 3-3 Nano coated PZT crystal	28
14. Figure 3-4a Schematic of experimental setup for adsorption test	30
15. Figure 3-4b Experimental setup for adsorption test	31
16. Figure 3-5 Flow rate of N ₂ vs evaporation rate of 2-nitrotoluene	34
17. Figure 3-6 Setup for plasma etching	37
18. Figure 4-1 Spectra of 2-nitrotoluene	40

19.	Figure 4-2 Sample M2 after exposure to mixture of concentration 43 ppm for 2 min	44
20.	Figure 4-3a Sample M3 after exposure to mixture of concentration 43 ppm for 1 min ..	45
21.	Figure 4-3b Sample M3 after exposure to mixture of concentration 43 ppm for 2 min ..	46
22.	Figure 4-4a Sample M4 after exposure to mixture of concentration 43 ppm for 50 sec .	47
23.	Figure 4-4b Sample M4 after exposure to mixture of concentration 43 ppm for 1 min ..	48
24.	Figure 4-4c Sample M4 after exposure to mixture of concentration 43 ppm for 2 min ...	49
25.	Figure 4-5a Sample M5 after exposure to mixture of concentration 43 ppm for 40 sec .	50
26.	Figure 4-5b Sample M5 after exposure to mixture of concentration 43 ppm for 50 sec .	51
27.	Figure 4-5c Sample M5 after exposure to mixture of concentration 43 ppm for 1 min ..	52
28.	Figure 4-5d Sample M5 after exposure to mixture of concentration 43 ppm for 2 min ...	53
29.	Figure 4-6a Sample M6 after exposure to mixture of concentration 43 ppm for 1 min	54
30.	Figure 4-6b Sample M6 after exposure to mixture of concentration 43 ppm for 2 min ...	55
31.	Figure 4-7a Sample M3 after exposure to mixture of concentration 23 ppm for 1 min ..	58
32.	Figure 4-7b Sample M3 after exposure to mixture of concentration 23 ppm for 2 min ..	59
33.	Figure 4-8a Sample M4 after exposure to mixture of concentration 23 ppm for 1 min .	60
34.	Figure 4-8b Sample M4 after exposure to mixture of concentration 23 ppm for 2 min ..	61
35.	Figure 4-9a Sample M5 after exposure to mixture of concentration 23 ppm for 1 min ..	62
36.	Figure 4-9b Sample M5 after exposure to mixture of concentration 23 ppm for 2 min ..	63
37.	Figure 4-10 Plasma etched sample M2 exposed to 43 ppm mixture for 1 min	67
38.	Figure 4-11a Plasma etched sample M3 exposed to 43 ppm mixture for 35 sec	68
39.	Figure 4-11b Plasma etched sample M3 exposed to 43 ppm mixture for 50 sec	69
40.	Figure 4-11c Plasma etched sample M3 exposed to 43 ppm mixture for 60 sec	70

41.	Figure 4-12a Plasma etched sample M4 exposed to 43 ppm mixture for 25 sec.....	71
42.	Figure 4-12b Plasma etched sample M4 exposed to 43 ppm mixture for 60 sec	72
43.	Figure 4-13 Plasma etched sample M2 exposed to 23 ppm mixture for 2 min	76
44.	Figure 4-14a Plasma etched sample M3 exposed to 23 ppm mixture for 50 sec	77
45.	Figure 4-14b Plasma etched sample M3 exposed to 23 ppm mixture for 60 sec	78
46.	Figure 4-15a Plasma etched sample M4 exposed to 23 ppm mixture for 30 sec	79
47.	Figure 4-15b Plasma etched sample M4 exposed to 23 ppm mixture for 40 sec	80
48.	Figure 4-15c Plasma etched sample M4 exposed to 23 ppm mixture for 50 sec	81
49.	Figure 4-15d Plasma etched sample M4 exposed to 23 ppm mixture for 60 sec	82
50.	Figure 4-16 Plasma etched sample M5 exposed to 23 ppm mixture for 25 sec	83
51.	Figure 4-17 Plasma etched sample M4 exposed to 19 ppm mixture for 4 min	87
52.	Figure 4-18 Plasma etched sample M4 exposed to 19 ppm mixture for 5 min	88
53.	Figure 4-19 Plasma etched sample M4 exposed to 19 ppm mixture for 6 min	89
54.	Figure 4-20 Polyethyleneimine amount vs adsorption time of sensors at different concentrations	90

CHAPTER 1

INTRODUCTION

After the terrorists attack of September 11, 2001, several measures are being taken to strengthen security of the country. One of these measures is detection of explosives by security screening in airports, train and bus stations, federal buildings, etc. A number of different technologies have been used in these areas which are probable targets of terrorists. Increasing the sensitivity, reliability and speed of these detection equipments is the current challenge for the scientific community.

There are two major types of explosive detection, trace detection and bulk detection. Trace explosives detection is detection of explosives by collecting and analyzing tiny amounts of explosive vapor or particles with some sensitive sensor. It seeks to detect residue or contamination from handling or being in proximity of explosive materials. Bulk detection, on the other hand, is a means of detecting a visible amount of an explosive. It seeks to detect the actual explosive material.

Trace explosive detection can be performed by two different sampling methods, vapor trace detection and particulate trace detection. Vapor trace detection is a method which senses gas phase molecules that are emitted from a solid or liquid explosive. It is not concerned with any direct contact with the explosive, but it is concerned with the concentration of particles of the explosive material in the surrounding air. This type of detection method is mainly affected by the vapor pressure of the explosive. As far as vapor pressure is concerned, explosives can be

classified into three groups: high, medium, and low vapor pressure. Those explosives with concentration up to 1 ppm (1 part explosive per 1 million parts in air) are called high vapor pressure explosives. Examples are Triacetone Triperoxide (TATP), Ethylene Glycol Dinitrate (EGDN), Nitroglycerin (NG), and Dinitrotoluene (DNT). Medium vapor pressure explosives are those with a concentration of 1 ppm-1ppb. Ammonium Nitrate (NH_4NO_3) and Trinitrotolluene (TNT) are some examples. Low vapor pressure explosives are those with 1ppt or less concentration. Pentaerythritol Tetranitrate (PETN), Cyclonite (RDX) and Octogen (HMX) are those explosives classified under this category. Such low vapor pressure explosive materials present a challenge in the successful detection of trace amounts of explosives via a vapor sample. On the other hand, particulate trace detection involves direct contact with the explosive, or indirectly, through contact with someone who has been handling the explosive.

The other major category of explosive detection is bulk detection. Bulk detection can be either by imaging or nuclear based detection. Imaging technology uses some sort of energy to create the exact image of the material. This technology is being used in conjunction with software which involves the comparison of the suspected material with preloaded material data in a library.

Depending on the level of security and other factors, either trace detection or bulk detection methods may be employed. Current explosive detection technologies with their basic working principle are reviewed below.

1.1 Raman Spectrometry

Raman spectroscopy involves shining a laser onto a sample and examining the interaction between this light and the chemical bonds in the sample. This interaction is known as the Raman effect. When the sample is irradiated, most of the incident light is scattered at the same

wavelength. This "elastic" type of scattering is known as Rayleigh scattering. However, a small fraction of the laser light will excite molecular vibrations in the sample and will be inelastically scattered, or scattered at a slightly different wavelength. This shift in the wavelength can be detected and used to make determinations about the sample.

Tiffany Miller [1] explained how Raman spectrometer works as described below. Raman scattering is a type of inelastic scattering. Inelastic scattering means that energy is lost, so the scattered light has different energy (frequency) than the incident light. It is usually very weak in comparison with elastic scattering. However, Raman scattering depends heavily on the structure of the molecules that are scattering the light, and thus can be useful for characterizing the structures of materials [2].

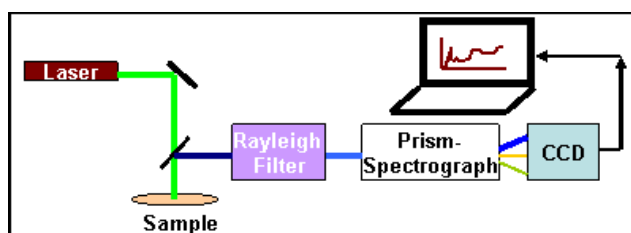


Figure 1-1. Principle of Raman Spectroscopy [1].

A laser beam is focused onto the sample. The molecules within the sample scatter the light and the scattered light is collected. Most of the scattered light is due to elastic scattering and has the same frequency as the incident laser. This frequency is filtered out. The remaining scattered light is due to Raman scattering. Since Raman is an inelastic scattering, the scattered light is not at the incident frequency, but has been shifted from that frequency. This shifted light is sent through a prism like spectrograph that separates it into the different frequencies present, which are detected and sent to the computer.

1.2 Microcantilever

According to Larry Sensac and Thomas Thundat [3], microcantilever sensor technology has been demonstrated in sensitive detection of chemical, physical and biological analytes. Microcantilever sensors can be operated in a dynamic mode where mass loading due to molecular adsorption is monitored as variation in resonance frequency of the cantilever occurs. In static mode adsorption of molecules from trace amounts of explosives on the coated side of cantilever (upper side of the cantilever in Figure 1-2) makes the cantilever bend. The bending is not because of the added weight-when the molecules bind to the cantilever's coated surface; they cause it to stretch relative to its uncoated surface. This makes the structure curve. The more explosives present, the greater is the curvature.

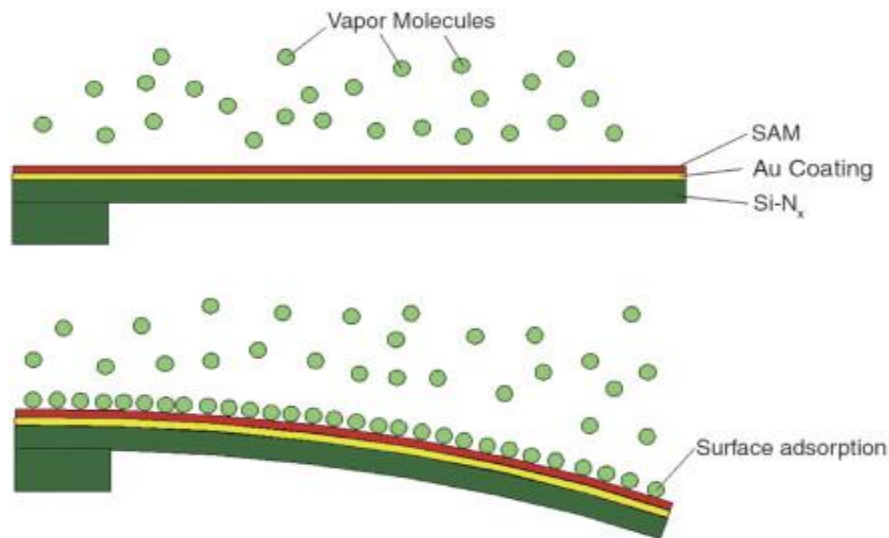


Figure 1-2. Schematic diagram of Microcantilever bending due to adsorption [3].

Thundat [4] explains the details of operation of the microcantilever as shown in Figure 1-3. Air is drawn into chamber 2 containing microcantilever 4 with coating 6. Coating 6 may comprise platinum or transition metal oxides or other compositions well known as absorbers of explosive vapor molecules. Dust and other particulates are removed by filter 8. The molecules of

the explosive vapor will be adsorbed and accumulate on microcantilever surface 10. Then the microcantilever will be heated to a high temperature by piezoresistive track 12. The microcantilever undergoes drastic bending as it is heated.

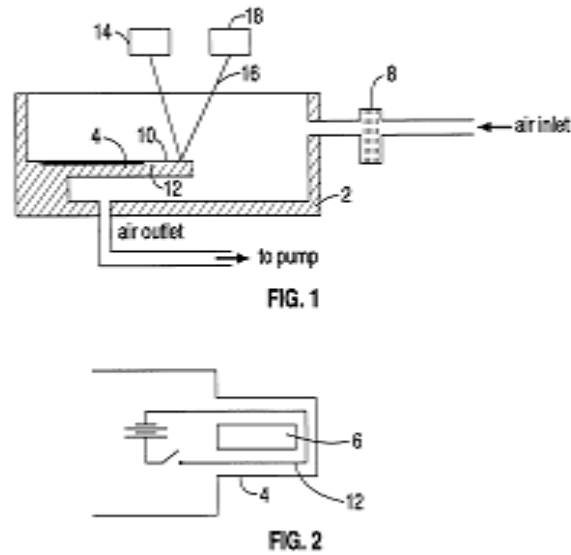


Figure 1-3. Microcantilever sensor.

Once the steady state is reached, the microcantilever bending stabilizes. Once the auto combustion temperature is maintained for a period of time, the adsorbed molecules of explosives undergo auto-combustion, producing a sudden variation in the microcantilever deflection. The auto-combustion temperature and the time the temperature needs to be maintained for the combustion to occur are characteristics of the individual explosive. The sudden deflection of the microcantilever due to auto combustion produces a transient resonance response where the deflection amplitude falls off exponentially as the function of time. The transient resonance response is detected by a photo detector 14 which detects the laser light beam 16 emitted from a laser diode 18 and reflected by the microcantilever surface. A plot of normalized microcantilever

bending with respect to a reference microcantilever will indicate if the explosive molecule is present.

The work of G.Murahdharan, et.al. [5] showed that microcantilevers can adsorb TNT to a level of picograms. The sensitivity of detection depends on the resonance frequency of the cantilever, and the resonance frequency of a cantilever beam varies with mass adsorption [6].

1.3 Surface Acoustic Wave (SAW) Sensors

Surface acoustic wave detection of explosive materials is based on frequency changes that occur when materials are deposited on the SAW crystal surface (detector surface). As the acoustic wave propagates through or on the surface of the material, any changes to the characteristics of the propagation path affect the velocity and/or amplitude of the wave [7]. Changes in velocity can be monitored by measuring the frequency or phase characteristics of the sensor. The frequency shift is dependent upon the properties (mass and the elastic constants) of the material being deposited, the temperature of the SAW crystal, and the chemical nature of the crystal surface. The core of the SAW sensor is a piezoelectric crystal that is capable of converting an electric field into an acoustic wave. The surface of this crystal is coated with a polymer that adsorbs the explosive. As the polymer adsorbs the material of interest, there is a change in mass that results in a shift in frequency. This shift in frequency is the means by which the change in mass is detected and is the basis for this method of explosive detection. A pattern recognition algorithm is then used to identify the materials of interest.

Figure 1-4 shows the configuration of a typical acoustic wave device [7]. The Interdigital transducer (IDT) of each sensor provides the electric field necessary to displace the substrate and thus form an acoustic wave. The wave propagates through the substrate, where it is converted back to an electric field at the IDT on the other side. The range of phenomena that can be

detected by acoustic wave devices can be greatly expanded by coating the devices with materials that undergo changes in their mass, elasticity, or conductivity upon exposure to some physical or chemical stimulus. For its application as a vapor chemical sensor, it can be coated with chemically selective coatings that adsorb the vapors of interest and results in an increased mass loading on the device.

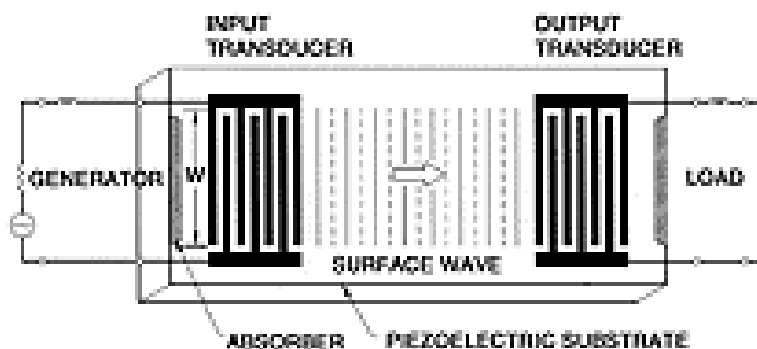


Figure 1-4. SAW system.

Some polymers which can sense certain explosives are listed in Table 1-1 below [8]. This can be useful in improving the selectivity of the sensor under research. For example, a study on adsorption by SAW sensors with Carbowax-1000 presented a very good chemical interface for detection of low level chemical spectra of explosive material [9].

Table 1-1. Different polymers for different explosives

Polymer	Explosive
Polyacetylenes	DNT
Poly (p-phenylenevinylenes) (PPV)	TNT and DNT
poly(p-phenyleneethynylenes) (PPE)	TNT
Polymeric porphyrins	TNT and trinitrobenzene (TNB).
silicone polymers (SXPFA)	Nitrobenzene
Carbowax-1000	Nitroaromatic
Cyclodextrins	DNT and TNT

1.4 Surface Enhanced Raman Spectroscopy (SERS)

Surface Enhanced Raman Spectroscopy (SERS) is a Raman Spectroscopic (RS) technique that provides greatly enhanced Raman signal from molecules that have been adsorbed onto certain specially prepared metal surfaces. Increases in the intensity of Raman signal have been regularly observed with SERS. The importance of SERS is that it is both surface selective and highly sensitive where as RS is neither. RS is ineffective for surface studies because the photons of the incident laser light simply propagate through the bulk and the signal from the bulk overwhelms any Raman signal from the analytes at the surface. SERS selectivity of surface signal results from the presence of surface enhancement (SE) mechanisms only at the surface. Thus, the surface signal overwhelms the bulk signal, making bulk subtraction unnecessary.

There are two primary mechanisms of enhancement: an electromagnetic and a chemical enhancement. The electromagnetic enhancement (EME) is dependent on the presence of the metal surface's roughness features, while the chemical enhancement (CE) involves changes to the adsorbate electronic states due to chemisorption of the analyte [10].

1.5 Amplifying Fluorescent Polymer

The basis of detection is that the sensor contains a fluorophore that will emit light until the material of interest is attached to a receptor site. Once the material is adsorbed, there is a decrease in light signal that can be measured. This technology was developed by MIT scientists and currently used in FIDO explosive detection device [11].

1.6 Ion Mobility Spectrometer (IMS), Differential Mobility Spectrometer (DMS), and Ion Trap Mobility Spectrometer (ITMS)

Ion Mobility Spectrometer (IMS), Differential Mobility Spectrometer (DMS), and Ion Trap Mobility Spectrometer (ITMS) have similar principle of operation [12], [13], [14]. An IMS

system measures how fast a given ion moves in a uniform electric field through a given atmosphere. It has a tube called drift tube which is divided into two regions: the ionization region and the drift region (Figure 1-5). A sample is taken either by drawing air from the surroundings of the suspected material or by swiping the suspected material itself. The sample is drawn first into the ionization region of the drift tube of the IMS, and is ionized there. The source of the ionizing electron is either nickel-63 ($^{63}\text{Ni}^{28}$), Americium (^{241}Am) or carbon nanotube technology. These ions are periodically admitted into the drift region through an electronically shuttered gate. Once in the drift tube, the ions are subjected to a homogeneous electric field ranging from a few volts per centimeter to many hundreds of volts per centimeter depending on the class of compounds targeted. Once set, the field does not change. This electric field then drives the ions through the drift tube where they interact with the neutral drift molecules contained within the system. Separation of chemical species is achieved based upon the ion mobility (a parameter that is dependent of ion mass, size, and shape) where they arrive at the detector for measurement. This time spent in the drift region is known as the time of flight (TOF). Ions are recorded at the detector in order from the fastest to the slowest, generating a response signal characteristic of the chemical composition of the measured sample. Upon collision with a detector plate the ions impart current flow that is amplified and converted into voltage. This electric charge or potential difference is measured by an electrometer. The time required for the ions to travel the length of the drift region is called the drift time. The voltage response vs. drift time, called a mobility spectrum or plasmagram, is used for chemical identification, and is a complex function of the charge, mass, and size of the ion. The pattern of separation is compared to a library of known patterns to identify the substance collected. The sample collection can be either by drawing in air near the object or by swiping a surface to

collect particles. Early IMS systems generally operate in either positive or negative mode. But recent IMS developments use oscillating negative and positive polarities in the drift tube to capture both negative and positive ions.

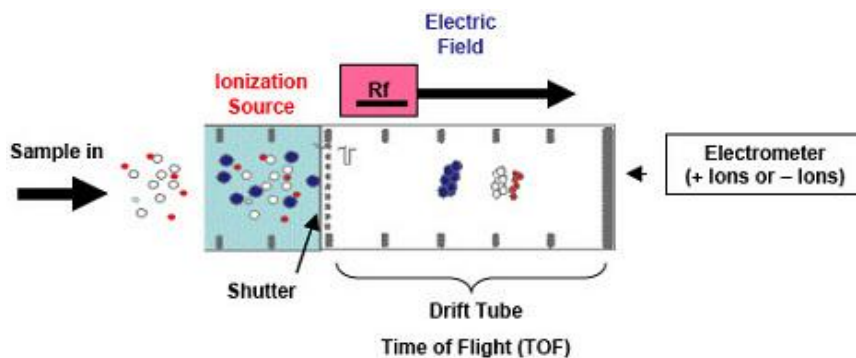


Figure 1-5. Principle of Ion Mobility Spectrometer (IMS) [13].

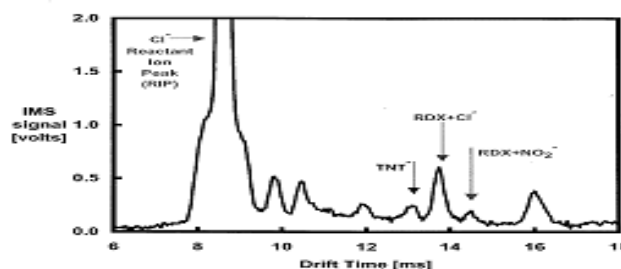


Figure 1-6. Plot of IMS signal Vs drift time [15].

DMS technology is a version of IMS [16]. In IMS, once the samples are ionized they will periodically flow through a constant electric field. On the other hand, in DMS systems, ions continuously flow through low and high electric fields. Ionized samples flow continuously via a carrier gas, such as air, into the detector area with its parallel plates spaced 0.5mm apart. Once in the detector area, the ions experience a uniform oscillating asymmetric radio frequency (Rf) electric field which is typically 1MHz and ranges from 500-1500V. As applied, the Rf causes a perpendicular motion of the ions, resulting in a zigzag motion. Each ion species will exhibit discrete mobility characteristics. Whereas IMS measures the ions velocity in a given electric

field, DMS measures its change of velocity (mobility) when exposed to low and high electric fields (Figure 1-7).

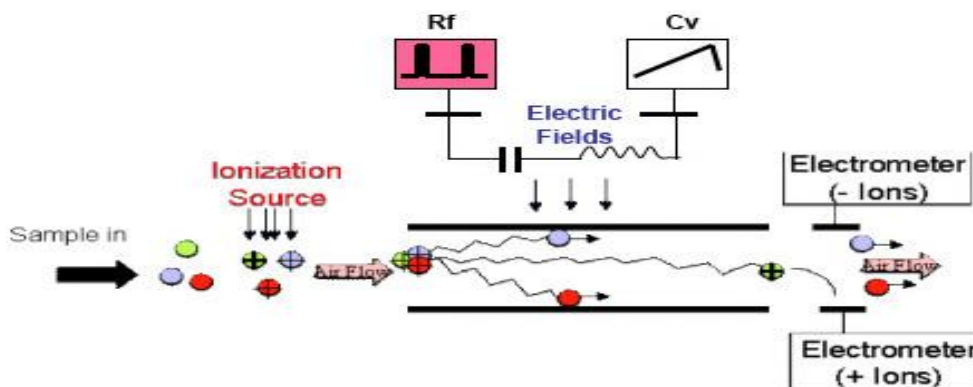


Figure 1-7. Principle of Differential Mobility Spectrometer (DMS) [13].

There are some pros and cons in regard to IMS and DMS systems. The basic strength of IMS is its ability to quickly separate ions [1], [5]. It is stated that IMS gives result in 3-15 ms [13]. The ability of IMS to operate under ambient condition is the other advantage to use it in airports. It is simple that it doesn't need any vacuum system unlike mass spectrometry [14]. The chemical information gleaned from IMS includes quantitative information, often with low limits of detection, and structural information or classification of chemical family.

IMS has some disadvantages. It is stated that IMS has high false alarm rate at lower alarm thresholds. It is explained that current airport IMS system use ionization chemistry, dopants and negative ion sensing to detect specific explosives and have inherently lower chemical specificity [12]. Two different materials that form ions of similar size and mass may appear as a single broad peak rather than two distinct peaks in an IMS spectrum. This leads to an increased false alarm rate. Use of gas chromatography to separate ions before they reach the IMS is one method of minimizing this problem. Because it uses ionization conditions, dopant gas and drift time for existing explosives, IMS has limited capability to detect new threats [12]. Lots of

paper work requirement is also mentioned as another drawback. Since it is source of radioactivity (but no significant effect on health), it requires extra paper work.

On the other hand, DMS is more advantageous than IMS [13]. In DMS there is no shutter which discards 99% of samples, and as a result, DMS is 10-100 times more sensitive than IMS. It can also simultaneously detect both positive and negative ions whereas IMS can detect one or the other. Hence DMS has more data-rich environment to reduce false alarms. Additionally, DMS is smaller in size and less costly. [13].

A hybrid detector developed by Sionex is observed to utilize pros of each technology [16]. IMS uses a discrete pulsed flow and consequently uses only 1%–2% of the available ions while DMS uses a continuous flow and uses 80%–90% of the available ions. IMS is mono-polar and uses sequential polarity switching to see both positive and negative ions while DMS sees both positive and negative ions simultaneously. As a result, there is a benefit to using first DMS and then IMS. Because DMS generates both positive and negative ions simultaneously, Sionex used two discrete IMS flow chambers, one of which has a positive polarity and the other has a negative polarity.

The other family of IMS is ITMS. ITMS technology significantly improves the performance of traditional IMS [17]. Like IMS, ITMS separates ionized vapors and then measures the mobility of the ions in an electric field. The gaseous samples enter an ionization chamber where an ionizing source emits low-energy beta particles, resulting in ion formation in the gaseous phase. However, ITMS breaks new ground by eliminating the shutter grid and the associated loss of ions and sensitivity. With ITMS, ionization reaches equilibrium in a field-free region and is then pulsed into the drift tube where an electric field guides the ions to the

collector. Without a shutter grid, a much greater number of ions enter the drift tube. Compared to IMS technology, ITMS can deliver increased sensitivity, flexibility, and practicality for security applications.

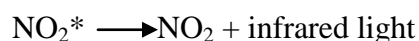
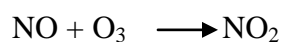
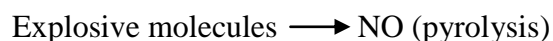
1.7 Mass Spectrometry

The survey and guide for selection of explosive detection system [12] and [15] describe that mass spectrometry (MS) is one of the most powerful techniques available for laboratory chemical analysis. Although it is rarely used in routine field applications and may thus be of little interest doing explosive detection on the field. It uses an explosive material's molecular weight and fragmentation patterns for identification. While there are different types of mass spectrometers, it is basically a mass filtering technique. Molecules are ionized and passed through a filter (e.g., magnetic, ion trap, time-of-flight), which allows ions to be identified based on their charge-to-mass ratio. These papers point out that the technology takes relatively longer time, and hence are used in laboratories rather than at check points.

1.8 Chemiluminescence(CL)

The survey and guide articles [12], [15] presented as references explain that chemiluminescence is the production and emission of light that occurs as a product of a chemical reaction(s). Most explosive compounds contain either nitro (NO_2) or nitrate (NO_3) groups. The compounds commonly used as taggants in plastic explosives also contain NO_2 groups. Detectors based on chemiluminescence take advantage of this common property of most explosives by detecting infrared light that is emitted from electronically excited NO_2 molecules, denoted as NO_2^* . In a chemiluminescence system, explosive molecules are first pyrolyzed (pyrolysis is the chemical decomposition of organic materials by heating in the absence of oxygen or any other

reagents, except possibly steam to produce nitric oxide (NO). The NO molecules are then reacted with ozone (O_3) in an evacuated reaction chamber maintained at a pressure of about 3 torr = 0.4 kPa. This reaction produces the excited state molecules, NO_2^* , which later decay to unexcited NO_2 and infrared light. The signal output measured by the photomultiplier is directly proportional to the amount of NO present in the reaction chamber, and this signal is thus used to detect the presence of explosives in a chemiluminescence system.



The survey paper [12] points one drawback of this technology that it cannot detect explosives which are not nitro-based.

1.9 Electron Capture Detector (ECD)

In an ECD, a vapor sample is drawn into an inlet port, and this vapor mixes with a stream of inert carrier gas (usually helium or argon). The gas flow then travels through an ionization region to an exhaust line. In transit, the gas flow passes through a chamber with a radioactive material that acts as an electron source, as in an IMS. The source material is usually either nickel-63 ($^{63}\text{Ni}28$) or tritium. The emitted electrons become thermalized through collisions with the gas in the chamber, and eventually are collected at an anode. Under equilibrium conditions, there is thus a constant standing current at the anode. The basic principle behind an ECD is that this standing current is characteristic of the gas mixture being drawn into the system. If the gas mixture originally consists, e.g., of helium and room air, the standing current will be reduced if the vapor of an explosive enters the chamber. This happens because the explosive molecules have a high electron affinity and thus a tendency to capture free electrons and form stable

negative ions, leaving fewer electrons to reach the anode. Thus, a reduction of the measured standing current is evidence that an explosive or some similar species is present. As with a chemiluminescence detector, the ECD by itself cannot distinguish individual types of explosives from each other or certain interferents, so a gas chromatograph is placed on the front end to allow temporal identification of different explosives. Mostly this type of technology is referred to as GC/ECD detectors [15], [18].

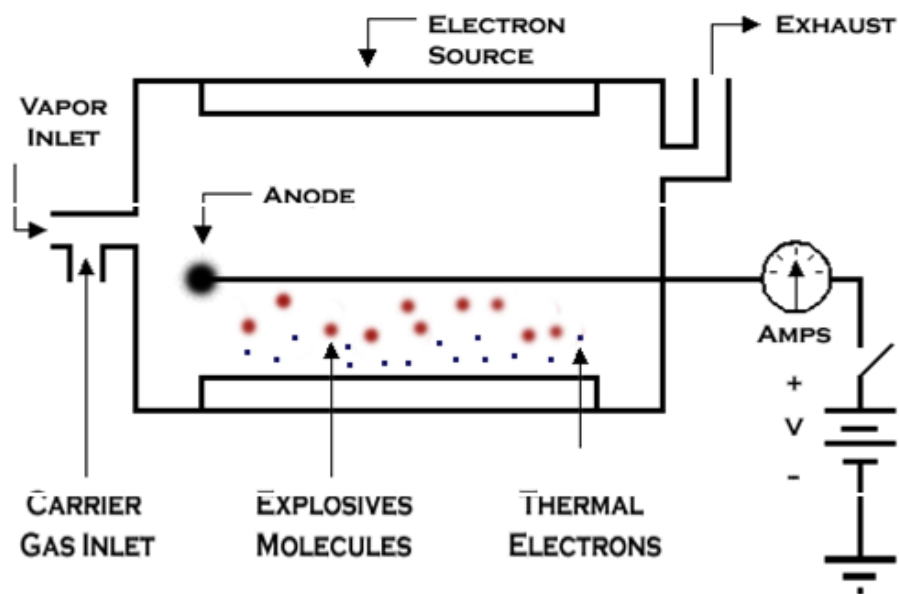


Figure 1-8. Schematic diagram of operation of Electron Capture Detector [15].

This type of detector has typical sensitivities of about 1 ppb. An electron-capturing compound which is somewhat less than the sensitivity of a typical IMS or chemiluminescence system, but it is still adequate for some applications. However, GC/ECD detectors usually cost less than IMS or chemiluminescence systems, and are also smaller, lighter, and more portable [15].

1.10 Micro Analyzer

This is equipment developed by Sionex to take advantage of GC and DMS. The instrument is a vapor analyzer incorporating an ambient sampling system, pre-concentrator, GC separation module and the microDMx detection system. The device has ability to incorporate a variety of heated GC columns and pre-concentrator materials to meet a specific application [19].

1.11 Thermo-Redox

Thermo-redox technology is an electrochemical technique based on the thermal decomposition of explosive molecules and the subsequent reduction of NO₂ groups. A sample is drawn into the system and is passed through a concentrator tube, which selectively traps explosive-like materials. The sample is heated rapidly to release NO₂ molecules, and these molecules are detected using proprietary technology. This technology detects only the presence of NO₂ groups and cannot distinguish explosives materials and potential interferents that contain NO₂ groups. Thus, the system identifies the presence of an “explosive-like” material, without identifying a specific explosive [12].

1.12 More Research

Research in the Department of Chemistry, North University of China, Peoples Republic of China showed that Polyethyleneimine (PEI) on silica gel can be used to adsorb TNT. Polyethyleneimine (PEI) was grafted onto the surface of silica gel particles in order to produce the novel adsorption material PEI/SiO₂. Then these novel materials adsorption properties of TNT were investigated and experimental results showed that PEI/SiO₂ possessed strong adsorption ability for TNT [20].

Another research done in Defense R and D Organization (DRDO) of India showed that Carbowax-1000 and Poly dimethyl siloxane (PDMS) have good adsorption towards nitro

aromatic vapors [21]. Reference [9] stated that Carbowax can also be used as a polymer on SAW sensors to adsorb DNT.

In Portugal at the University of Algarve, organic thin film transistors are found to sense TNT vapors [22]. Polymers are deposited by spin coating and, oligomers (or small molecules) deposited by vacuum sublimation. When vapors of nitro aromatic compounds bind to thin films of organic materials, which form the transistor channel-the conductivity of the thin film increases and change the transistor electrical characteristic.

In 2006, different polymers were coated on SAW and found to be selective for chemical warfare agents such as dimethylmethylphosphonate (DMMP), acetonitrile (CH_3CN), dichloromethane (CH_2Cl_2) and dichloropentane (DCP) [23]. An array with five SAW sensors using different kinds of polymers was fabricated to detect chemical agents and their gas response characteristics were extensively investigated. The SAW devices with different inter-digital transducer (IDT) electrode line widths of 3, 4, 6, 8 and $20\mu\text{m}$, which corresponded to the central frequencies of 264, 198, 132, 99 and 39.6 MHz, respectively, were designed. The IDT electrodes consisted of 100 finger pairs of 200 nm thick aluminum films. The polymers used as the sensing materials were polyisobutylene (PIB), polyepichlorohydrin (PECH), polydimethylsiloxane (PDMS), polybutadiene (PBD) and polyisoprene (PIP). The thin films were coated on a quartz substrate by spin coating technique. Four simulant gases of chemical warfare agents of dimethylmethylphosphonate (DMMP), acetonitrile (CH_3CN), dichloromethane (CH_2Cl_2) and dichloropentane (DCP) were used as target gases, instead of the real nerve, blood, choking and vesicant agents. After spin coating of PIB and PECH, the substrate was heated at 65°C in N_2 ambient for 1hr to remove the cyclohexane and ethylacetate, which were used as solvents. PDMS films were heated at 75°C in a N_2 flow for 2 hr to remove the ethylacetate used as a solvent. And

PBD and PIP were heated at 60 °C in a N₂ flow for 1 hr to remove the benzene used as a solvent. The sensing characteristics of the SAW sensors were measured by using E-5061A network analyzer. The polymer SAW sensor array showed good selectivity to simulant gases.

Chapter two of this thesis presents the statement of problem of this study. It states the need for nano technology in explosive detection, current challenges to counterterrorism, and the impact of nano sensors. The concept of this research is explained in detail.

CHAPTER 2

STATEMENT OF PROBLEM

History and records of terrorist attacks since 2011 show that hidden explosives have become the most common type of terrorists' act worldwide. Such explosives are inexpensive, easy to make, difficult to detect at a distance, use components which are cheap and available, rather they are highly explosive. Detecting explosives is a challenging task because of a number of issues, such as the low vapor pressures of most explosives, and frequent introduction of novel explosive compositions. Most of the detecting devices currently used are, however, rather bulky, expensive, and require time-consuming procedures. Because of these limitations, such systems are sparsely deployed only at strategic locations such as airports and government buildings. Further complications arise when one considers not only airports, where there is a reasonably controllable environment for sensing and detection, but also the virtually uncontrollable entry points to public places, transportation networks, infrastructures, and road networks with unpredictable vehicular and pedestrian traffic. Thus, protecting against explosive-based terrorism can only be accomplished by mass deployment of miniature sensors that are sufficiently fast, sensitive, selective, inexpensive, and amenable for mass production.

Creating a sensor that is both sensitive and selective is only the first part of the current challenge. The second part involves bringing explosives from the environment to the sensor element. Sample collection is the front end of any integrated sensor system, and for trace explosive detection it is the most challenging task. Since vapor pressures of most explosives are

extremely low, a large amount of air must be sampled in order to obtain enough molecules of a particulate for detection. Such collection of selective and enough amount of air sample will enable the device detect the explosive at lower concentration then by increasing the sensitivity. Typically, a large volume of air, which is a mixture of many molecules including very low concentrations of explosives, is collected, and explosives and particulates are trapped using special materials. The trapping material is then heated to desorb the trapped molecules which will be analyzed in some sort of analyzer for identification. The mechanism of trapping particles on the surfaces is called adsorption.

Adsorption, as distinguished from absorption, is a process in which gas or liquid particles (adsorbate) are attracted and contact to surface of a solid substance (adsorbent). The rate of adsorption is governed by rate of arrival of molecules at the surface and the sticking probability of incident molecules on the substrate.

$$R = \frac{f(\theta).P}{\sqrt{2\pi mkT}} \exp\left(\frac{-Ea}{RT}\right) \quad (2.1)$$

where:

R = Rate of adsorption

Ea = Activation energy for adsorption

$f(\theta)$ = Some function of the existing surface coverage

P = Gas pressure [N.m²]

m = Mass of one molecule [kg]

T = Temperature [K]

Among the factors affecting adsorption of gases on solids, surface area of the solid (adsorbent)

has a prominent effect since it influences the activation energy for adsorption. The larger the surface area of the adsorbent, greater is the extent of adsorption. The specific area of the adsorbent increases tremendously when finely divided forms of the solid adsorbent are used (the smaller the particle size, greater is its surface area). Based on this fact the focus of this research is increasing the surface area by nanoparticles coating with a mixture containing ferrofluid. The unique nature of ferrofluid to form fluid cone patterns on the substrate will increase the surface area. This will clearly increase the amount of gas particles collected which in turn increases the probability of trapping the explosive particles, thus enabling the sensor to be more sensitive. In addition to increasing the amount collected, the trapping process is intended to be selective to explosive or explosive-like materials. This is done by including (in the mixture) a polymer known as polyethyleneimine which has special affinity to explosive nature chemicals.

Figure 2-1 shows structure of the nano coated sensor. Lead zirconate titanate (PZT) material is to be used as a substrate base on which the coating is done. PZT material develops voltage across two of its faces due to mechanical stress or when it experiences heat. It has large dielectric constant and has a spontaneous electric polarization which can be reversed in the presence of an electric field. All these properties enable PZT materials selected for manufacturing of different sensors.

The nano coating solution is a mixture of ferrofluid, polyethyleneimine, and epoxy resin. Details of the sensor development are discussed in chapter 3.

The main constituent of the mixture is ferrofluid. When ferrofluid is subjected to a strong vertical magnetic field, the surface spontaneously forms a regular pattern of cones (Figure 2-1). This formation of the pattern of cones increases the surface area and the surface free energy.

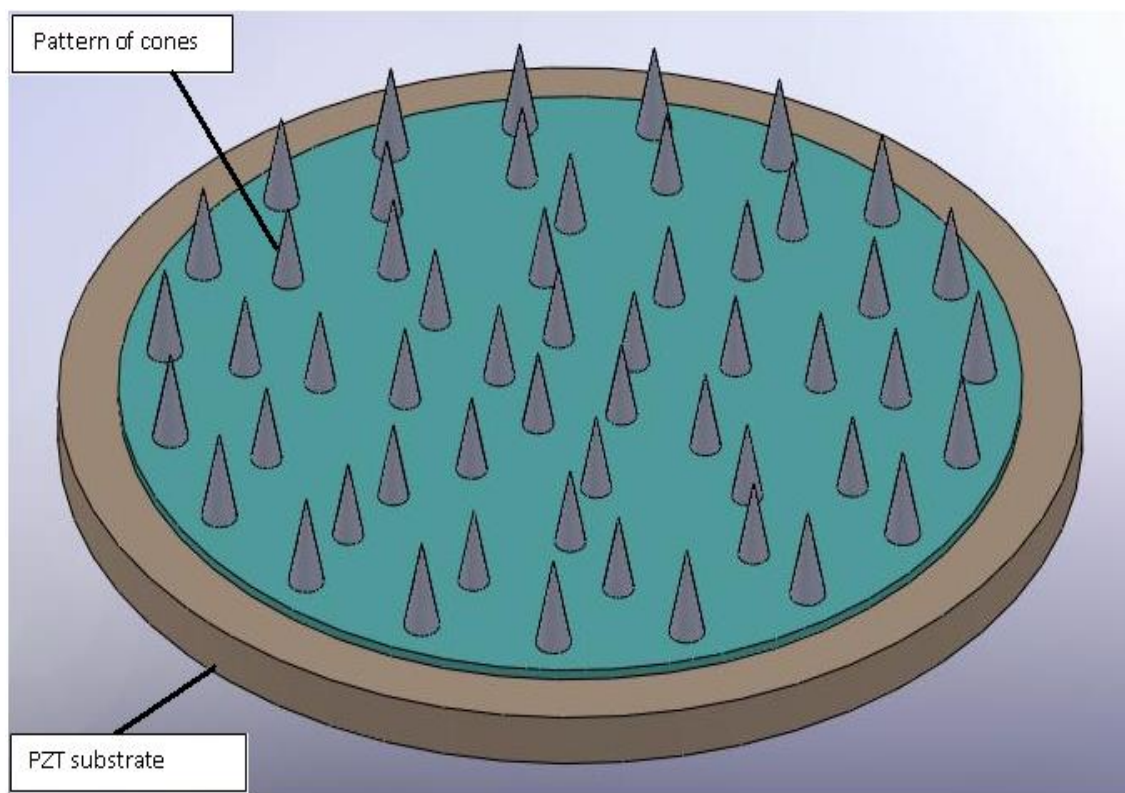


Figure 2-1. Structure of nano-coated sensor.

The magnetization of the ferrofluid responds immediately to changes in the applied magnetic field, and when the applied field is removed the moments randomize quickly, and the formed cones will disappear. To keep these cones in their position after removal of the magnetic field, curing with ultraviolet (UV) lamp is required. The forces holding the magnetic fluid in place are proportional to the gradient of the external field and the magnetization value of the fluid. This implies that the retention force of a ferrofluid can be adjusted by changing either the magnetization of the fluid or the magnetic field in the region.

The purpose of including polyethyleneimine in the mixture is to increase the selective adsorption of particles. Previous research [20] showed that polyethyleneimine (PEI) on silica gel can be used to adsorb TNT.

In this thesis the effects of polyethyleneimine and plasma etching to improve the speed and sensitivity of trace explosive detection are presented in detail. The next chapter discusses how to form the cone patterns on the substrate, the experimental setups, and the experimental procedures.

CHAPTER 3

EXPERIMENTAL SETUP

3.1. Sensor Preparation

Ferrofluid is liquid which becomes magnetized when exposed to a magnetic field. This liquid is actually a colloid which consists of a carrier liquid and ferromagnetic particles. The ferromagnetic particles are very small, and hence do not settle down. When a ferrofluid is subjected to magnetic fields, they exhibit peculiar physical formations. As opposed to the plain flat surface of liquids, a ferrofluid will organize itself into tiny cones projecting outwards. This formation appears to be a solid substance whose surface is composed of cone patterns. This dark magnetic fluid, under the influence of a magnet, becomes a dome or ball having spikes all over its surface. Also referred to as normal field instability, this phenomenon causes the magnetic field to be strong at the cone peaks and weak at their troughs. This experiment uses ferrofluid, provided by Ferrofluid Ferrotech Corp., which consists of 5% magnetic particles, 10 % surfactant and 85% carrier fluid. The size of ferromagnetic nanoparticles is 10nm.

Another ingredient used to make up the sensor is polyethyleneimine. Polyethyleneimine is a polymer which has special affinity to attract explosives like trinitrotoluene (TNT). Polyethyleneimine provided by Alfa Aesar is used for this experiment.

The third ingredient used is epoxy resin. This material helps in regards to the stability of the cones on the piezoelectric crystal.

Figure 3-1 shows the experimental set up for the coating of the sensor. The set up is composed of two bar magnets in an acrylic transparent chamber.

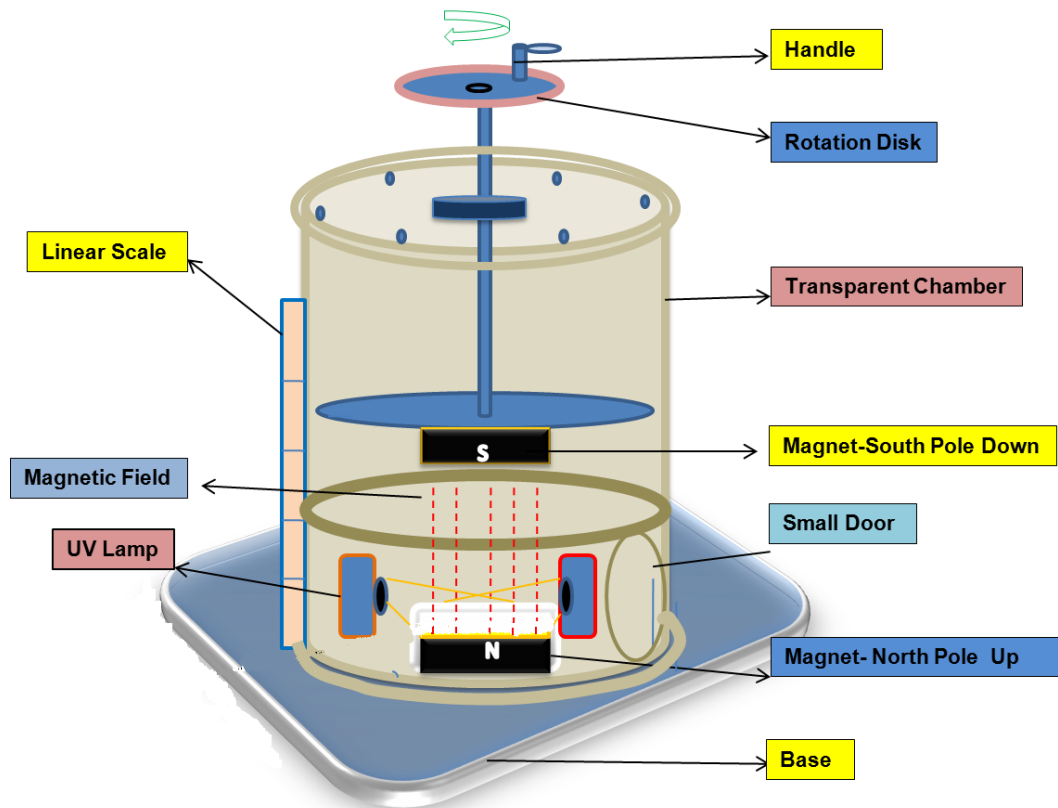


Figure 3-1a. Experimental set up for coating of nano particles.

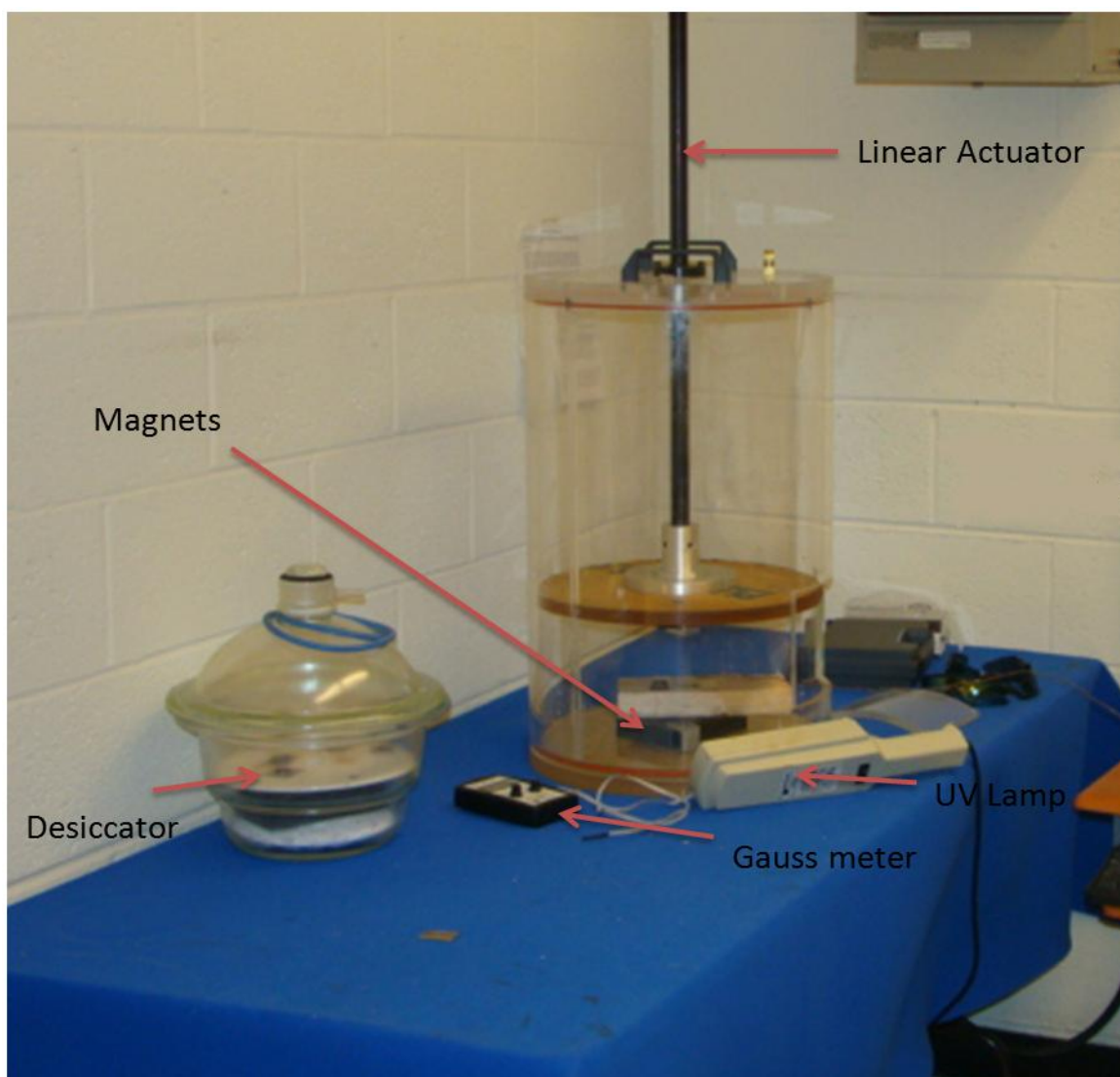


Figure 3-1b. Experimental set up for coating of nano particles.

The two magnets are arranged so that the north pole and south pole of the magnets are facing each other. One magnet is fixed at the lower base of the cylindrical chamber and the other magnet attached to a linear actuator can be moved to vary the distance between the two magnets. The magnetic strength is the main factor affecting the formation of cone patterns. The magnetic strength is controlled by the distance between the two poles which is manipulated by rotating the handle. Keeping the distance between the two magnets constant, it is possible to locate the sensor at the height which corresponds to the appropriate magnetic strength reading (gauss) reading.

The relationship between the magnetic strength and the distance between lower magnet and the sensor for this experimental set up is determined by measuring the magnetic strength at different distances. Table 3-1 tabulates the magnetic field strength at different distances.

Table 3-1. Magnetic strength at distance from top of the lower magnetic source

Distance [mm] from lower magnet	Magnetic Strength [gauss]
0	515
2	501
4	494
9	470
12	467
14	449
16	440
19	428
21	411
23	397
28	387

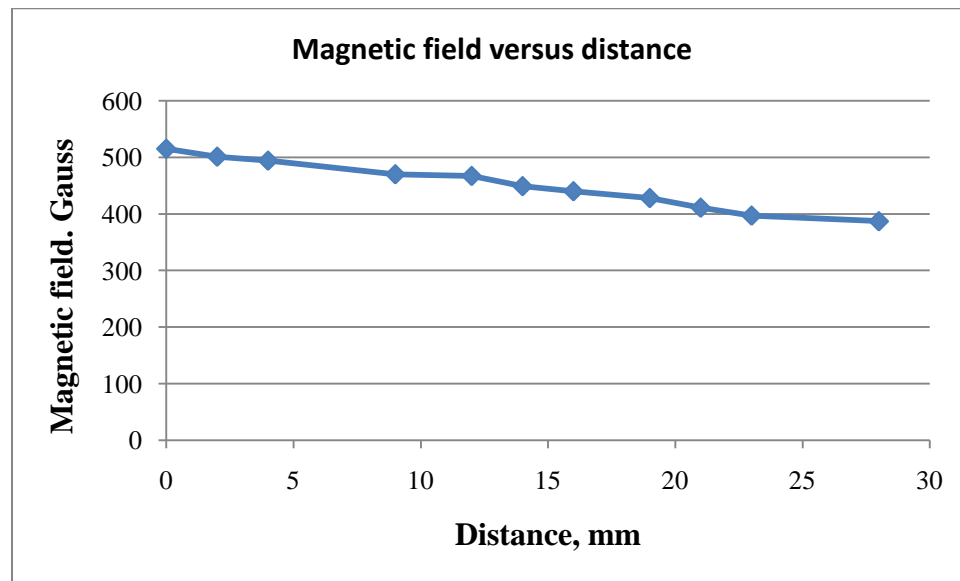


Figure 3-2. Magnetic field strength at a distance from the top of the magnet.

Experiments showed that the best formation for density and distribution attained at 450 gauss of magnetic field and at 14 mm above the top of the lower bar magnet.

This magnetic strength is used to make the sensors with the following three procedures:

1. The first step is preparation of the mixture. The percentage amount of each ingredient has effect in the speed, and the adsorption capacity of the sensor. Different combination of ferrofluid, polyethyleneimine on silica beads and epoxy are studied by using adsorption test.
2. Once the mixture is made, a very fine layer of nano coating solution is coated on the surface of PZT crystal.
3. Finally the nano coated piezo crystal is subjected to a magnetic field. This time, spikes of cones will be shown on the piezo crystal (substrate). These must be cured by applying ultraviolet ray for at least 24 hr. Ultraviolet light (UV) of wavelength 130 nm is used for curing the coated PZT. Figure 3-3 show the surface texture of the nano coated sensor.

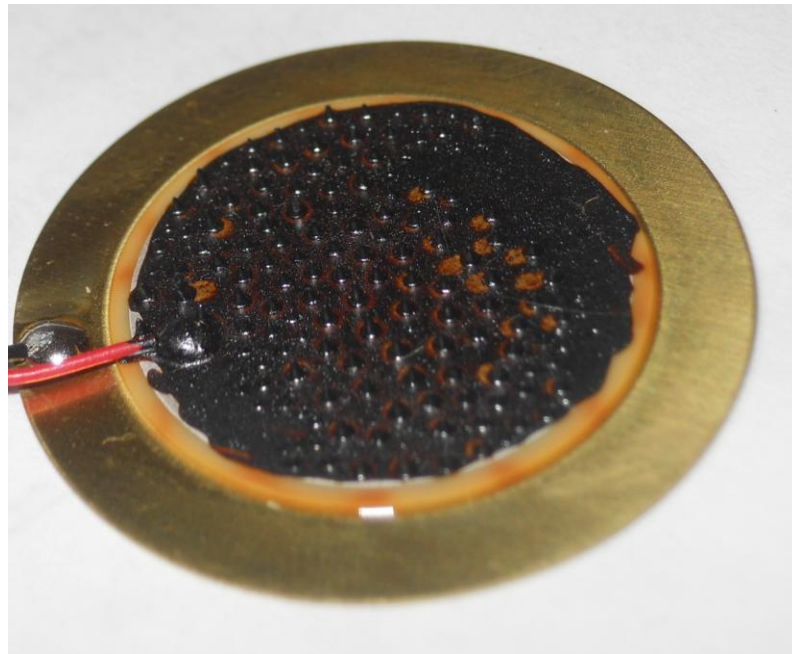


Figure 3-3. Nano coated PZT crystal.

3.2. Adsorption Test for Trace Particles

Solid surfaces show strong affinity towards gas molecules that comes in contact with and some amount of them are trapped on the surface. The process of trapping or binding of molecules to the surface is called adsorption. Almost all the solids adsorb gases to some extent. However, the exact amount of a gas adsorbed depends upon a number of factors, as highlighted below:

One of the factors affecting adsorption is nature of surface area of the adsorbent. The same gas is adsorbed to different extents by different solids at the same experimental conditions. Further, the greater the surface area of the adsorbent, greater is the volume of the gas adsorbed. It is for this reason that substances like charcoal and silica gel are excellent adsorbents because they have highly porous structures and hence large surface area.

The other factor is nature of the gas being adsorbed. Different gases are adsorbed to different extents by the same adsorbent at the same experimental conditions. The higher the critical temperature of a gas, greater is the amount of that gas adsorbed. In other words, a gas which is more easily liquefiable is more readily adsorbed.

Temperature and pressure are also the other factor affecting the process. Adsorption decreases with increase of temperature and vice versa. At constant temperature, the adsorption of a gas increases with increase of pressure.

The other factor is activation of the solid adsorbent. It means increasing the adsorbing power of an adsorbent. This is usually done by increasing the surface area of the adsorbent which can be achieved by either by making the surface of the adsorbent rough or by substituting the adsorbent into smaller pieces or grains or by removing the gases already adsorbed on the surface.

Taking these factors into consideration, the following experimental set up (Figure 3-4) is

used for adsorption test, and the procedures are described below.

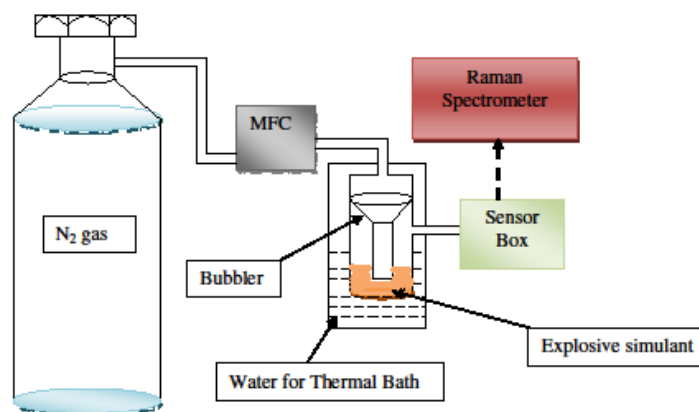


Figure 3-4a. Schematic of experimental setup for adsorption test.

The carrier nitrogen gas will be passed through the mass flow controllers (MFC). The manifold will be kept inside the thermal bath to keep the sample warm. This will help to facilitate the evaporation of the mock explosive sample. As the nitrogen gas pass through the manifold, it will pick some trace particles of the mock explosive from the sample and direct them to the sensor box. This process will be conducted for limited time. After a certain period of time, the sensor will be taken to Raman Spectrometer for spectra reading. These spectra will be compared to pre-known spectra of the mock explosive. If there is adsorption on the surface, the spectra read on output of Raman Spectrometer will show the same peaks to that of the mock explosive.

The trace particle detection will be a progressive process i.e. the compounds to be adsorbed will start form a basic compound to the more complex ones as the results come in. For this particular test the mock explosive used is 2-nitrotoluen.

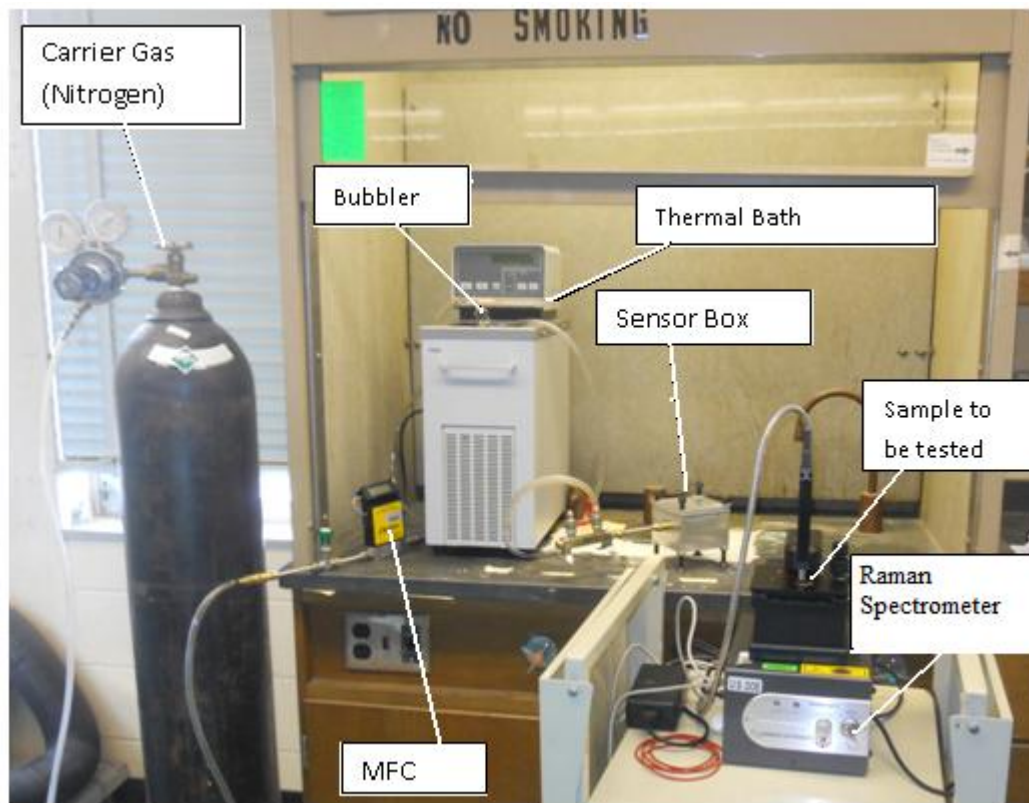


Figure 3-4b. Experimental setup for adsorption test.

The following procedures are used for the adsorption test.

1. Using the Raman Spectrometer, take the spectra of the sensor on which adsorption test is to be conducted.
2. Save this spectrum as reference for subtraction.
3. Set the thermal bath to 100°C, and wait till this temperature is attained.
4. Set the flow rate of the Mass flow Controller to the required flow rate to obtain the required concentration. The relation between flow rate and concentration are discussed in the following section (Section 3.3).
5. Once the mixture of nitrogen gas and nitrotoluene starts to come out of the bubbler to the sensor, set the stop watch on.

6. Once the sensor is exposed to the mixture for a predetermined time, remove the sensor and take the spectral reading on the Raman Spectrometer.

3.3. Concentration of Mock Explosive in Carrier Gas

All solids and liquids emit a certain amount of vapor at all temperatures above absolute zero (-273°C), and at a given temperature the amount of vapor emitted is characteristic of the particular substance. Concentration of the mock explosive is the measure of how much of the 2-nitrotoluene vapor is mixed with the carrier gas (nitrogen). There are a number of different ways of expressing solute concentration (2-nitrotoluene) in the solvent (nitrogen gas). Some of the units of concentration are: molarity (moles solute/liter of solution), normality (equivalents of solute/liter of solution), mass per volume (mass of solute /mass of solution), and molality (moles of solute/mass of solvent), and parts per million (ppm). The most common units used to express explosive chemicals is parts per million (ppm), parts per billion (ppb) and parts per trillion (ppt).

Parts per million concentrations are essentially mass ratios (solute to solution) multiplied by a million (10^6).

$$\text{ppm} = \frac{\text{mass of solute in mg}}{\text{mass of solvent in Kg}} \quad (3.1)$$

To calculate the concentration of the 2-nitrotoluene in the carrier gas, evaporation rate of 2-nitrotoluene at a specific flow rate of carrier gas at some working temperature and pressure should be known. Experiment is done to find the evaporation rate of 2-nitrotoluene at temperature of 100°C.

1. Measure 10 ml of 2-nitrotoluene in the bubbler
2. Fill the thermal bath with water, and set the temperature to 100°C.

3. Determine the required volume flow rate (cm^3/min), and read the corresponding reading from the calibration chart of the flow meter used. The flow meter used for this experiment is OMEGA model1814S.
4. Monitor the temperature till it reads 100°C .
5. Open the valve and turn the stop watch on.
6. Once the evaporation takes place for sufficient time, stop the process,
7. Take the new reading of the 2-nitrotoluene.
8. Divide the evaporated amount of 2-nitrotoluene to the duration of evaporation to get the evaporation rate in volume/time.

Experiments were done as per the above procedures, and table 3-2 shows the evaporation rate of 2-nitrotoluene using nitrogen as a carrier gas.

Table 3-2. Evaporation rate of 2-nitrotoluene at different flow rates of N_2 carrier gas

Flow rate of Carrier gas (N_2) Cm^3/min	Evaporation rate of 2-nitrotoluene [ml/min]
350	1/152
450	1.2/120
600	1.5/60
800	2.1/60
1000	2.8/60

This table can be used to calculate the concentration, (in ppm, ppb, or ppt) of 2-nitrotoluen in the nitrogen gas.

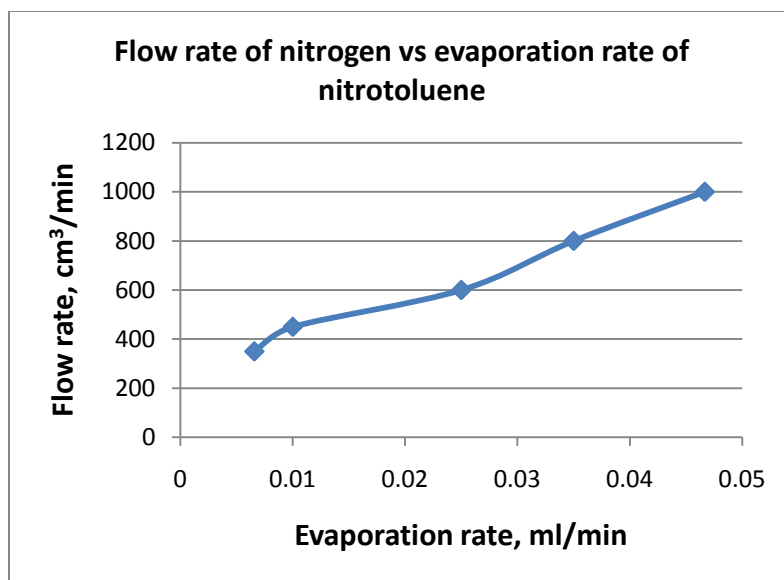


Figure 3-5. Flow rate of N₂ vs evaporation rate of 2-nitrotoluene.

For example, if the adsorption test is done for T min with nitrogen flow rate of 350 cm³/min, the concentration of the nitrotoluene (the solute) in the nitrogen gas can be calculated as follows:

$$ppm = \frac{\text{mass of solute in mg}}{\text{mass of solvent in Kg}}$$

$$\text{Density of nitrotoluene} = 1.29 \frac{\text{gm}}{\text{ml}}$$

$$\text{Density of Nitrogen} = 1.25 \frac{\text{gm}}{\text{l}} = 0.00125 \frac{\text{gm}}{\text{ml}}$$

$$\text{Mass of solute} = \text{Density of nitrotoluene} \times \text{volume of nitrotoluene}$$

$$\text{volume of nitrotoluene} = \frac{1}{152} \frac{\text{ml}}{\text{min}} * T \text{ min} = 0.006578947 T \text{ ml}$$

$$\text{Mass of solute} = 1.29 \frac{\text{gm}}{\text{ml}} * 0.006578947 T \text{ ml} = 0.008486842 T \text{ gm}$$

$$\text{Mass of solvent} = \text{Density of nitrogen} \times \text{volume of Nitrogen}$$

$$= 1.25 \frac{\text{gm}}{\text{l}} * (350 \frac{\text{ml}}{\text{min}} * T \text{ min})$$

$$= 0.00125 \frac{\text{gm}}{\text{ml}} * (350 \frac{\text{ml}}{\text{min}} * T \text{ min}) = 0.4375 T \text{ gm} = 0.0004375 T \text{ kg}$$

$$\text{ppm} = \frac{0.008486842 T \text{ mg}}{0.0004375 T \text{ Kg}} = 19.4 \text{ ppm}$$

To convert ppm to other units of concentration:

$$= 19.4 \text{ ppm} \times 1000 \frac{\text{ppb}}{\text{ppm}} = 19400 \text{ ppb}$$

$$= 19.4 \text{ ppm} \times 1000000 \frac{\text{ppt}}{\text{ppm}} = 19400000 \text{ ppt}$$

Based on this, the concentration of 2-nitrotoluene in Nitrogen is calculated for different rates and presented as follows.

Table 3-3 Concentration of 2-nitrotoluene at different flow rates of N₂ carrier gas

Flow rate of Carrier gas (N ₂) Cm ³ /min	Concentration of 2-nitrotoluene
350	19 ppm
450	23 ppm
600	43 ppm
800	45 ppm
1000	48 ppm

3.4. Plasma Etching of Sensors

Surfaces of solid materials contain irregularities or hills and valleys. These surface irregularities are commonly called asperities. Asperities are found on metals, polymers, ceramics, and carbon bodies. In addition to the presence of surface irregularities, the solid surface itself may be covered with number of films. For example on the outer most surface there may be a layer of adsorbate, which is water vapor or hydrocarbons from the environment that may be condensed and become physically adsorbed to the solid surface. On metal surfaces or alloys, beneath this layer of adsorbate is generally a layer of metal or alloy oxide. Thickness of the oxide layer depends on nature of the substrate and the environment. Beneath the oxide layer on alloy surfaces is a region of surfacial material which may be highly worked or deformed as a

result of the forming process with which the metal surface was prepared. With ceramic materials the oxide layer may or may not be present. However, adsorbates are still present. These layers are extremely important because of their properties, from surface chemistry point of view, can be entirely different from the bulk metal. Likewise the mechanical behavior is also influenced by the amount and depth of deformation of the surface layers.

Therefore, a surface treatment is required to bring out characteristic features of the substrate surface. Plasma technology is used as surface treating tool in this experiment. Plasma can be used for cleaning surfaces of any residues or contamination, activation of various materials before adhering together, and etching and partial removal of surfaces. Plasma etching of the substrate before cone formation will enhance the binding of the cones to the substrate to increase stability. On the other hand, etching the sensor after the cones are formed on the substrate will increase the adsorption performance of the sensor. The plasma etching setup will be composed of the etching gas (argon), compressed air, vacuum pump and the plasma etching machine. Figure 3-5 shows the schematic for plasma etching of the sensor.

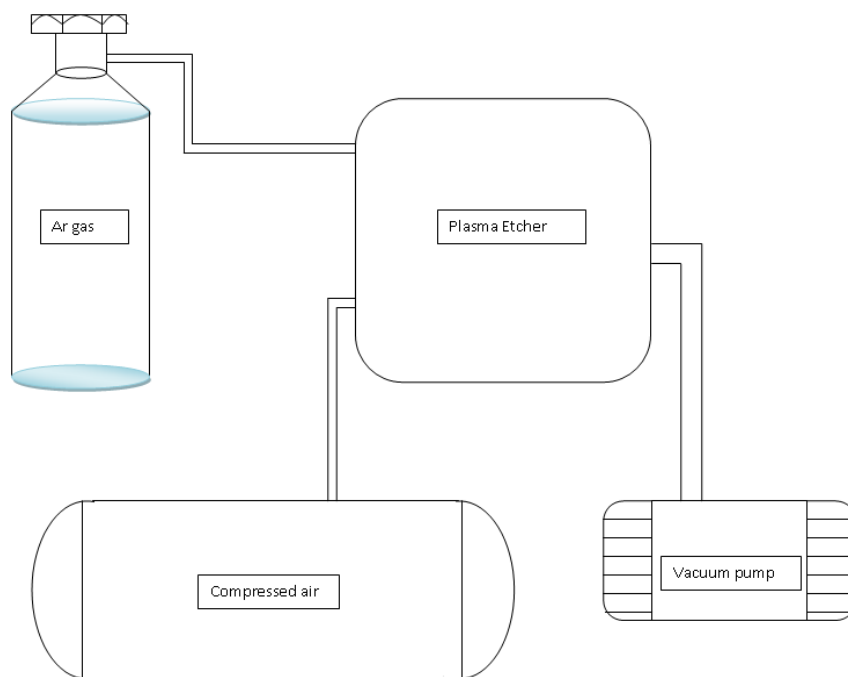


Figure 3-6. Setup for plasma etching.

Chapter four of this report presents the results of the adsorption tests to show the effect of polyethyleneimine and plasma etching on different samples. These test results are summarized in tabular and graphical form.

CHAPTER 4

RESULTS

In the previous chapter, the experimental setups and procedures were outlined for cone formation, plasma etching, and adsorption testing. Using these setups, several experiments have been performed to study the effects of polyethyleneimine and plasma etching on the adsorption of a mock explosive onto the newly developed nano coated sensor. This chapter presents the results of these experiments.

4.1 Absorption Spectra of 2-Nitrotoluene

The absorption spectrum is defined as the fraction of incident radiation absorbed by a material over a range of frequencies. The absorption spectrum is primarily determined by the atomic and molecular composition of the material. When a sample is tested using a Raman spectrometer, energy will be absorbed by the test sample.

This energy is given by Einstein relation:

$$E = h\nu = \frac{hc}{\lambda} \quad (4.1)$$

Where:

E represents energy absorbed per photon

h represents Planck's constant = 6.626×10^{-34} J s / photon

ν represents the frequency

λ represents wave length

c represents speed of light

The frequencies where absorption lines occur, as well as their relative intensities, primarily depend on the electronic and molecular structure of the sample. Absorption spectroscopy is useful in chemical analysis because of its specificity and its quantitative nature. The specificity of absorption spectra allows compounds to be distinguished from one another in a mixture, making absorption spectroscopy useful in wide variety of applications.

For identification purposes the spectra of 2-nitrotoluene is obtained using a Raman spectrometer. Figure 4-1 shows the spectra of 2-nitrotoluene. As shown in this figure, peaks of 2-nitrotoluen occur at wave numbers of 664, 791, 857, 1049, 1344. The highest intensity is at 791 and the lowest intensity is at wave number 664. This array of wave number peaks is used to identify the adsorbed 2-nitrotoluene on the nano coated sensor.

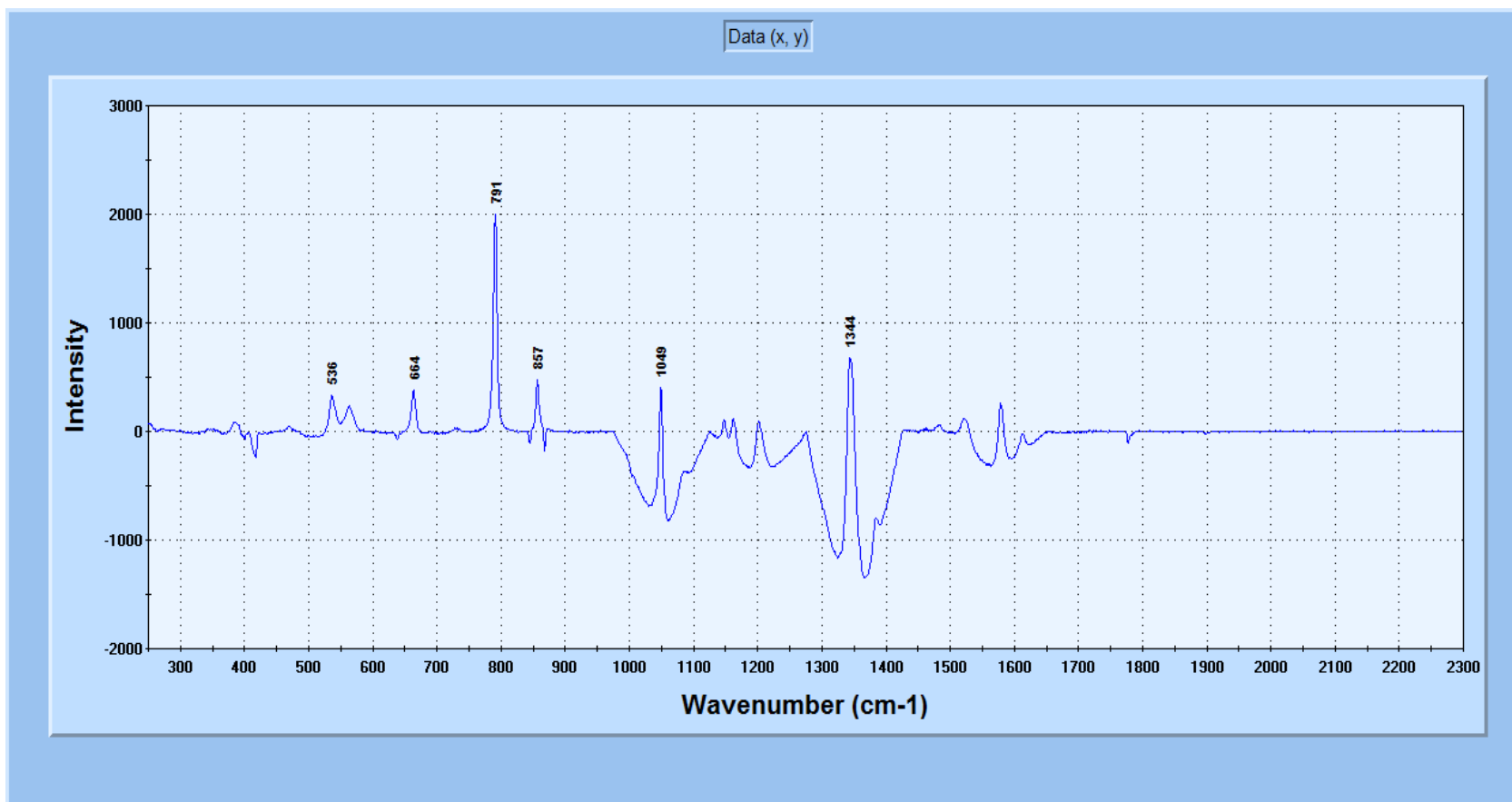


Figure 4-1. Spectra of 2-nitrotoluene.

4.2 Effect of Polyethyleneimine on Adsorption of Mock Explosive

To study the effect of polyethyleneimine, different sensors are made by varying the mass percentage of polyethyleneimine. The tests are done progressively by increasing the mass of polyethyleneimine. The following table shows the composition of each sensor sample.

Table 4-1. Composition of different sensor samples

Sample	Ferrofluid	Polyethyleneimine	VersaChem Epoxy
M2	90	5	5
M3	85	10	5
M4	80	15	5
M5	75	20	5
M6	70	25	5

Different adsorption experiments are conducted by exposing the sensor samples to different concentration mixtures at different exposure times. The samples are exposed to a vapor mixture of nitrogen gas and 2-nitotoluene at concentrations of 19 ppm, 23 ppm, and 43 ppm. After this test is complete, the Raman spectrometer is used to test whether 2-nitrotoluene has been adsorbed onto the sensor sample. The tests are performed in order of decreasing concentration: 43 ppm followed by 23 ppm and then 19 ppm.

4.2.1 Results of Adsorption Test with Mixture Concentration of 43 ppm

Figure 4-2 through Figure 4-6b show the results obtained after exposing the sensor samples to the mixture of mock explosive and carrier gas with a flow rate of 600 cm³/min of nitrogen gas. In addition these results are summarized in table 4-2.

Table 4-2. Adsorption test results at 43 ppm concentration

Duration of Exposure, Seconds	Reference peaks (2-nitrotoluene), wave numbers [cm ⁻¹]	Wave number [cm ⁻¹]				
		Sample M2 (Figure 4-2)	Sample M3 (Figure 4-3a) and (Figure 4-3b)	Sample M4 (Figure 4-4a) to (Figure 4-4c)	Sample M5 (Figure 4-5a) to (Figure 4-5d)	Sample M6 (Figure 4-6a) and (Figure 4-6b)
30	791	-	-	-	-	-
	1344	-	-	-	-	-
	857	-	-	-	-	-
	1049	-	-	-	-	-
	664	-	-	-	-	-
40	791	-	-	-	790	-
	1344	-	-	-	-	-
	857	-	-	-	-	-
	1049	-	-	-	-	-
	664	-	-	-	-	-
50	791	-	-	790	789	-
	1344	-	-	-	1344	-
	857	-	-	-	-	-
	1049	-	-	-	-	-
	664	-	-	-	-	-
60	791	-	791	791	790	791
	1344	-	1344	1345	1346	1346
	857	-	-	857	857	856
	1049	-	-	1050	1049	1049
	664	-	-	664	664	663
120	791	791	791	791	791	790
	1344	1345	1346	1345	1345	1346
	857	857	857	857	857	856
	1049	1049	1049	1049	1049	1049
	664	664	663	665	664	663

Sample M2 (which is composed of 90% ferrofluid, 5% polyethyleneimine and 5% epoxy) did not show any peak until the exposure time of 120 sec. As the exposure time was increased to 2 min, the spectra of 2-nitrotoluene was observed. Figure 4-2 shows the adsorption test results for sample M2 after exposing it to 43 ppm concentration for 2 min.

As can be seen from the table above, the fastest duration of exposure for sample M3, which is composed of 85% ferrofluid, 10% polyethyleneimine, and 5% epoxy, is 60 sec. Figure

4-3a and Figure 4-3b, are the adsorption test results for this sample. Figure 4-3a shows the results after the exposure time of 1 min while Figure 4-3b shows the results after 2 min. In both these graphs, the spectra of 2-nitrotoluene can be seen. In Figure 4-3a, some unknown gasses are also adsorbed. Even though the energy from these unknown gasses is more intense, there is still some energy absorbed at frequencies which specify 2-nitrotoluene. As the exposure time was increased to 2 min, the energy from the 2-nitrotoluene became more intense, and all the peaks of spectra of 2-nitrotoluene were observed.

Sample M4, which is composed of 15% polyethyleneimine adsorbed 2-nitrotoluene vapor after 50 sec exposure time. Figure 4-4a to Figure 4-4c show the results after 50 sec, 1 min and 2 min exposure time respectively. In all these graphs it is deemed that the mock explosive has been adsorbed. The wave number peaks are 1 unit more or less than the reference spectra of 2-nitrotoluene. This deviation is acceptable since the resolution of the Raman spectrometer was set to ± 1 . On this test the peaks of 2-nitrotoluene are dominant over any other gasses. Similarly, Figure 4-5a to Figure 4-6b showed that the mock explosive was adsorbed by samples M5 and M6.

At this particular concentration (43 ppm), it can be observed that for adsorption of the mock explosive to occur, either the sensor has to have more than 5% of polyethyleneimine or the sensor sample has to be exposed for longer time. It can be seen that increasing the amount of polyethyleneimine up to 20% in the nano coating mixture improves the adsorption speed of the sensor.

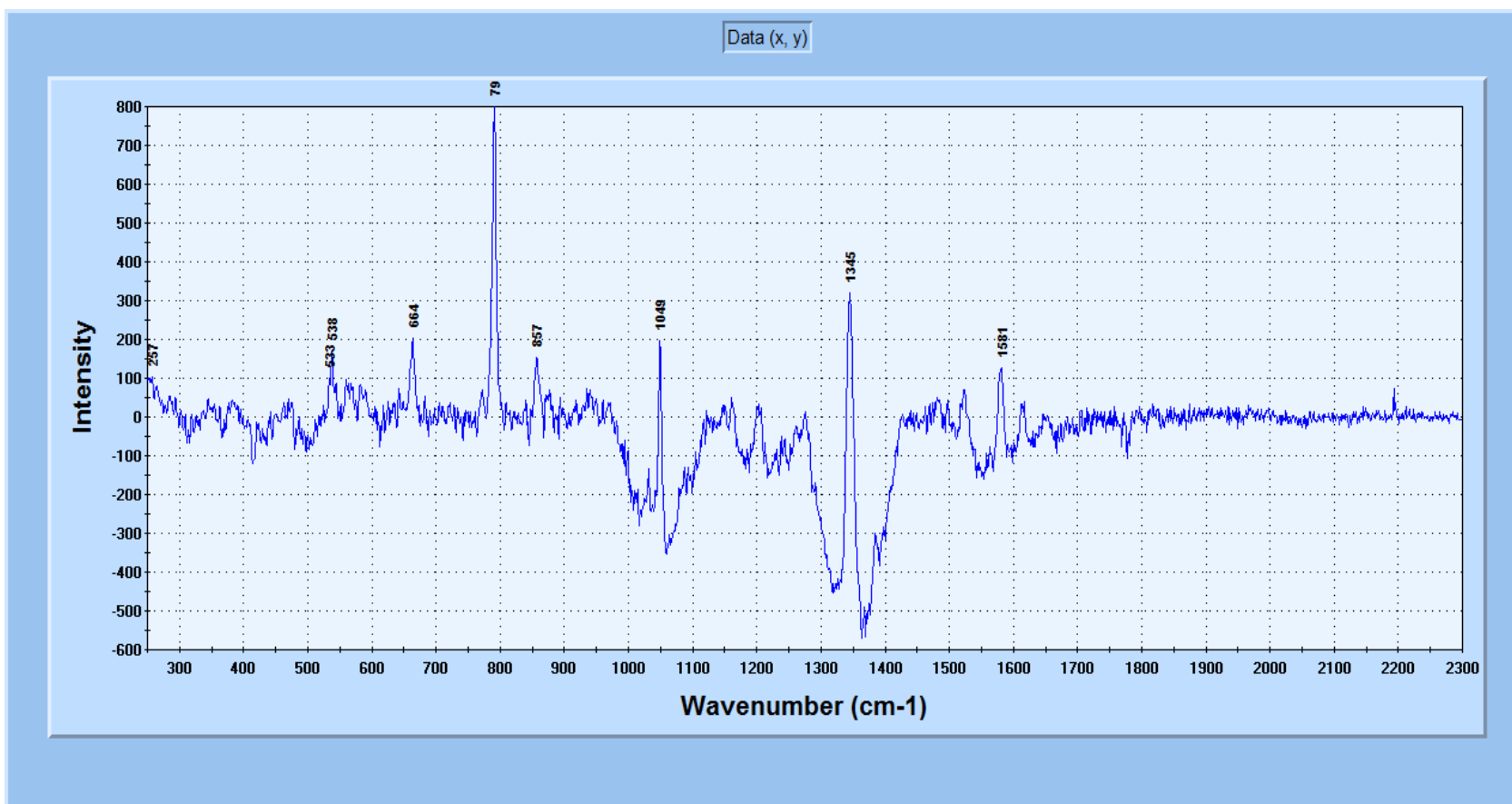


Figure 4-2. Sample M2 after exposure to mixture of concentration 43 ppm for 2 min.

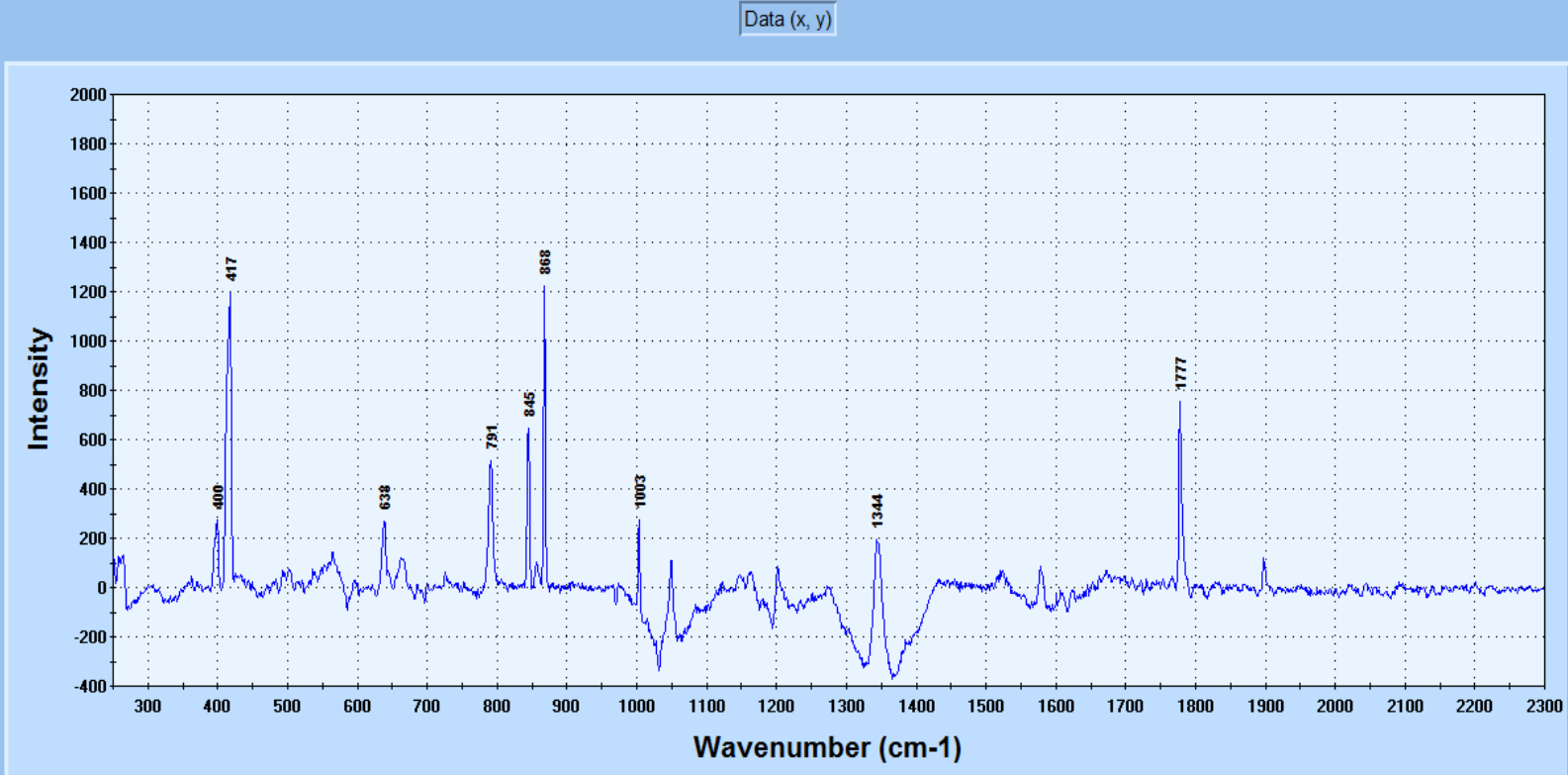


Figure 4-3a. Sample M3 after exposure to mixture of concentration 43 ppm for 1 min.

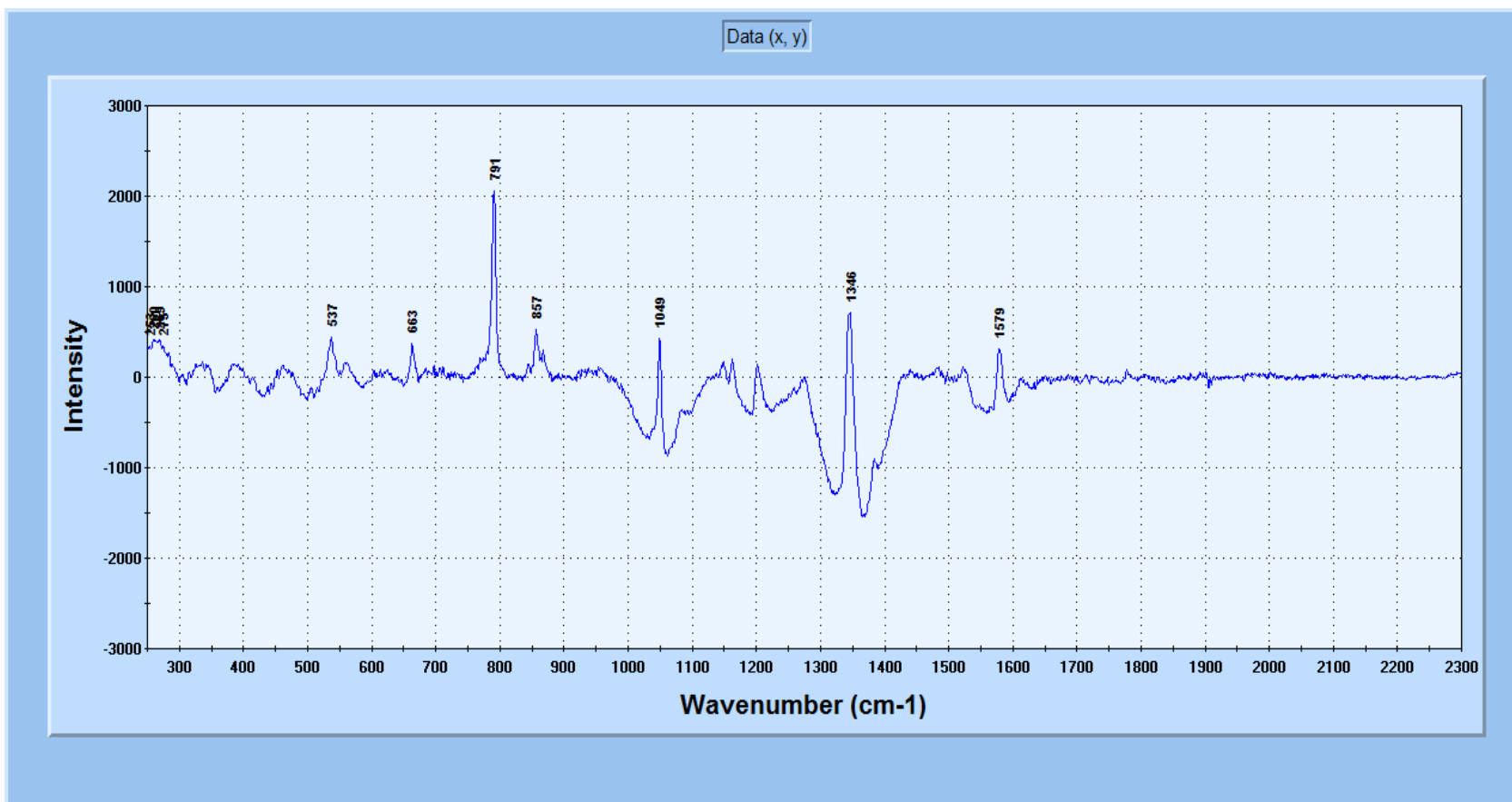


Figure 4-3b. Sample M3 after exposure to mixture of concentration 43 ppm for 2 min.

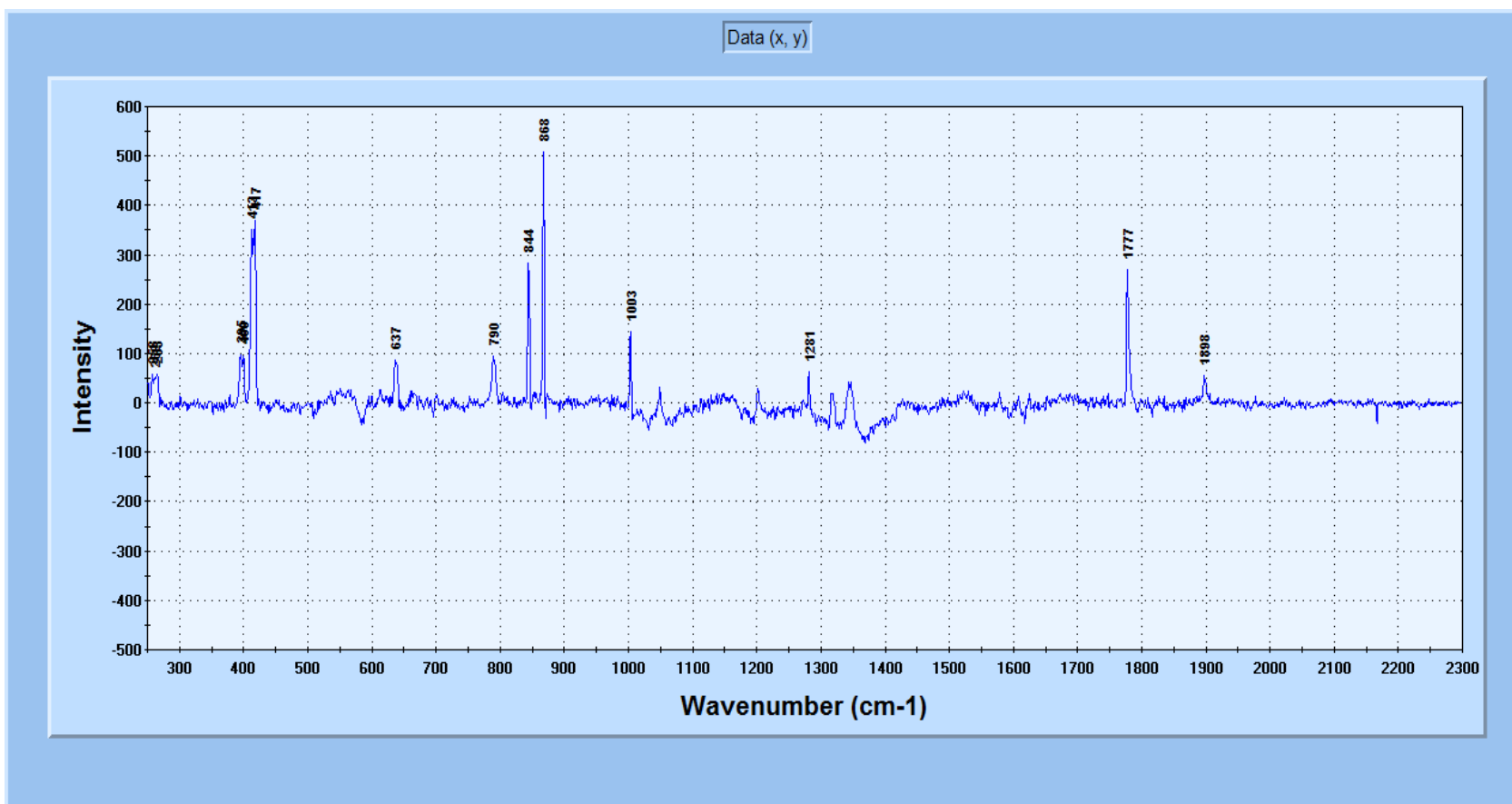


Figure 4-4a. Sample M4 after exposure to mixture of concentration 43 ppm for 50 sec.

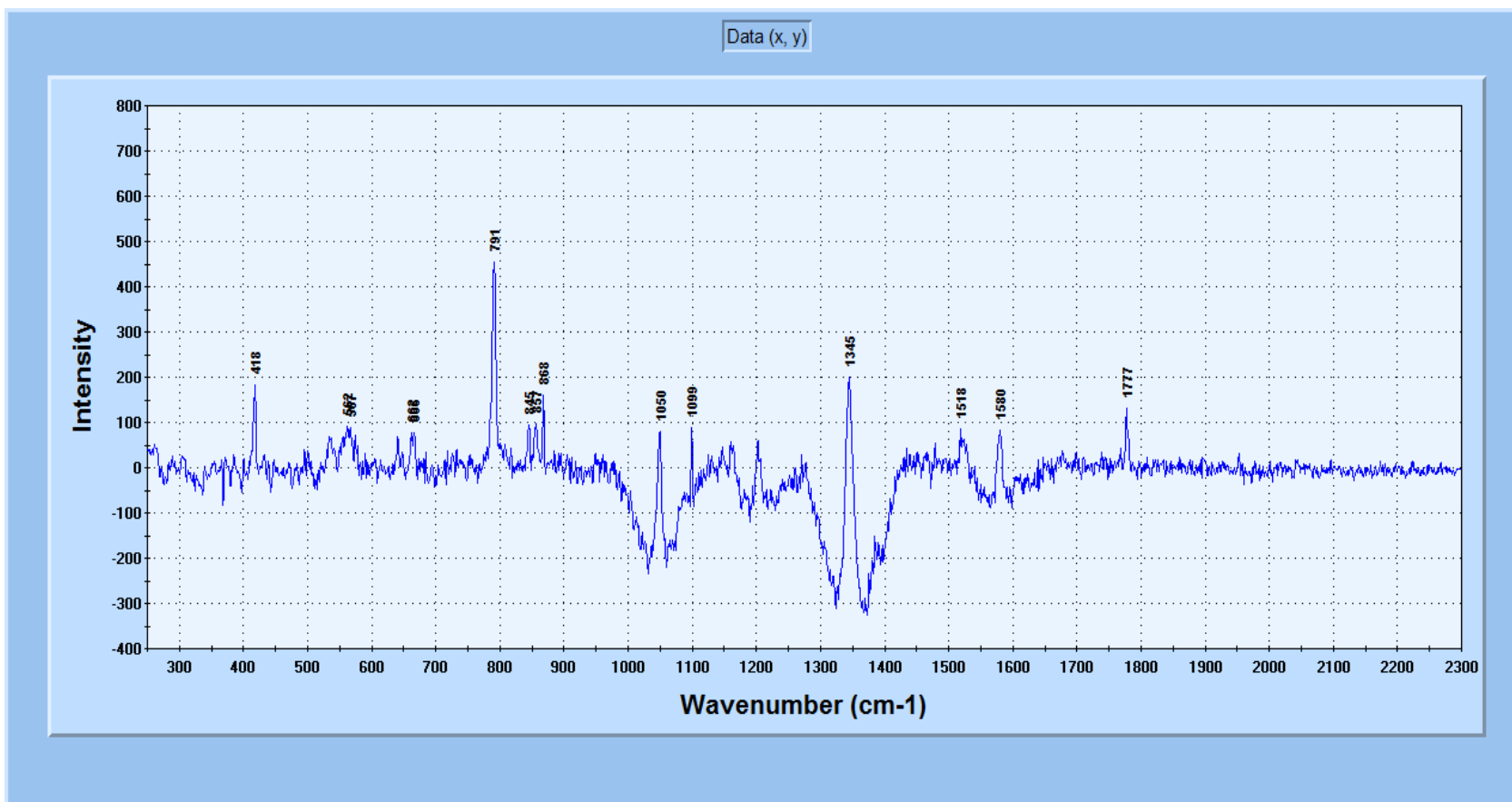


Figure 4-4b. Sample M4 after exposure to mixture of concentration 43 ppm for 1 min.

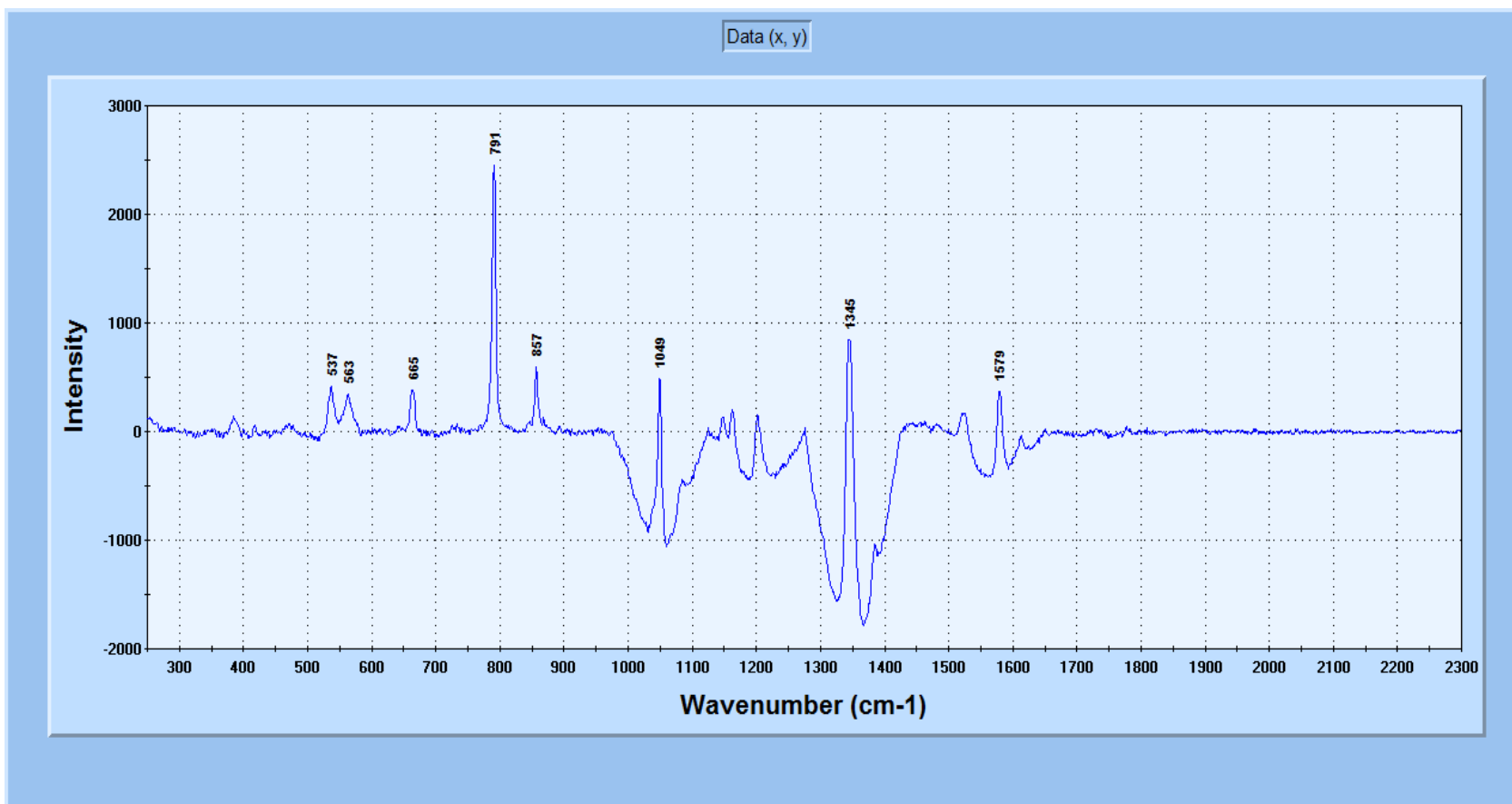


Figure 4-4c. Sample M4 after exposure to mixture of concentration 43 ppm for 2 min.

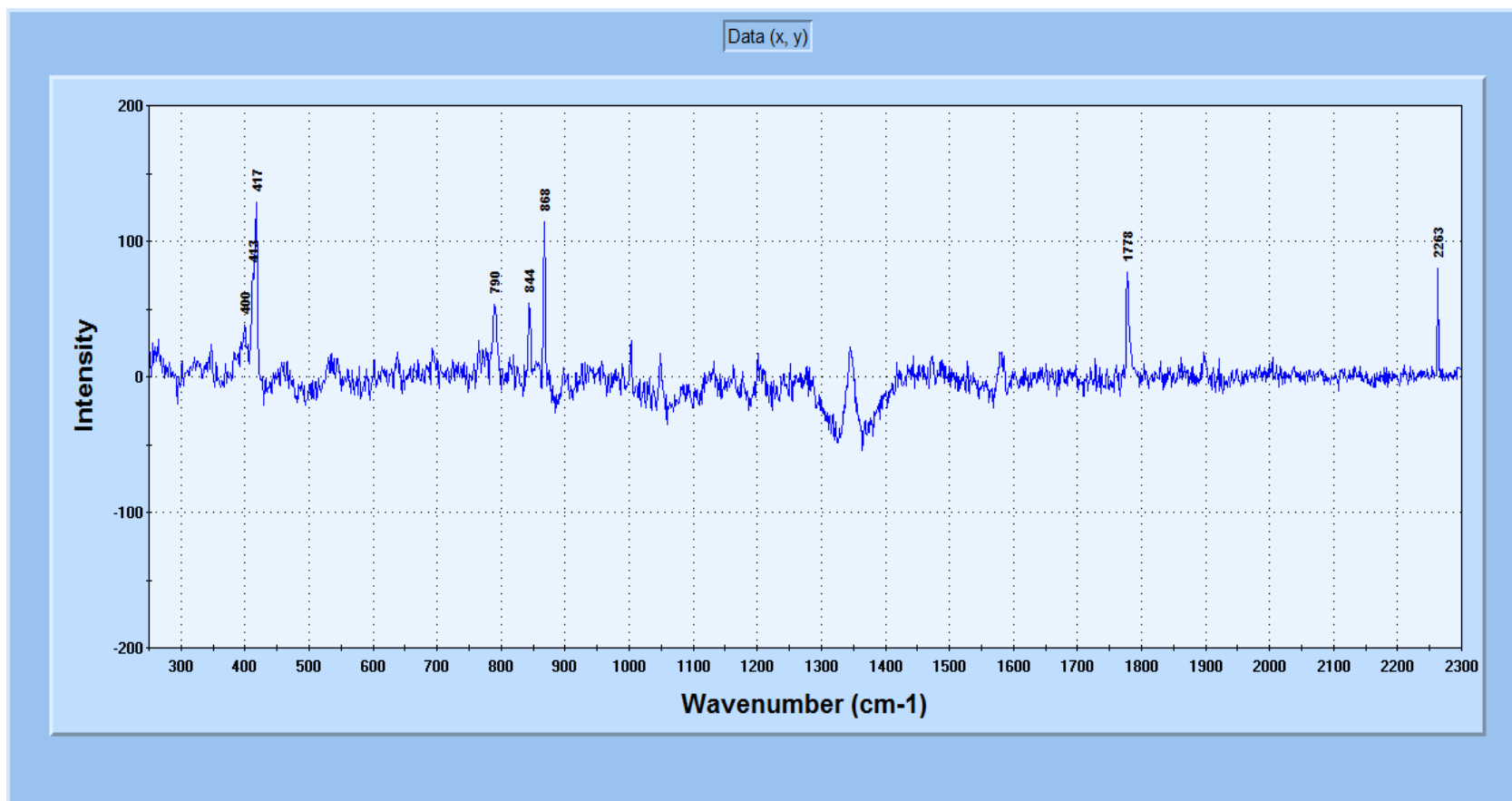


Figure 4-5a. Sample M5 after exposure to mixture of concentration 43 ppm for 40 sec.

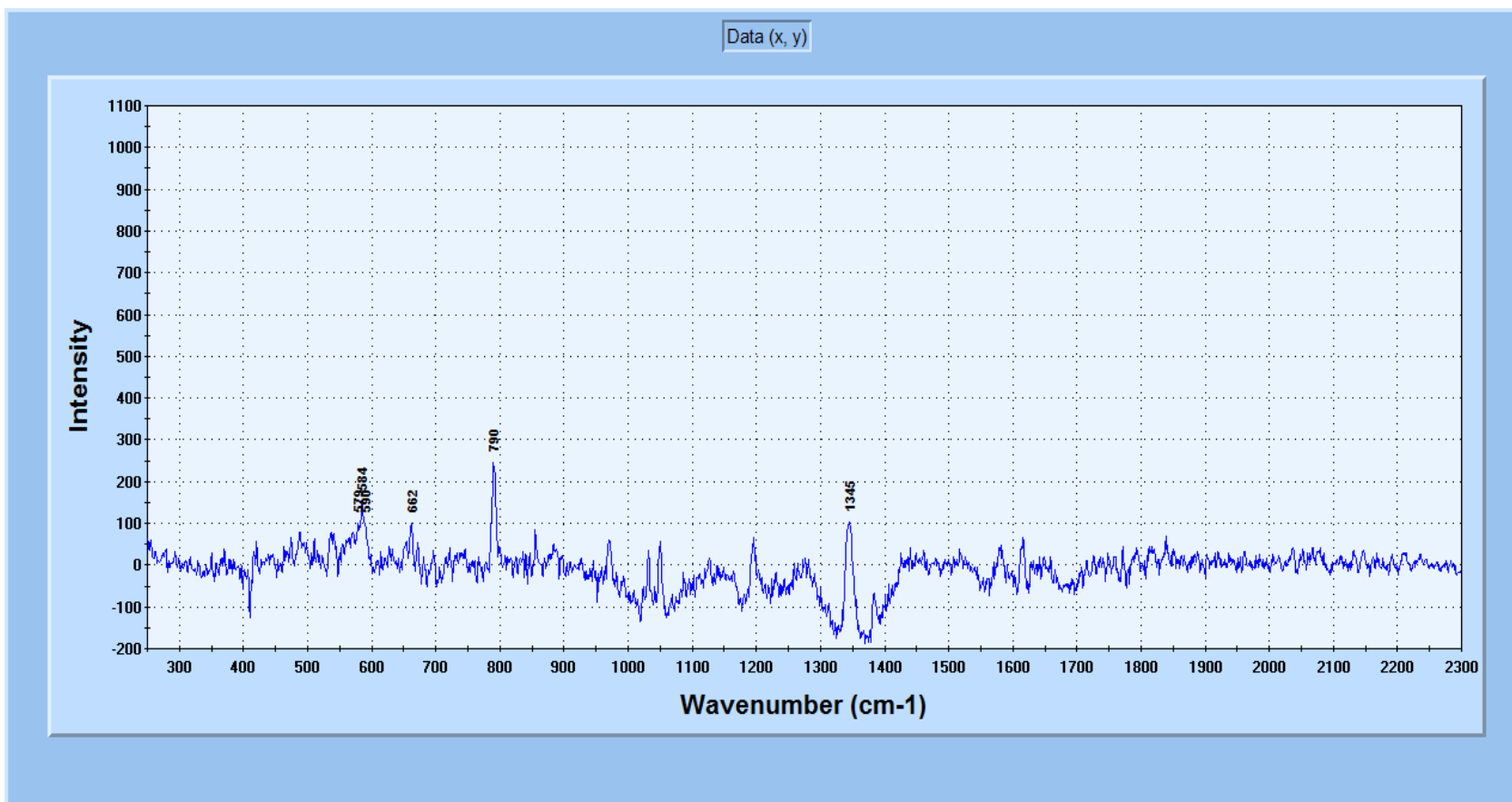


Figure 4-5b. Sample M5 after exposure to mixture of concentration 43 ppm for 50 sec.

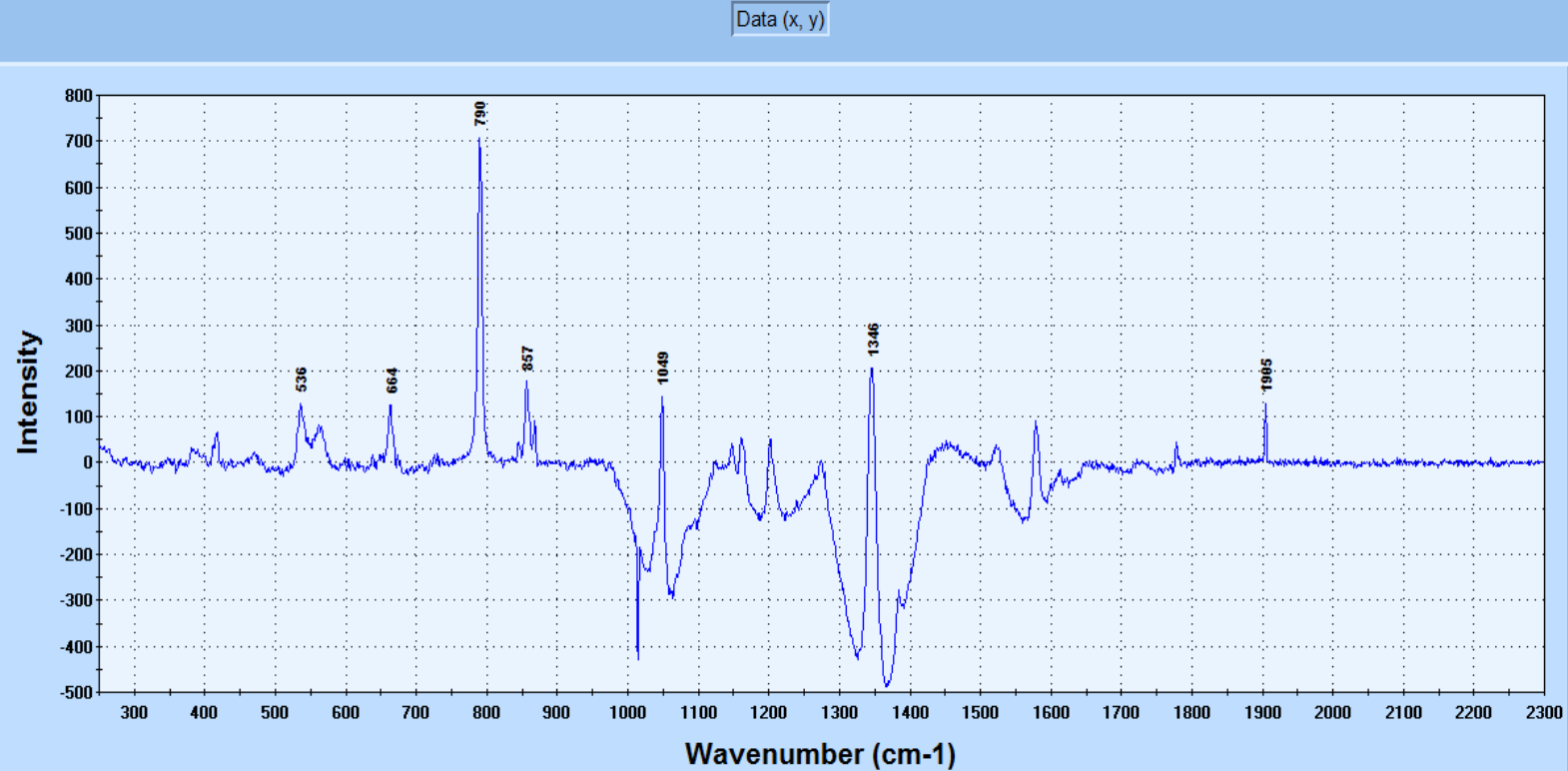


Figure 4-5c. Sample M5 after exposure to mixture of concentration 43 ppm for 1 min.

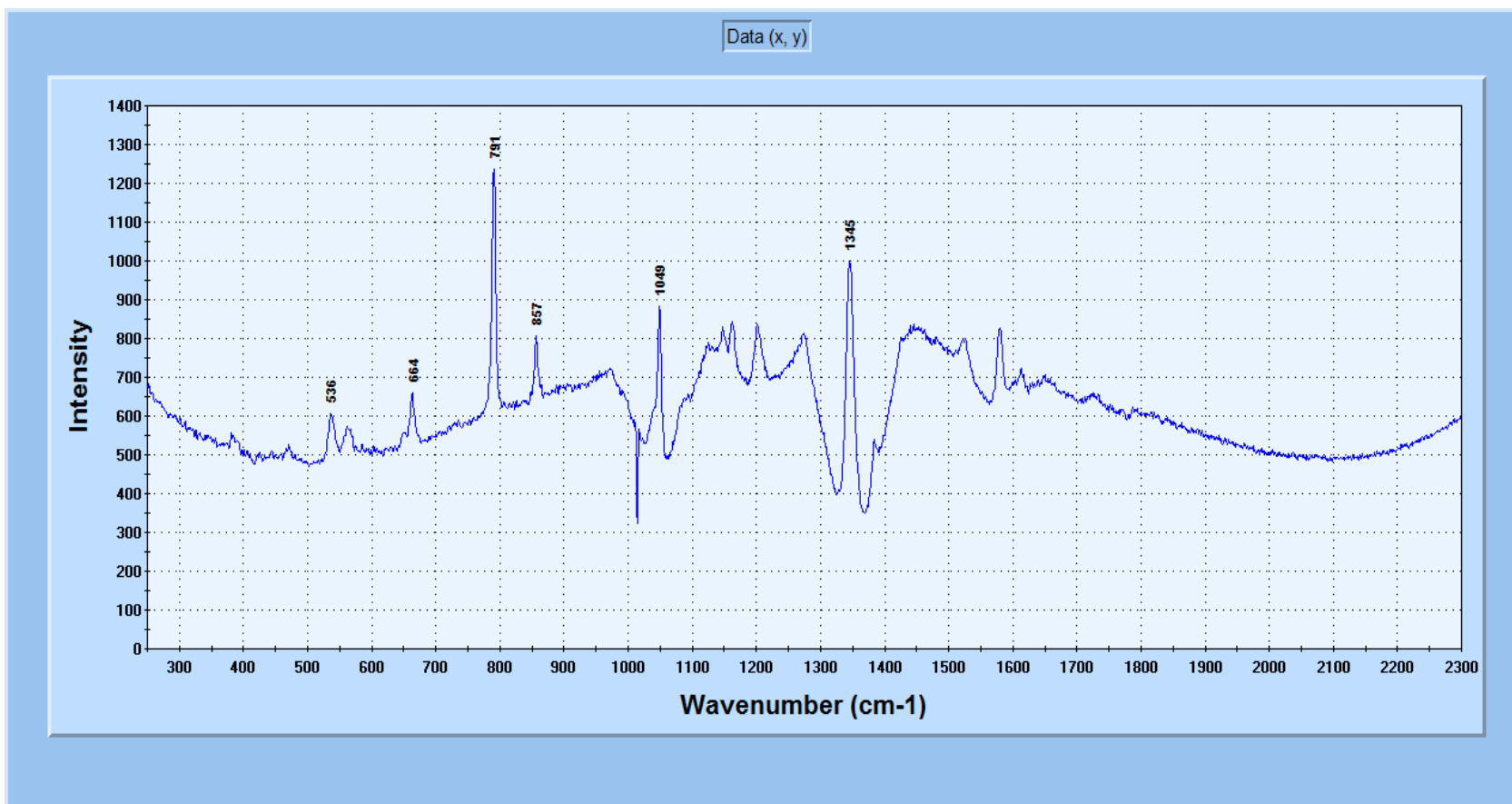


Figure 4-5d. Sample M5 after exposure to mixture of concentration 43 ppm for 2 min.

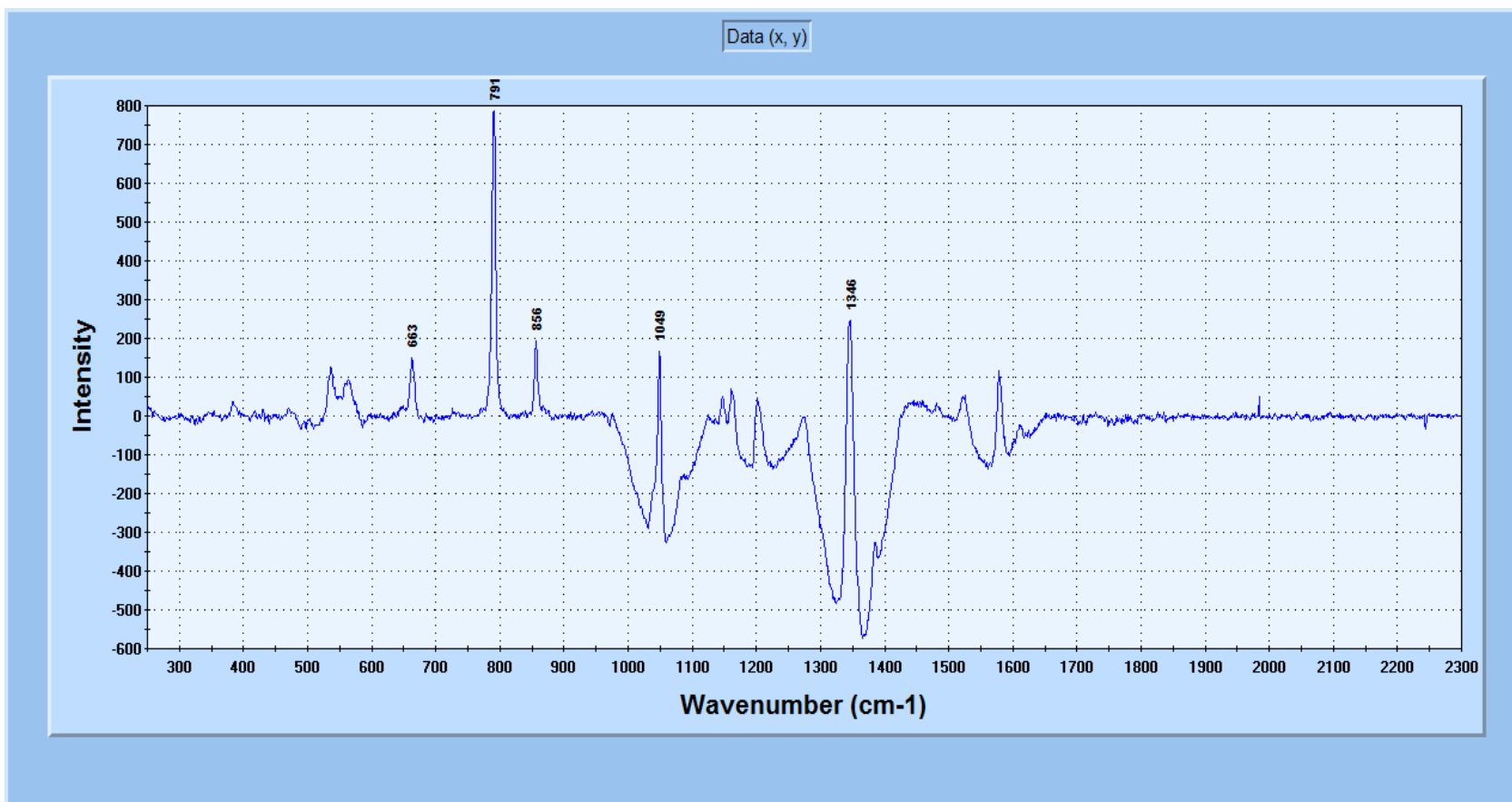


Figure 4-6a. Sample M6 after exposure to mixture of concentration 43 ppm for 1 min.

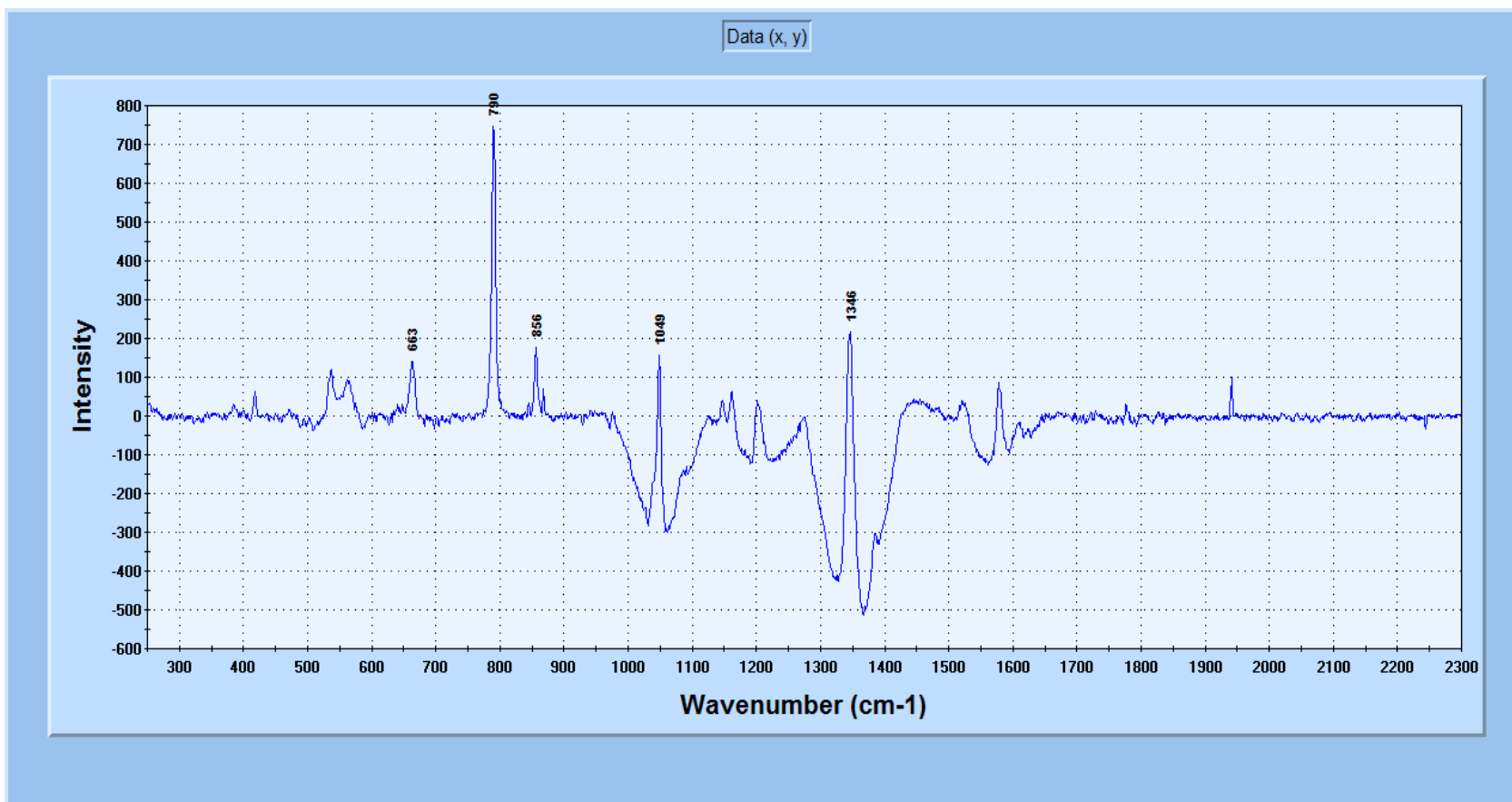


Figure 4-6b. Sample M6 after exposure to mixture of concentration 43 ppm for 2 min.

4.2.2 Results of Adsorption Test with Mixture Concentration of 23 ppm

In this section, the experiment is expanded to identify those samples which can capture polyethyleneimine vapor at a lower concentration. The same procedure is used except the concentration in this case is 23 ppm. The test results are summarized in Table 4-3 and Figure 4-7a to Figure 4-9b.

Table 4-3. Adsorption test results at 23 ppm concentration

Duration of Exposure, minutes	Reference peaks (2-nitrotoluene), wave numbers [cm^{-1}]	Wave number [cm^{-1}]				
		Sample M2	Sample M3 (Figure4-7a) and (Figure 4-7b)	Sample M4 (Figure4-8a) and (Figure 4-8b)	Sample M5 (Figure4-9a) and (Figure 4-9b)	Sample M6
0.5 min	791	-	-	-	-	-
	1344	-	-	-	-	-
	857	-	-	-	-	-
	1049	-	-	-	-	-
	664	-	-	-	-	-
1 min	791	-	-	790	791	-
	1344	-	-	1345	1344	-
	857	-	-	-	857	-
	1049	-	-	-	1048	-
	664	-	-	-	663	-
2 min	791	-	791	791	791	-
	1344	-	1344	1345	1345	-
	857	-	857	857	857	-
	1049	-	1050	1050	1049	-
	664	-	663	664	663	-

Sample M2, when exposed to a mixture with concentration of 23 ppm did not show any traces of 2-nitrotoluene after exposure times of 0.5 min, 1 min, and 2 min. On the previous test with concentration of 43 ppm, this sample was able to capture 2-nitrotoluene at 2 min exposure time.

Test results of sample M3 are shown in Figure 4-7a and Figure 4-7b. The results show no 2-nitrotoluene at exposure the times of 0.5 min and 1 min. However, for the exposure time of 2 min, 2-nitrotoluene was adsorbed onto the sensor sample.

For sample M4, the previous section verified that 1 min was long enough to detect 2-nitrotoluene at a concentration of 43 ppm. Similarly, the 2-nitrotoluene at a concentration of 23 ppm can be detected after a 1 min and a 2 min exposure time (Figure 4-8a and Figure 4-8b), but not after a 0.5 min exposure time.

Figure 4-9a and Figure 4-9b show the absorption spectra of sample M5 after 1 min and 2 min exposure times. This sample behaves similarly to the previous sample (M4) result that the fastest time is 1 min.

On the hand, sample M6 does not show any peak of 2-nitrotoluene. Sample M6 is made of 70% ferrofluid. Physical observation of this sample shows that the cone pattern distribution is not uniform and does not cover the whole surface. Since it does not have enough ferrofluid in the mixture, there were fewer cones formed and the cone pattern formed is not as uniform as the other samples with higher percentage of ferrofluid. This impacts the adsorption capacity of the sensor. Even though increasing the amount of polyethyleneimine increases the selectivity, this will reduce the amount of cones and the cone pattern will be less uniform. This inturn affects the adsorption capacity of the sensor negatively. But it was noted that the same sample captured the mock explosive at a higher concentration. Even though the effect is not reflected on adsorption at this time, the uniformity and number of cones formed on sample M5 (which is composed of 75% ferrofluid) was also not satisfactory either. In a later section, the effect of the non-uniformity of cone pattern for this sample, M5, is presented.

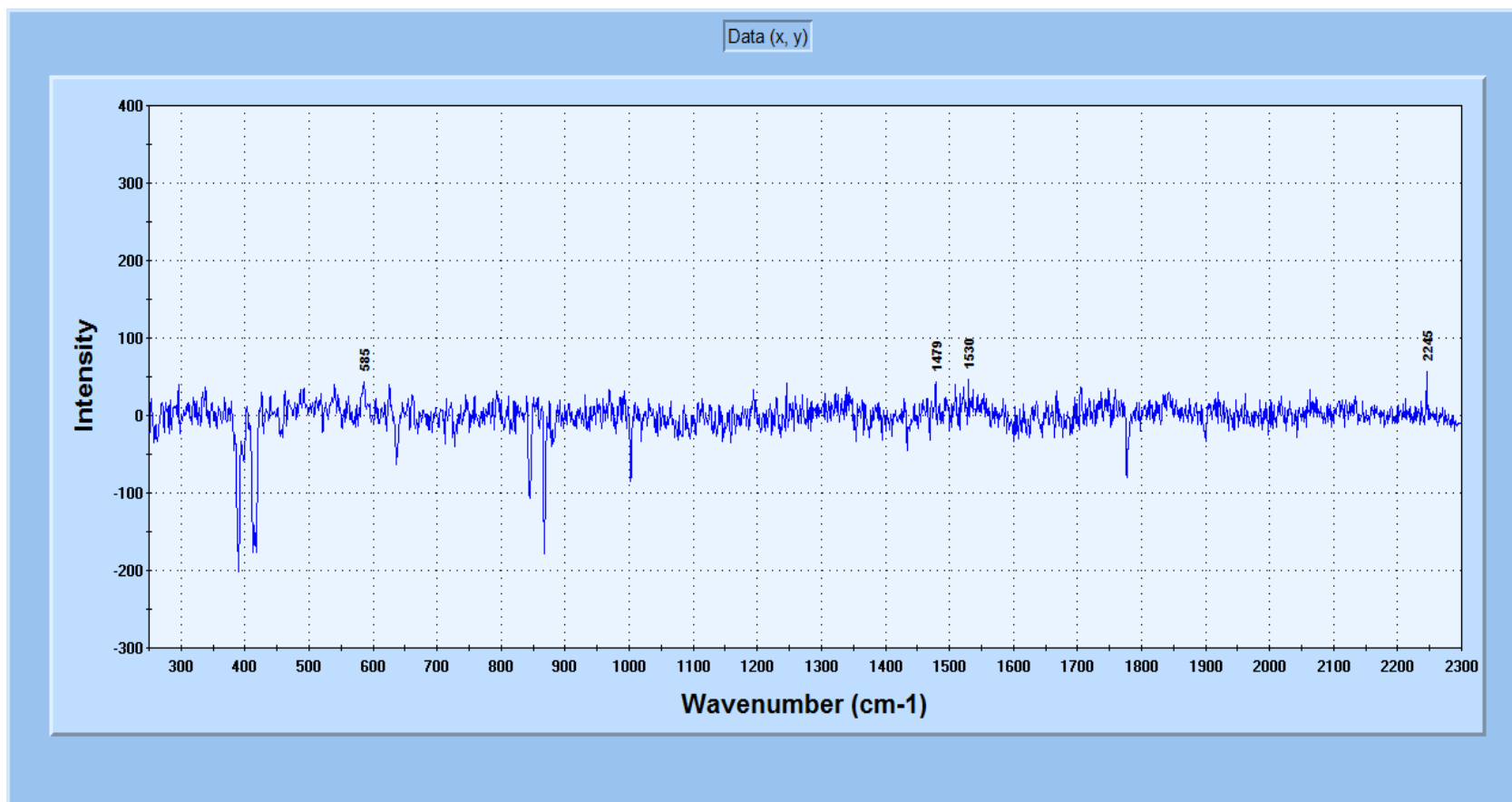


Figure 4-7a. Sample M3 after exposure to mixture of concentration 23 ppm for 1 min.

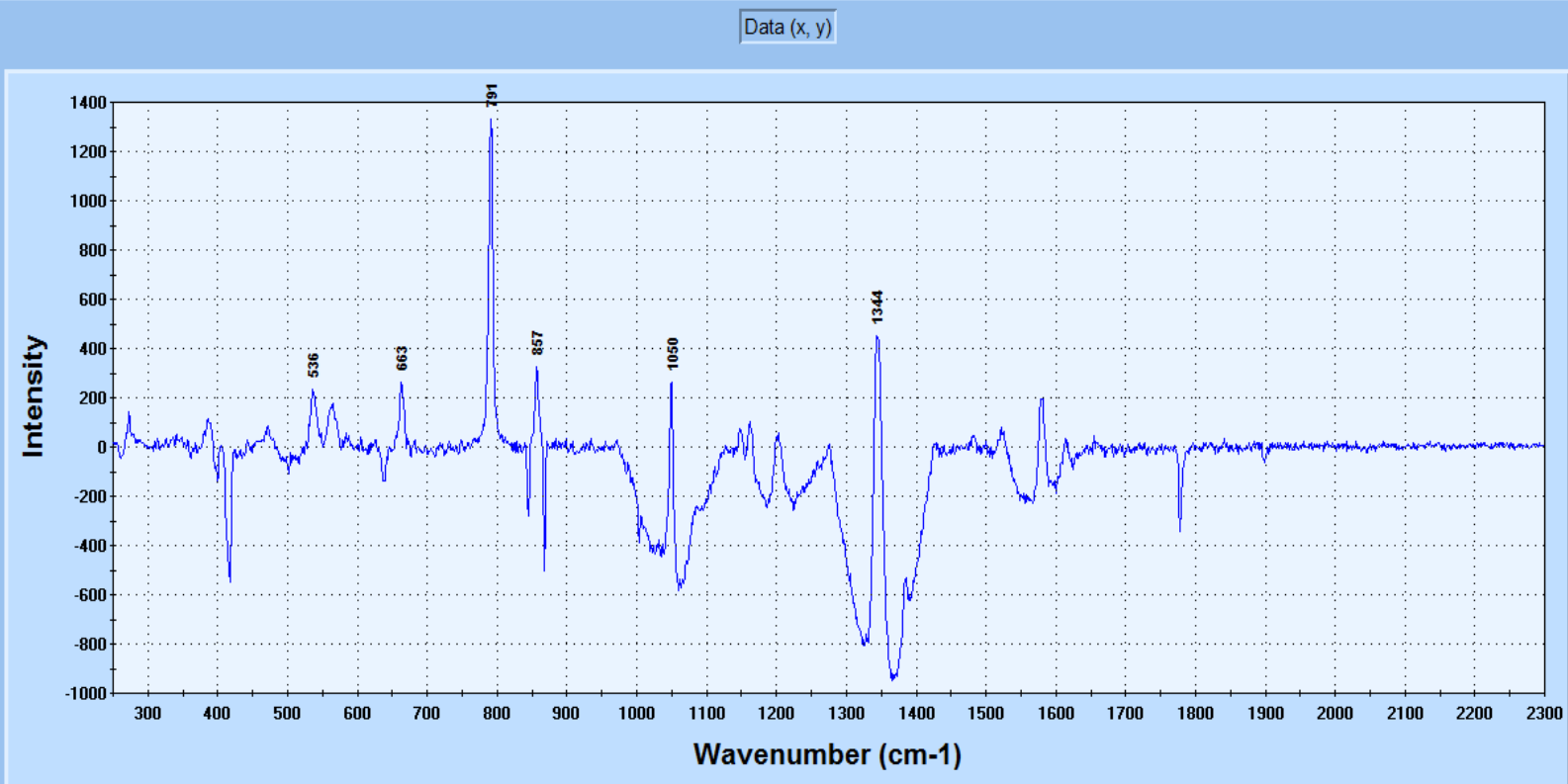


Figure 4-7b. Sample M3 after exposure to mixture of concentration 23 ppm for 2 min.

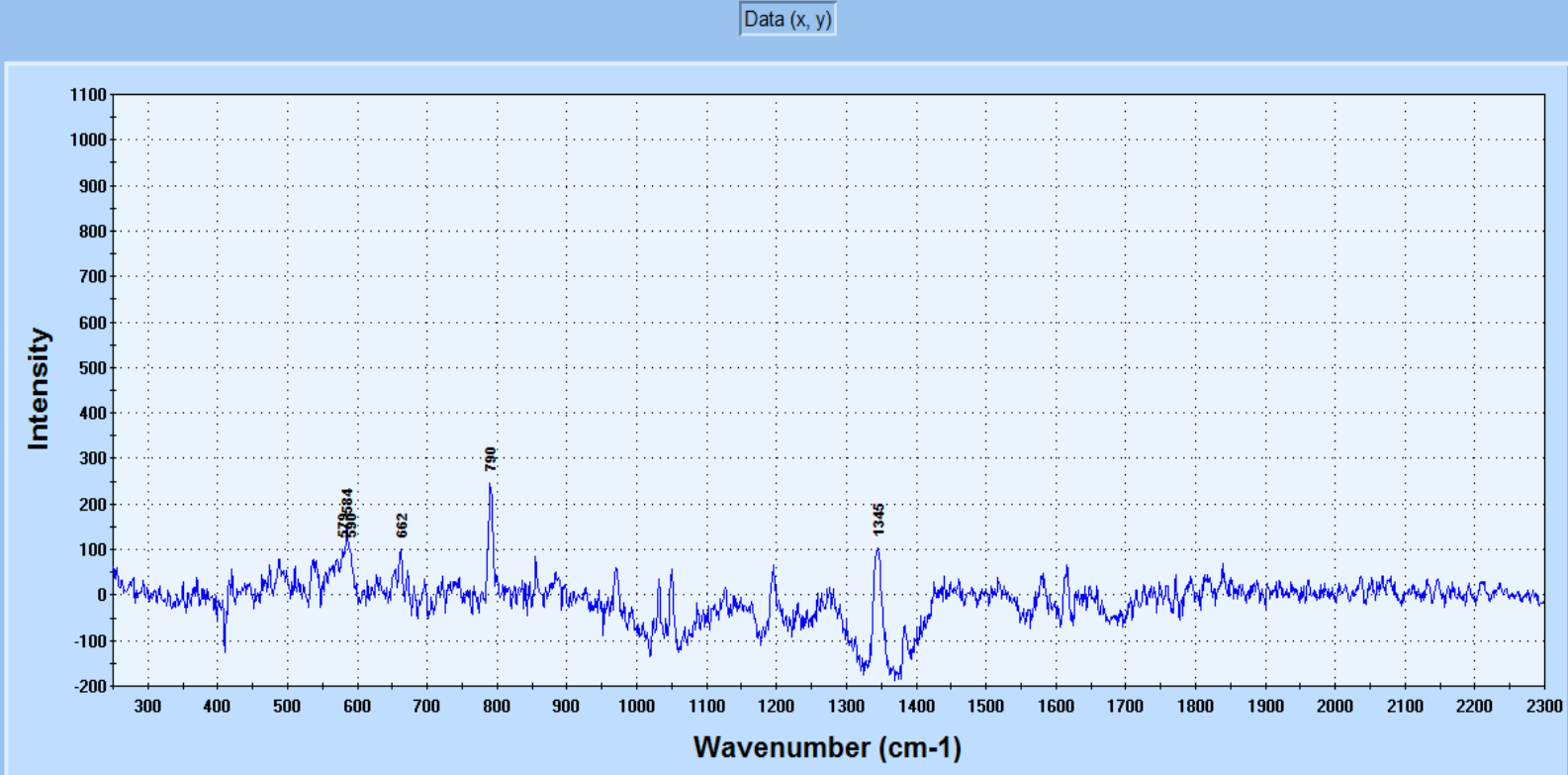


Figure 4-8a. Sample M4 after exposure to mixture of concentration 23 ppm for 1 min.

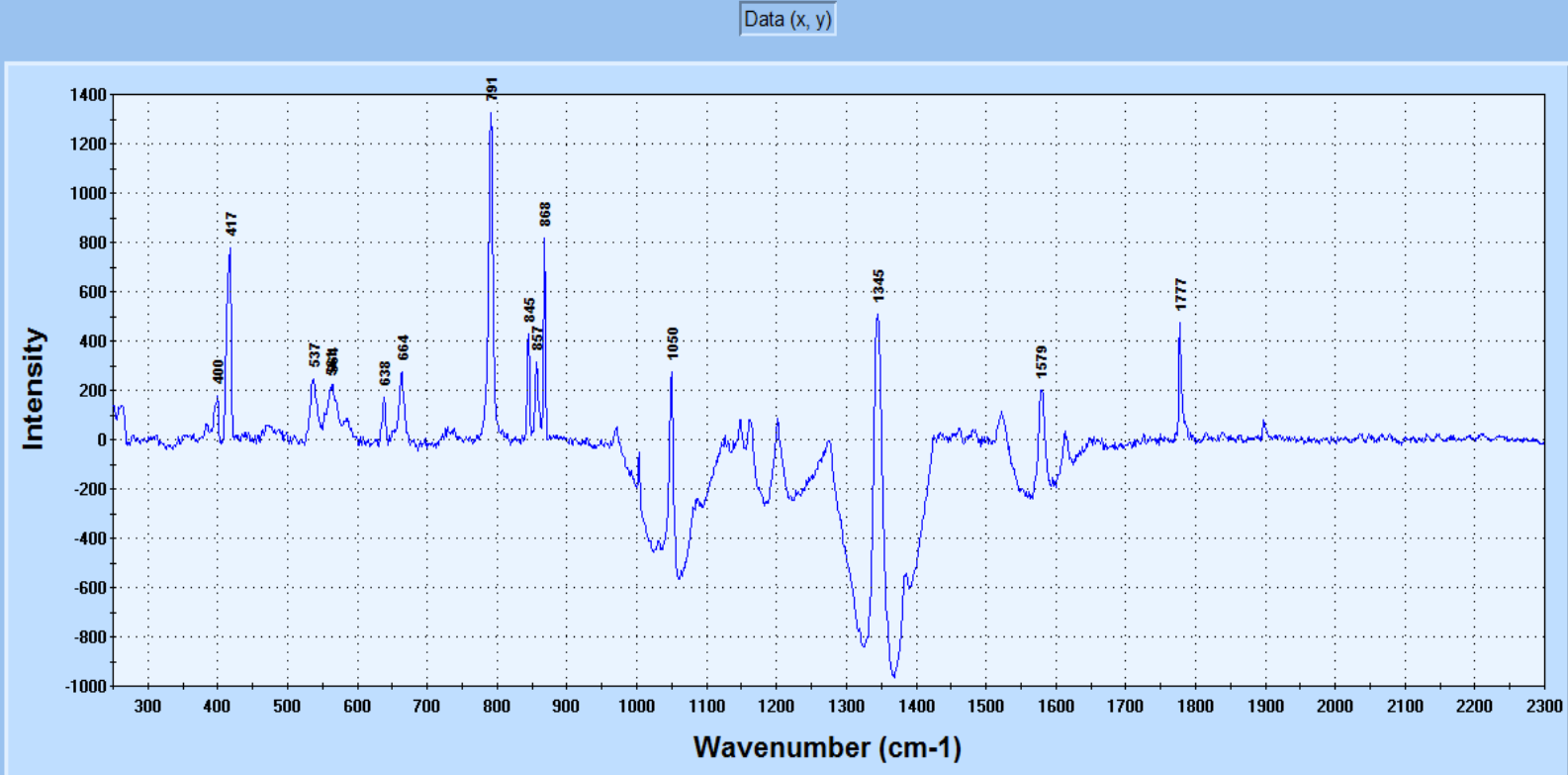


Figure 4-8b. Sample M4 after exposure to mixture of concentration 23 ppm for 2 min.

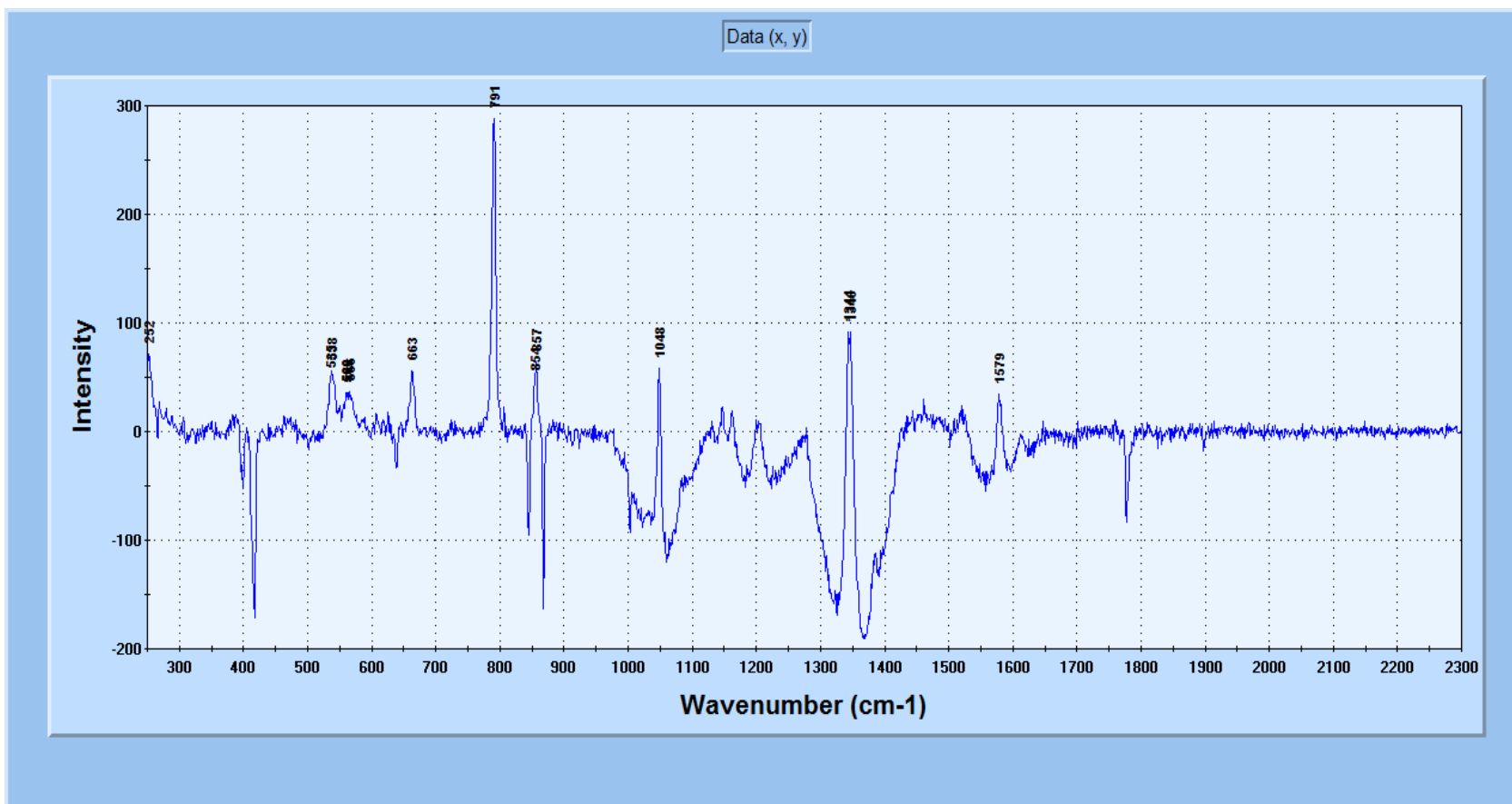


Figure 4-9a. Sample M5 after exposure to mixture of concentration 23 ppm for 1 min.

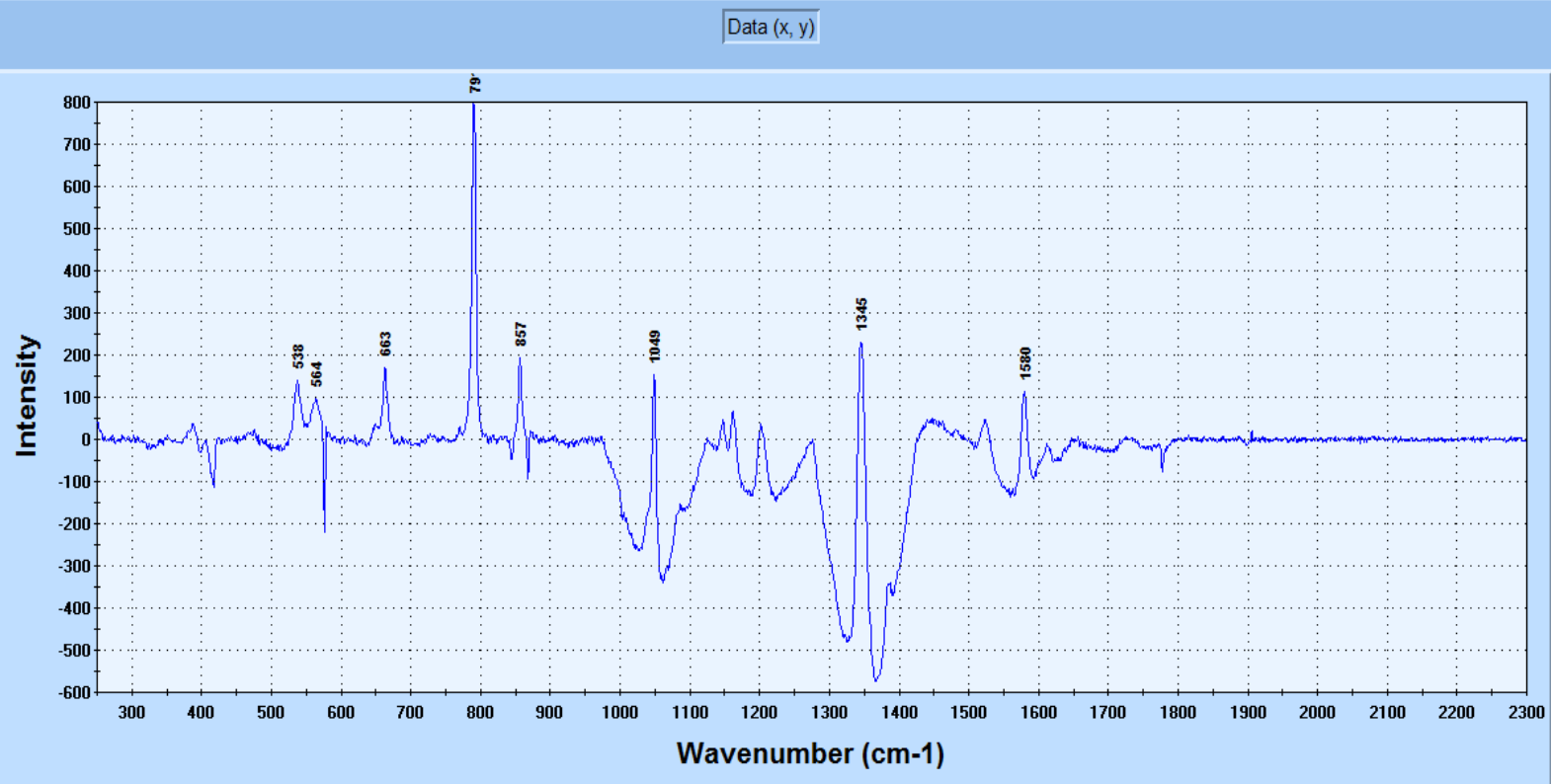


Figure 4-9b. Sample M5 after exposure to mixture of concentration 23 ppm for 2 min.

4.2.3 Results of Adsorption Test with Mixture Concentration of 19 ppm

In the previous two sections, it was seen that increasing the amount of polyethyleneimine in the nano coating mixture improved the adsorption efficiency of the sensor from 43 ppm to 23 ppm. In this section this experiment is expanded to deal with a lesser concentration of 19 ppm with exposure times up to 7 min.

All the results indicated that none of the samples adsorbed 2-nitrotoluene at this concentration.

Because of limitations on the percent of polyethyleneimine in the nano coating mixture, another avenue to improve the adsorption capability of the sensor at this lower concentration (19 ppm) was perused. In the following section, the effect of plasma etching on the sensor adsorption is studied.

4.3 Effect of Plasma Etching of the Sensor

To study the effect of plasma etching, different sensor samples are made with the same composition as listed in Table 4-1. These nano coated sensor samples are plasma etched for five minutes. The samples are then tested for adsorption with a vapor mixture of nitrogen gas and 2-nitrotoluene at concentrations of 43 ppm, 23 ppm, and 19 ppm successively.

4.3.1 Adsorption of 43 ppm Mixture Concentration on Plasma Etched Sensor

Table 4-4 summarizes the results obtained for adsorption test of different plasma etched sensor samples. The adsorption results of plasma etched sensors are also compared to the results obtained by those samples which are not plasma etched.

In previous section 4.2.1 it was discussed that sample M2 was not able to adsorb the 2-nitrotoluene vapor at a concentration of 43 ppm when exposed for 60 sec. The data obtained in this experiment, however, showed that plasma etched sample M2 could adsorb the mock

explosive at the same concentration as fast as 60 sec (Figure 4-10). This verified that plasma etching improved the speed of adsorption of sample M2 from 120 sec to 60 sec.

Similarly plasma etched samples M3 and M4 adsorbed the mock explosive at 35 sec and 25 sec respectively (Figure 4-11a and Figure 4-12a). In Table 4.2 it was noted that the minimum required exposure time for samples M3 and M4 without plasma etching were 60 sec and 50 sec respectively (Figure 4-3a and Figure 4-4a). Hence, this again verifies the importance that plasma etching plays in speeding up the process.

However, sample M5 does not show a definite course, and it is inconclusive in regards to the effect of plasma etching on the adsorption capability of the sensor. This sample showed adsorption at some exposure times, while at other instances it did not. The most probable cause of these flaws is the non-uniformity of the cone pattern. As mentioned in section 4.2.2, physical observation of samples M5 and M6 do not show many cones and the pattern was not uniform. This affected the consistency of the adsorption capability of these samples.

Table 4-4. Adsorption test results of plasma etched sensor at 43 ppm concentration

Duration of Exposure, Sec	Reference peaks (2-nitrotoluene), wave numbers [cm ⁻¹]	Wave number [cm ⁻¹]			
		Sample M2 (Figure 4-10)	Sample M3 (Figure 4-11)	Sample M4 (Figure 4-12)	Sample M5
15	791	-	-	-	790
	1344	-	-	-	1345
	857	-	-	-	-
	1049	-	-	-	-
	664	-	-	-	-
20	791	-	-	-	791
	1344	-	-	-	1344
	857	-	-	-	-
	1049	-	-	-	-
	664	-	-	-	-
25	791	-	-	792	-
	1344	-	-	1344	-
	857	-	-	-	-
	1049	-	-	-	-
	664	-	-	-	-
30	791	-	-	792	791
	1344	-	-	1344	1344
	857	-	-	-	-
	1049	-	-	-	-
	664	-	-	-	-
35	791	-	790	792	790
	1344	-	-	1344	1344
	857	-	-	-	-
	1049	-	-	-	1049
	664	-	-	-	-
40	791	-	790	792	-
	1344	-	1345	1344	-
	857	-	-	-	-
	1049	-	-	-	-
	664	-	-	-	-
45	791	-	790	792	-
	1344	-	1344	1344	-
	857	-	-	-	-
	1049	-	-	-	-
	664	-	-	-	-
50	791	-	790	792	791
	1344	-	1345	1344	1343
	857	-	-	-	-
	1049	-	-	-	-
	664	-	-	-	-
60	791	791	790	792	791
	1344	1344	1344	1344	1343
	857	-	858	857	-
	1049	-	1048	1050	1049
	664	-	-	665	-

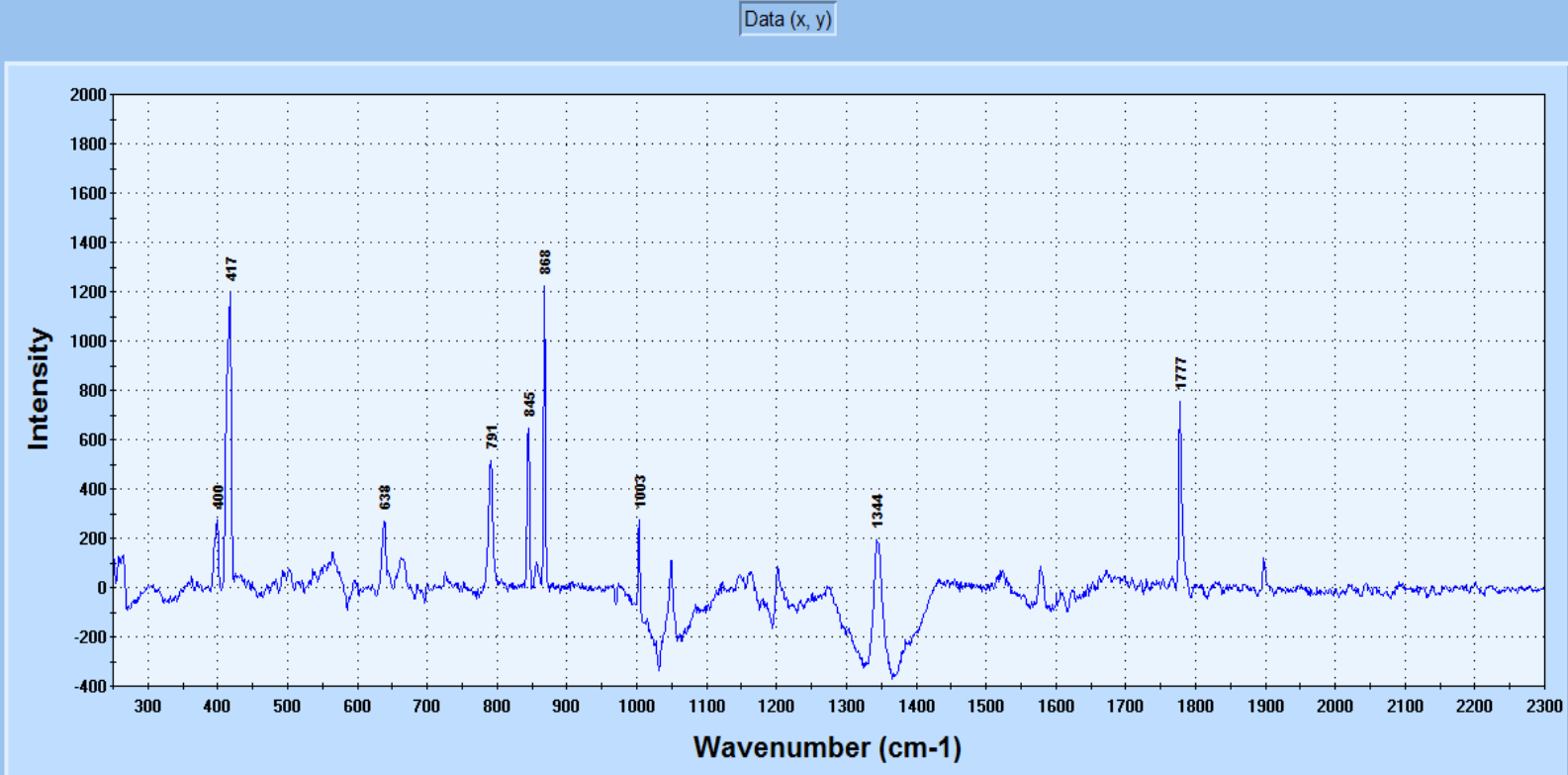


Figure 4-10. Plasma etched Sample M2 exposed to 43 ppm mixture for 1 min.

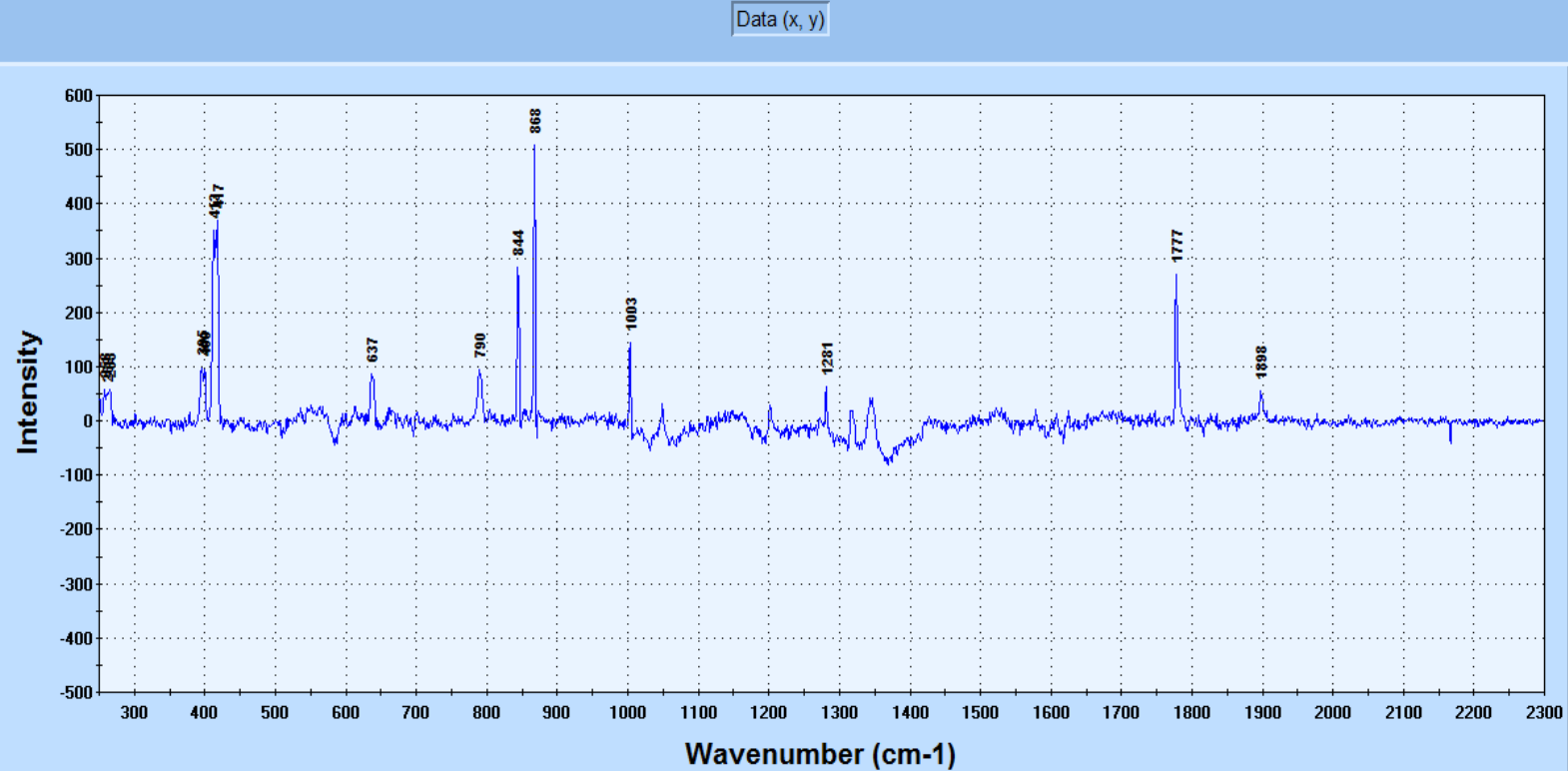


Figure 4-11a. Plasma etched sample M3 exposed to 43 ppm mixture for 35 sec.

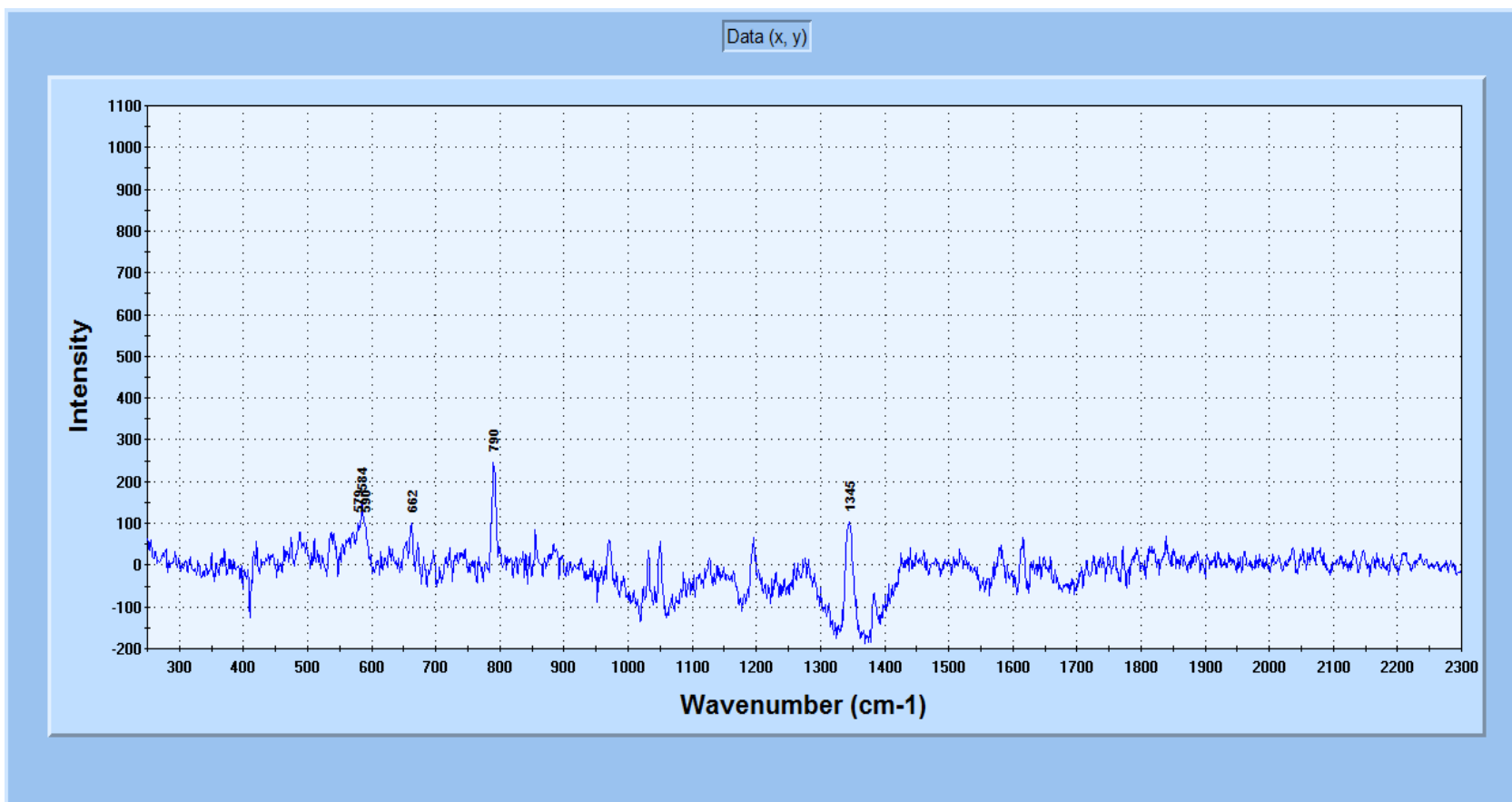


Figure 4-11b. Plasma etched sample M3 exposed to 43 ppm mixture for 50 sec.

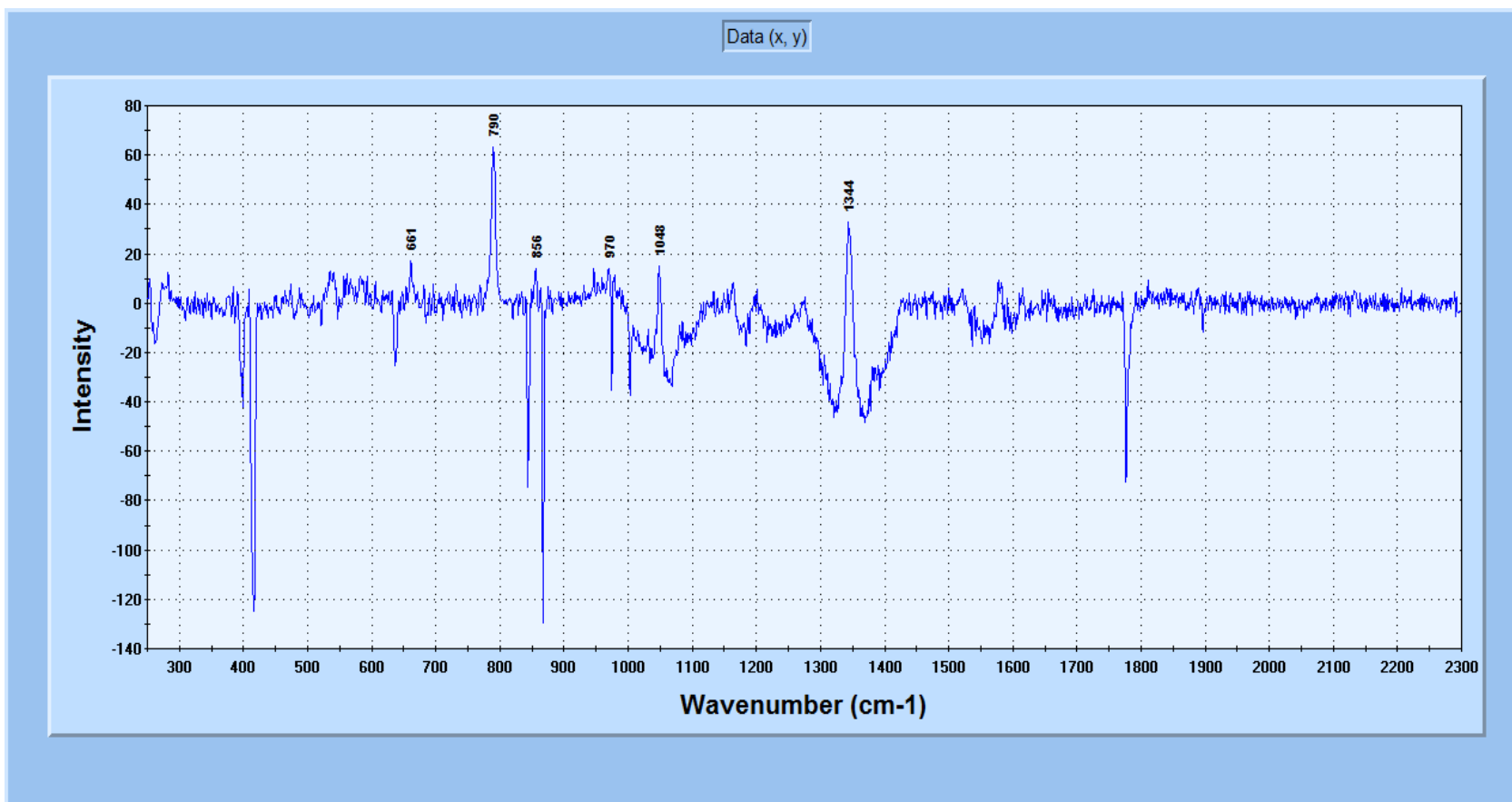


Figure 4-11c. Plasma etched sample M3 exposed to 43 ppm mixture for 60 sec.

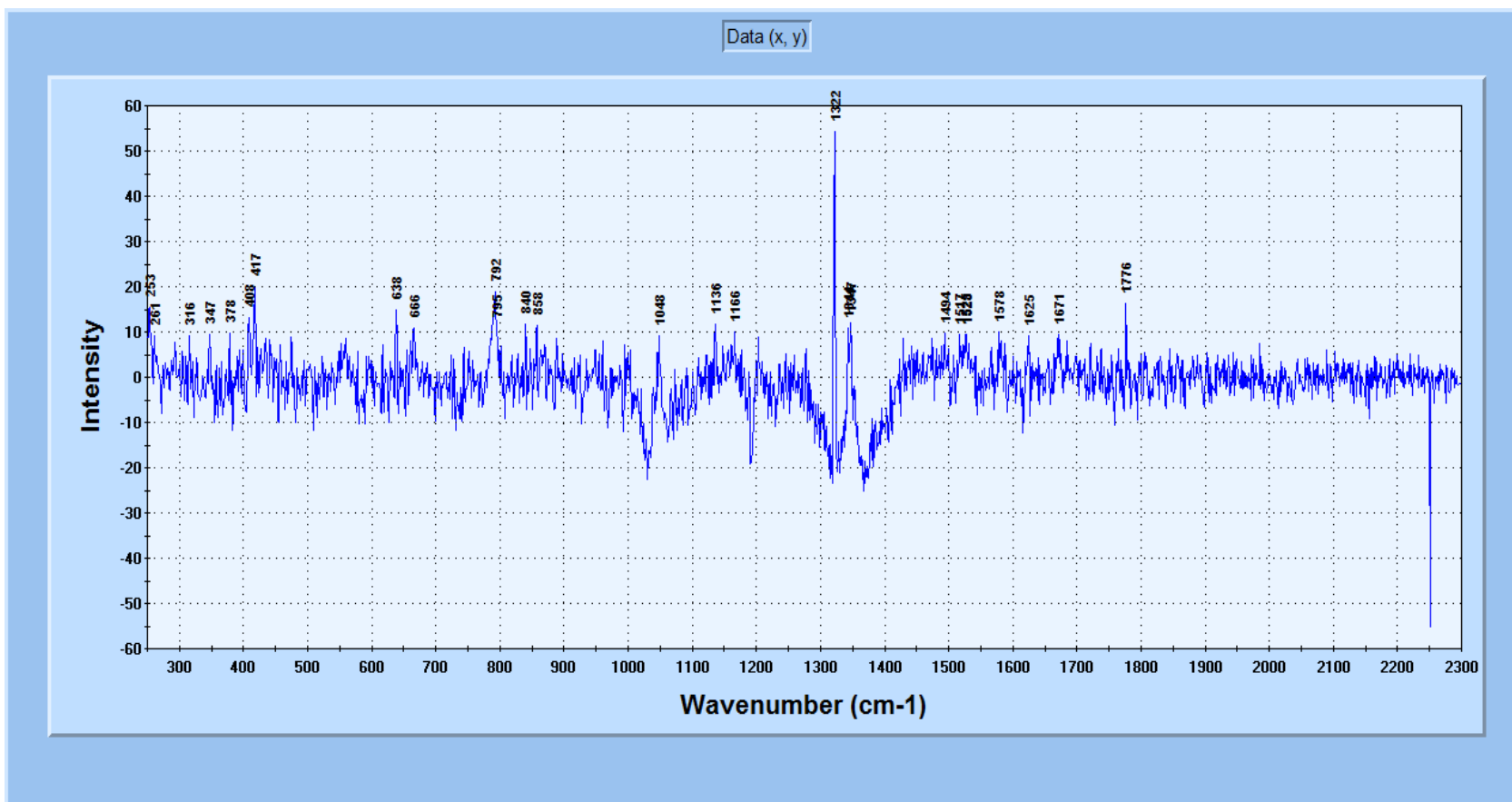


Figure 4-12a. Plasma etched sample M4 exposed to 43 ppm mixture for 25 sec.

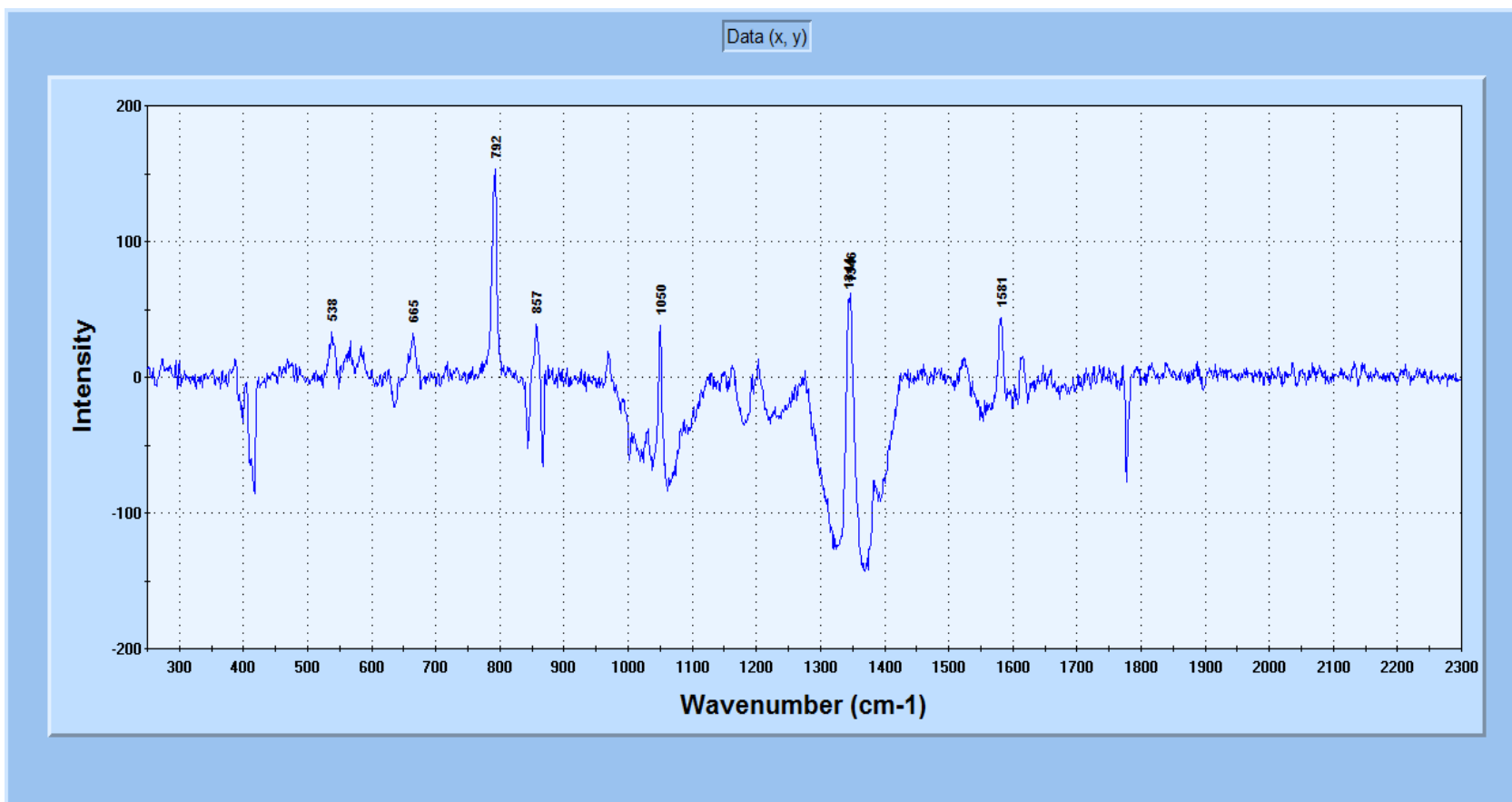


Figure 4-12b. Plasma etched sample M4 exposed to 43 ppm mixture for 60 sec.

4.3.2 Adsorption of 23 ppm Mixture Concentration on Plasma Etched Sensor

In the above experiment it was seen that plasma etching improved the adsorption speed of most samples when tested at 43 ppm concentration. Since the target is to capture trace particles at lower concentrations, more experiments are carried out by lowering the concentration from 43 ppm to 23 ppm and making the adsorption test on samples of the same composition. Comparisons between adsorption results of sensors with plasma etching and without plasma etching are made.

As it was discussed in section 4.2.2, sample M2 was not successful in adsorbing the 2-nitrotoluene vapor at a concentration of 23 ppm up to 2 min exposure time. But this experiment verified that the adsorption capability of this sample can be improved by plasma etching. Table 4-5 summarizes the results obtained after the adsorption test of plasma etched sample M2. After 60 sec and 90 sec exposure times, the sample did not show any adsorption. But after exposure time of 120 sec, the adsorption of vapor particles of the mock explosive was successful. This shows that the sensitivity of sample M2 was improved from 43 ppm to 23 ppm by plasma etching of the sensor.

Table 4-6, Figure 4-14, and Figure 4-15 present the results obtained on samples M3 and M4. Plasma etched sample M3 captured vapors of 2-nitrotoluene after an exposure time of 50 sec and up. Comparison of these results with the results obtained from adsorption test of sample M3 without plasma etching (Table 4-3) shows that the sample tested after plasma etching can adsorb the mock explosive at a faster rate than the sample without plasma etching.

Similarly, plasma etched sample M4 captured the mock explosive vapor at a faster rate than a sample which is not plasma etched. It is seen that adsorption is possible as fast as 30 sec.

But the same composition sample without plasma etching was not able to adsorb the mock explosive vapor at 30 sec.

On the contrary, plasma etched sample M5 did not show good results. The adsorption results of this sample were not consistent. It showed adsorption of the mock explosive vapor only at 25 sec exposure time (Figure 4-16). Increasing or decreasing the exposure time for this sample did not show any adsorption. Even repeating the test at 25 sec exposure time did not enable the capture of 2-nitrotoluene vapor. The non uniformity of the cone formation due to the insufficient amount of ferrofluid could be the most probable cause of this inconsistency.

Table 4-5. Adsorption test results of plasma etched sensor M2 at 23 ppm concentration

Duration of exposure, sec	Reference wave numbers (2-nitrotoluene)	Wave number [cm-1] of plasma etched Sample M2 (Figure 4-13)
60	791	-
	1344	-
	857	-
	1049	-
	664	-
90	791	-
	1344	-
	857	-
	1049	-
	664	-
120	791	792
	1344	1344
	857	-
	1049	-
	664	-

Table 4-6. Adsorption test results of plasma etched sensors M3 and M4 at 23 ppm concentration

Duration of exposure, sec	Reference wave numbers (2-nitrotoluene)	Wave number [cm-1] of plasma etched Samples	
		M3 (Figure 4-14)	M4 (Figure 4-15)
30	791	-	790
	1344	-	1344
	857	-	-
	1049	-	-
	664	-	-
40	791	-	790
	1344	-	1344
	857	-	856
	1049	-	-
	664	-	-
50	791	790	790
	1344	1343	1344
	857	-	-
	1049	-	1048
	664	-	-
60	791	790	790
	1344	1344	1344
	857	856	856
	1049	1049	1048
	664	663	-

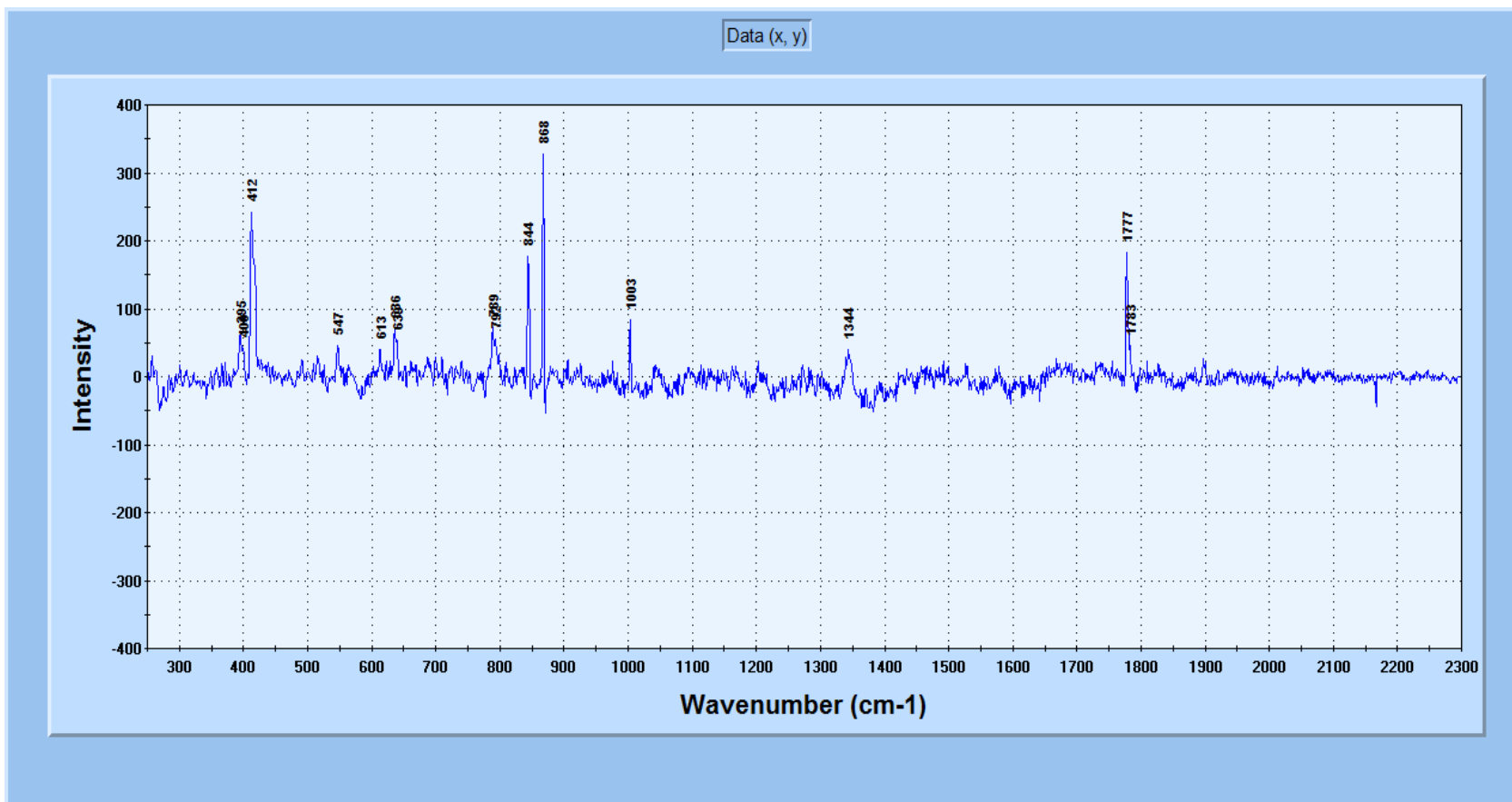


Figure 4-13. Plasma etched sample M2 exposed to 23 ppm mixture for 2 min.

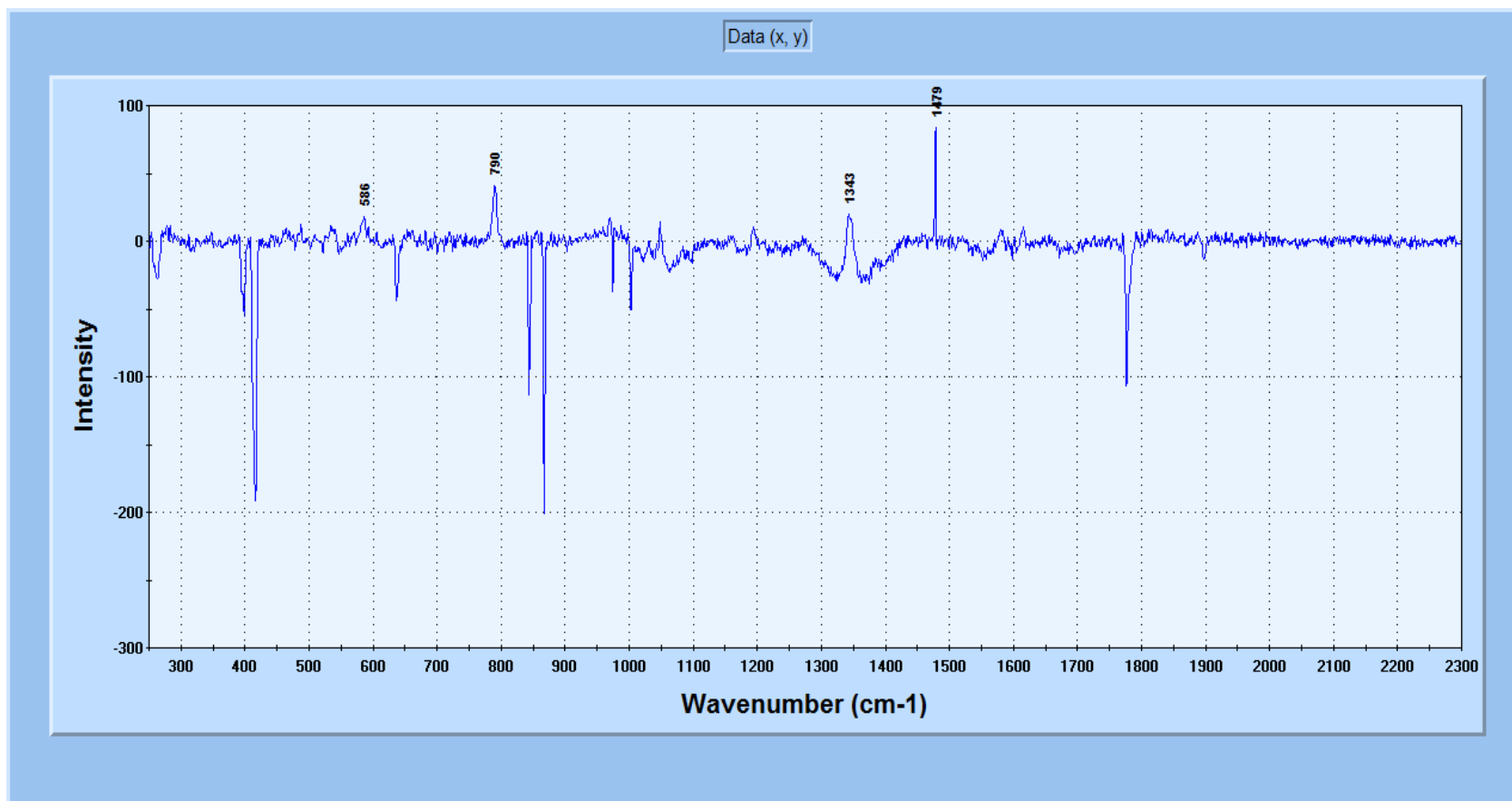


Figure 4-14a. Plasma etched sample M3 exposed to 23 ppm mixture for 50 sec.

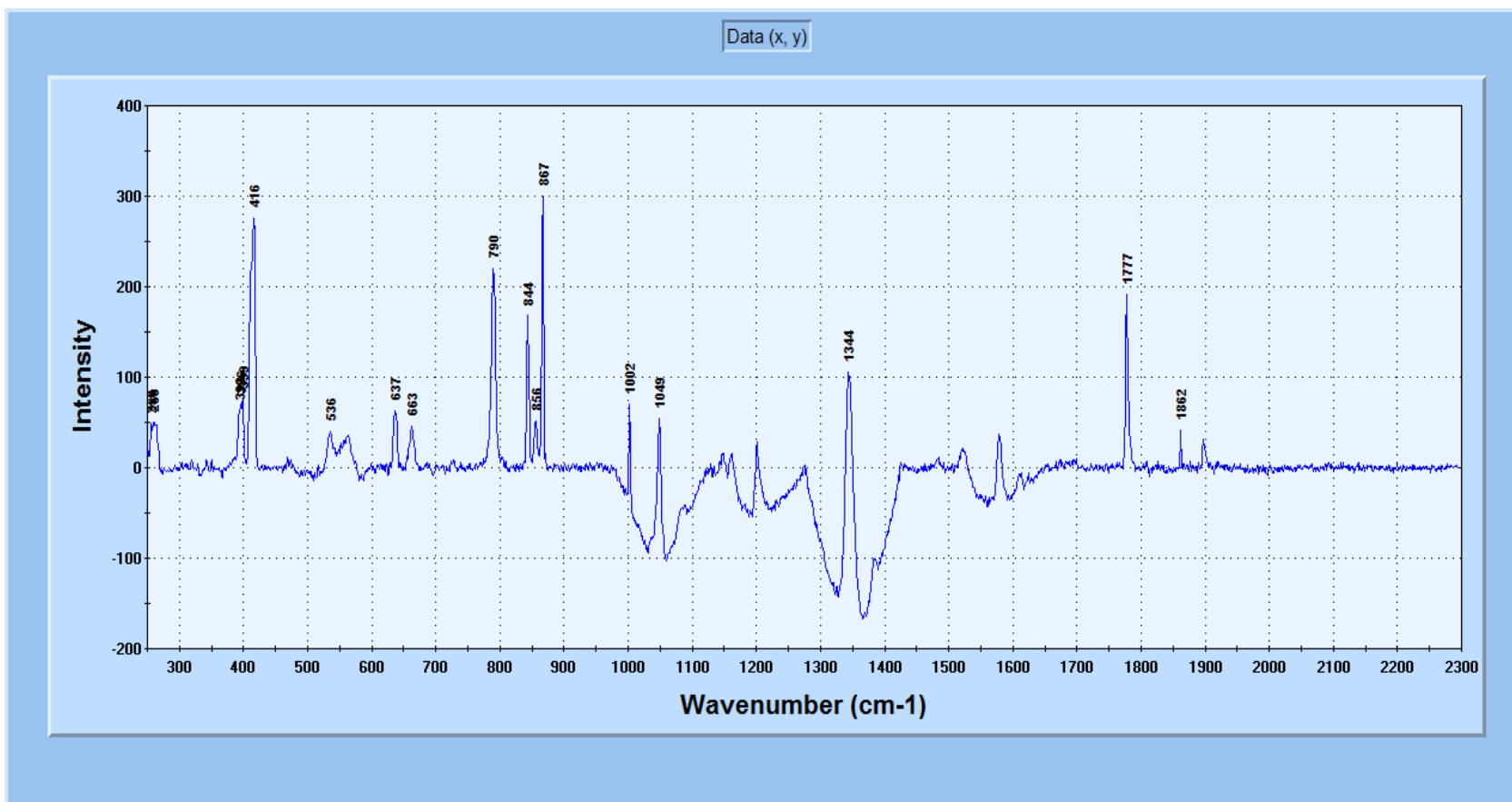


Figure 4-14b. Plasma etched sample M3 exposed to 23 ppm mixture for 60 sec.

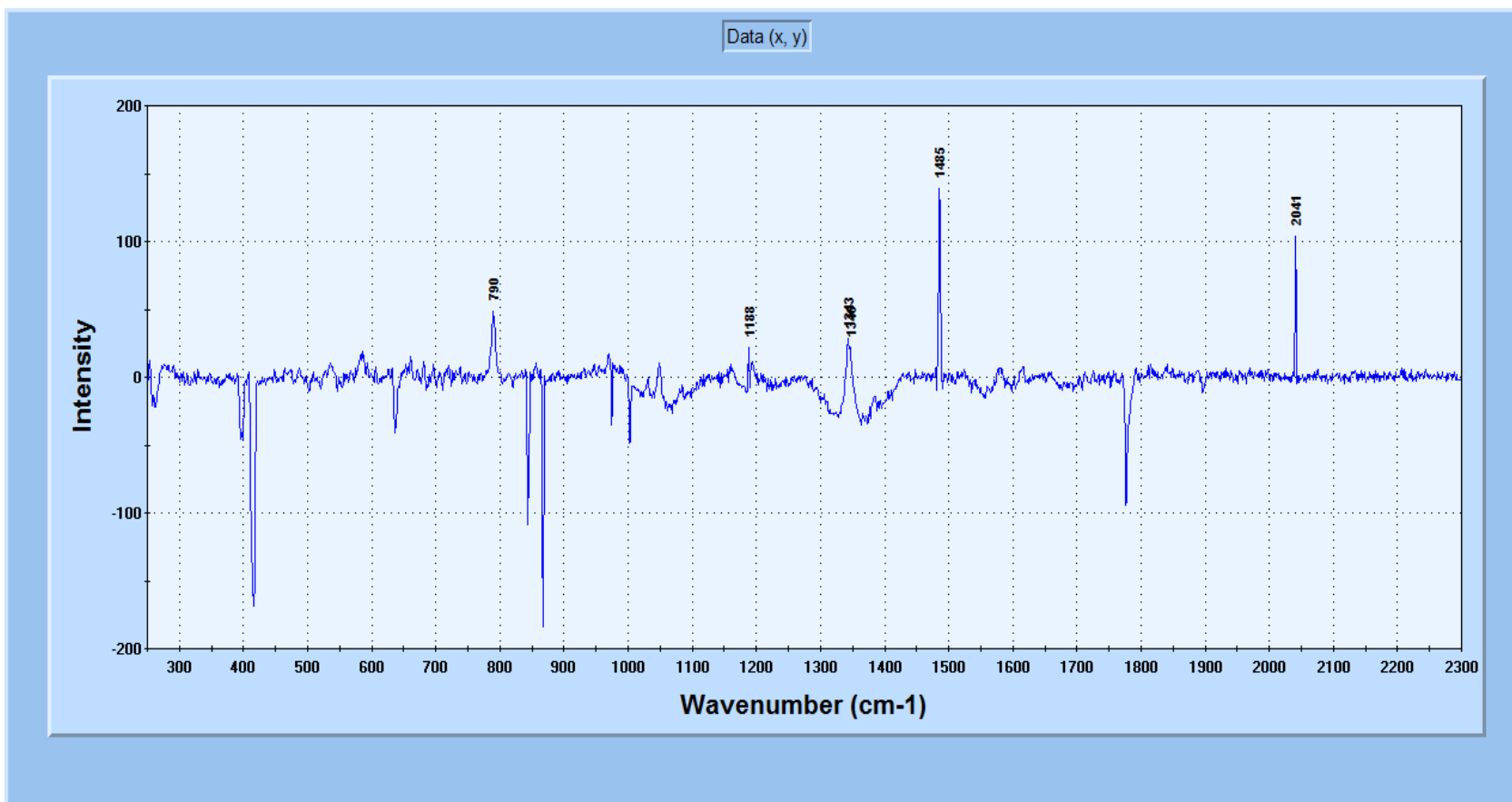


Figure 4-15a. Plasma etched sample M4 exposed to 23 ppm mixture for 30 sec.

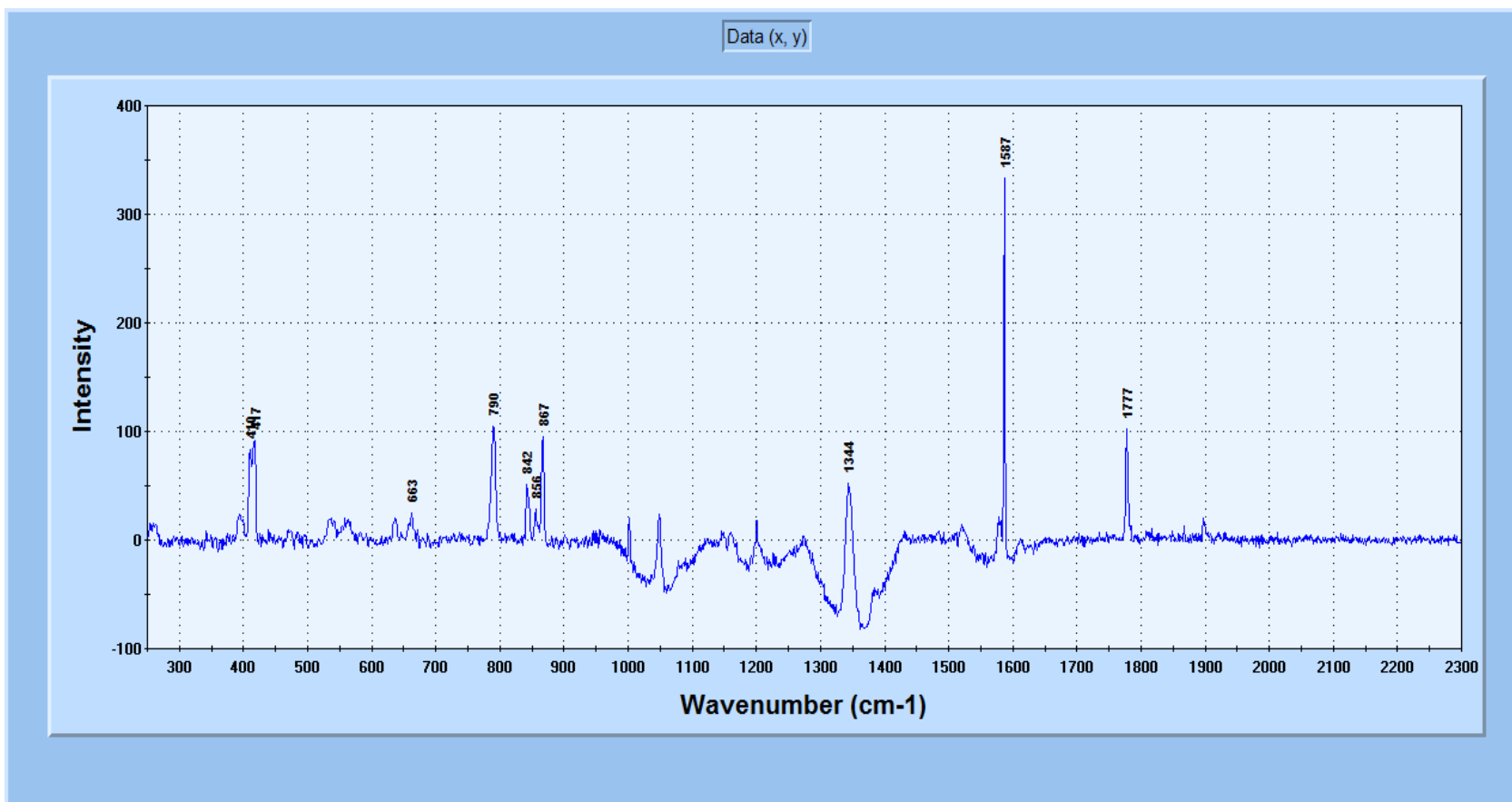


Figure 4-15b. Plasma etched sample M4 exposed to 23 ppm mixture for 40 sec.

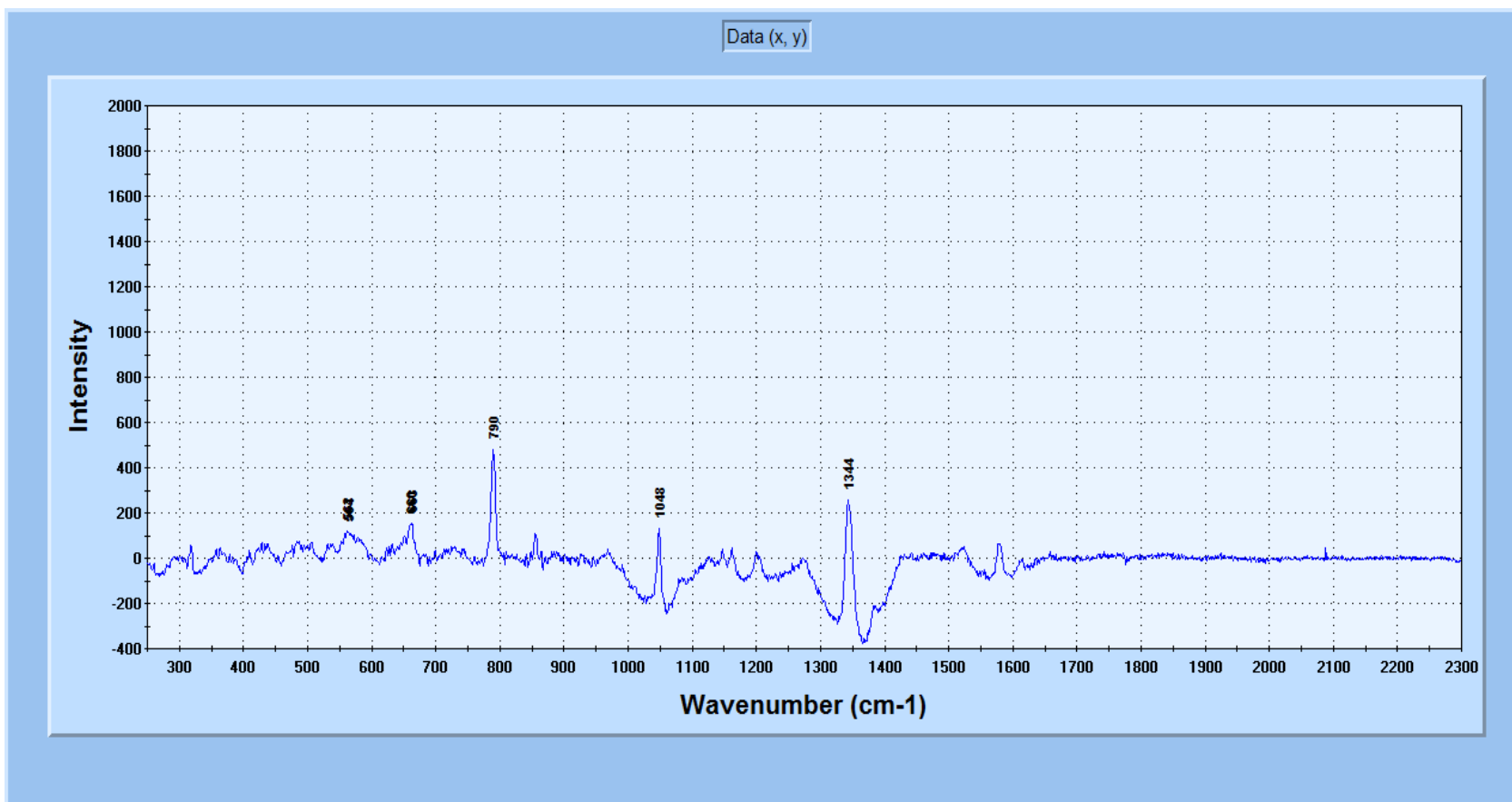


Figure 4-15c. Plasma etched sample M4 exposed to 23 ppm mixture for 50 sec.

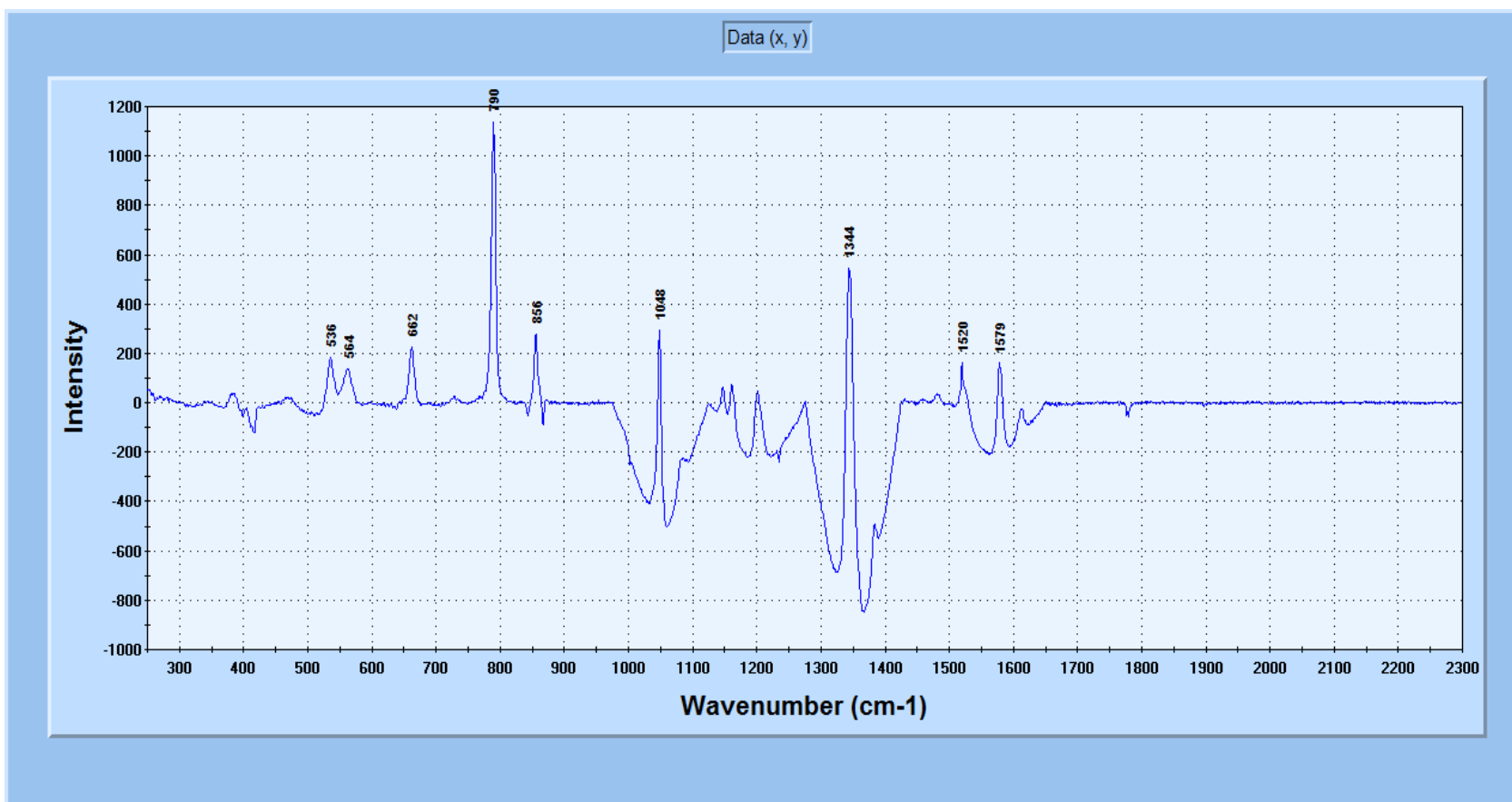


Figure 4-15d. Plasma etched sample M4 exposed to 23 ppm mixture for 60 sec.

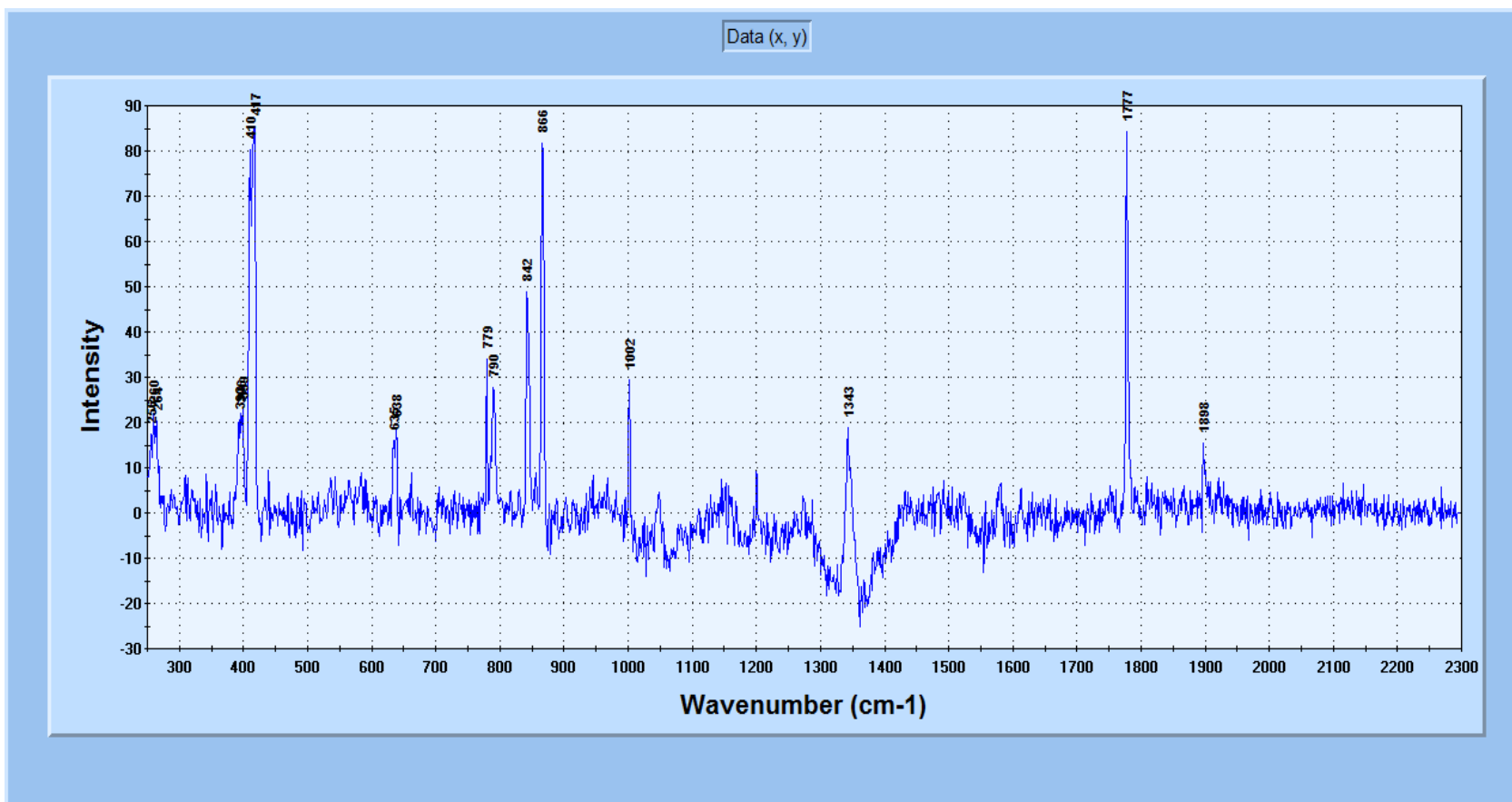


Figure 4-16. Plasma etched sample M5 exposed to 23 ppm mixture for 25 sec.

4.3.3 Adsorption of 19 ppm Mixture Concentration on Plasma Etched Sensor

As discussed in the preceding section, it was verified that plasma etching can improve the adsorption capability of the sensor samples from 43 ppm to 23 ppm. In this section, similar adsorption tests are performed at 19 ppm concentration. The results are summarized in Table 4-7.

In this experiment, three samples of plasma etched sensors M2, M3 and M4 are involved. As discussed in earlier sections of this thesis, samples M5 and M6 did not have uniform distribution of cones and had less number of cones as compared to other samples. It was noted that this affected the consistency of the results of the adsorption. For this reason samples M5 and M6 are not included in these tests.

As a result, plasma etched samples M2 and M3 do not show adsorption of the mock explosive. These samples were tested by successively increasing the adsorption exposure time up to 15 min. But no adsorption of the mock explosive vapor could be obtained.

Plasma etched sample M4 (80% ferrofluid, 15% polyethyleneimine and 5%) captured vapors of 2-nitrotoluene at this concentration (19 ppm). This sample is tested with different exposure times starting from 1 min. After the sample was exposed to the mixture vapor for 4 min, it showed adsorption of the mock explosive vapor. As shown in Figure 4-17, this adsorption is seen as Raman spectral peaks at wave numbers 791 and 1345 - which specify 2-nitrotoluene. Even though the energy intensities of the Raman spectral peaks at these wave numbers are less than intensities of Raman spectral peaks at other wave numbers (which specify unknown gases), there is still some energy absorbed at these wave numbers. As the exposure time is increased to 5 min and then to 6 min (Figure 4-18 and Figure 4-19), the Raman spectral peaks at wave numbers which specify the mock explosive became more intense and dominant over the Raman spectral peaks at other wave numbers which specify other unknown gasses.

In section 4.2.3 which discussed the adsorption results of sensors without plasma etching, it was noted that none of the sensor samples including M4 adsorbed the mock explosive. Hence, this experiment verified that plasma etching of the sensor improved the adsorption capability of the sensor at 19 ppm concentration. A combination of amount of polyethyleneimine in the coating mixture of sample sensor M4 and plasma etching of the sensor enabled this sensor to capture vapors of 2-nitrotoluene at a mixture concentration of 19 ppm.

Table 4-7. Adsorption test results of plasma etched sensor at 19 ppm concentration

Duration of Exposure	Reference wave numbers (2-nitrotoluene)	Wave number [cm ⁻¹]		
		Sample M2	Sample M3	Sample M4
1 min	791	-	-	-
	1344	-	-	-
	857	-	-	-
	1049	-	-	-
	664	-	-	-
2 min	791	-	-	-
	1344	-	-	-
	857	-	-	-
	1049	-	-	-
	664	-	-	-
3 min	791	-	-	-
	1344	-	-	-
	857	-	-	-
	1049	-	-	-
	664	-	-	-
4 min	791	-	-	791
	1344	-	-	1344
	857	-	-	-
	1049	-	-	-
	664	-	-	-
5 min	791	-	-	791
	1344	-	-	1344
	857	-	-	857
	1049	-	-	1049
	664	-	-	-
6 min	791	-	-	791
	1344	-	-	1345
	857	-	-	856
	1049	-	-	1049
	664	-	-	664

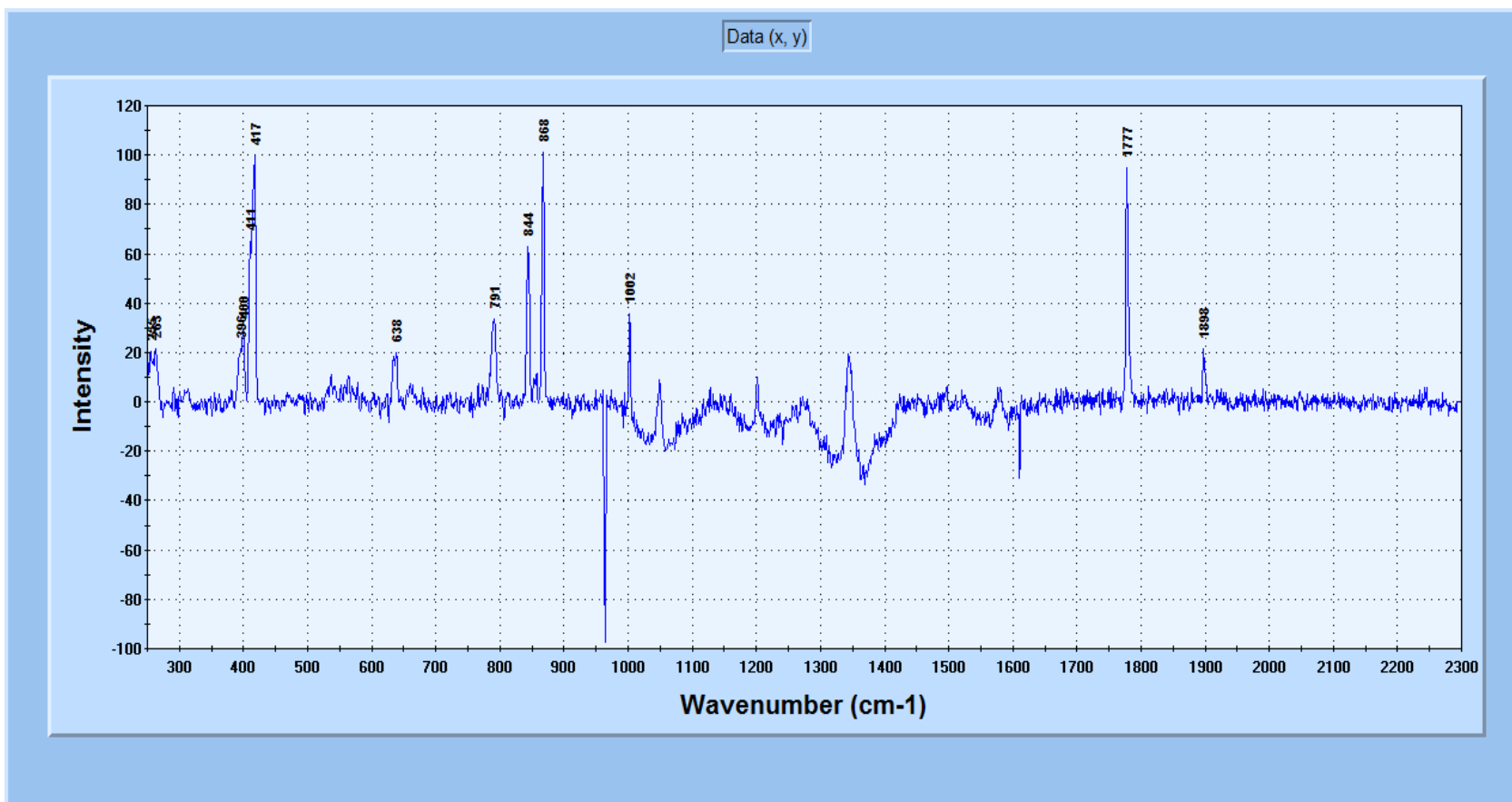


Figure 4-17. Plasma etched sample M4 exposed to 19 ppm mixture for 4 min.

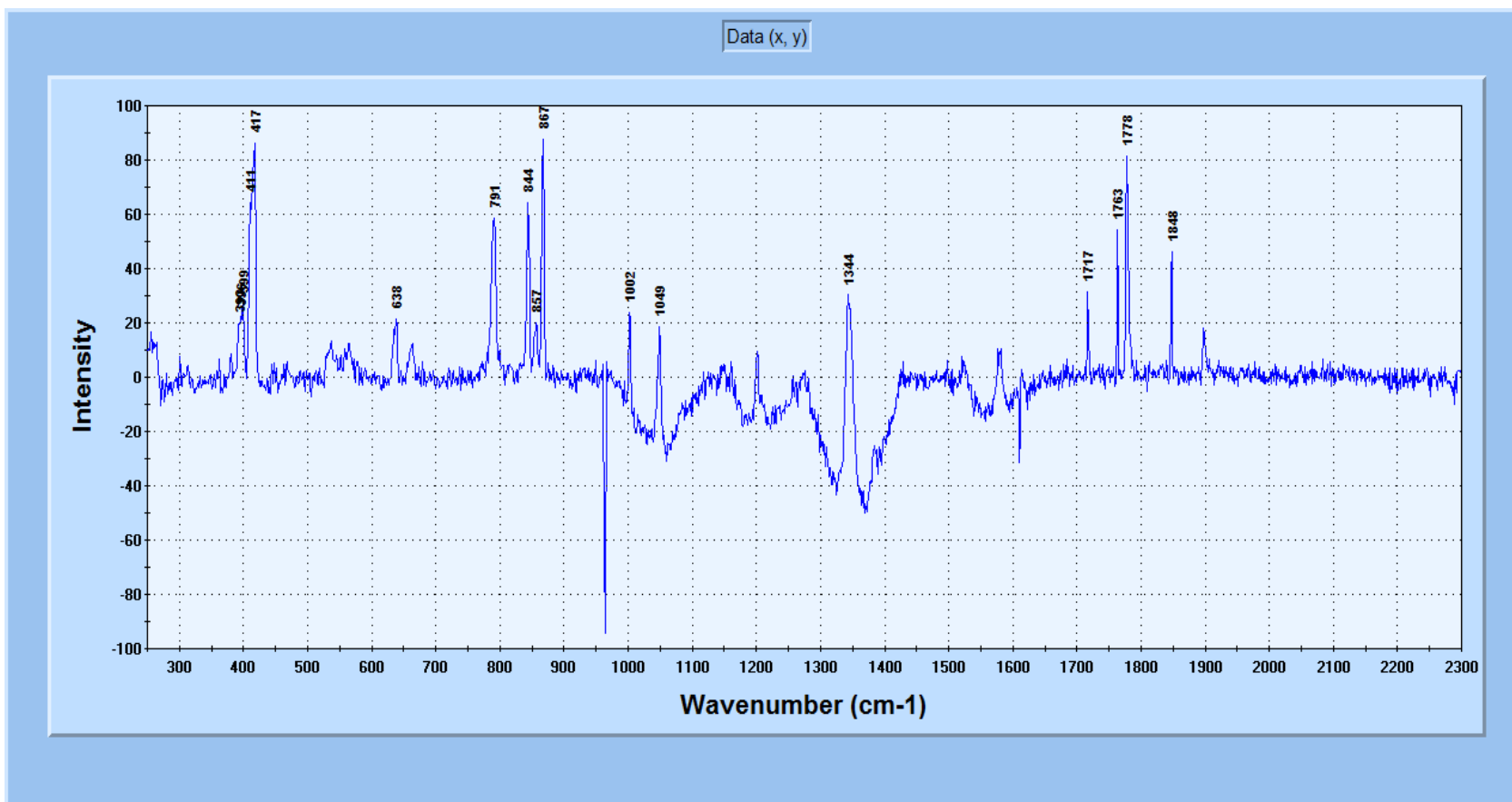


Figure 4-18. Plasma etched sample M4 exposed to 19 ppm mixture for 5 min.

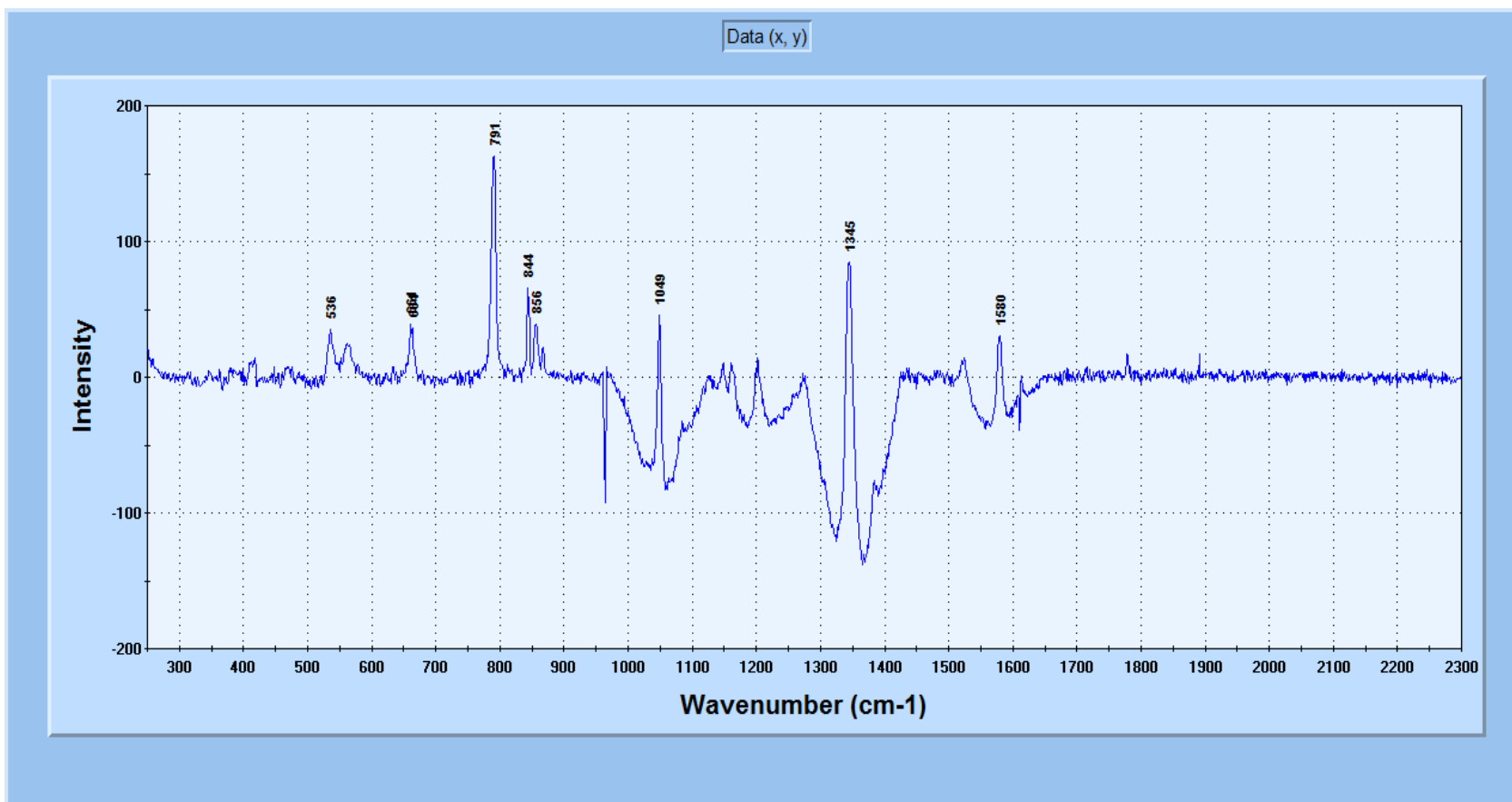


Figure 4-19. Plasma etched sample M4 exposed to 19 ppm mixture for 6 min.

In general, the results discussed in this chapter showed polyethyleneimine and plasma etching can improve sample collection of trace particles of mock explosives on ferrofluid coated sensor. The following plot (Figure 4-20) summarizes the effect of polyethyleneimine and plasma etching. Increasing the amount of polyethyleneimine from 5% to 15% improved the lowest concentration from 43 ppm to 19 ppm. And it can be seen also that plasma etching of the sensor improved both the speed and the minimum detectable concentration. Comparison of plots of plasma etched and un-etched sensor at 43 ppm, the plasma-etched one dropped the adsorption time significantly. In the same manner comparison of plots of plasma etched and un-etched sensor at 23 ppm, showed that the plasma etched one adsorb faster.

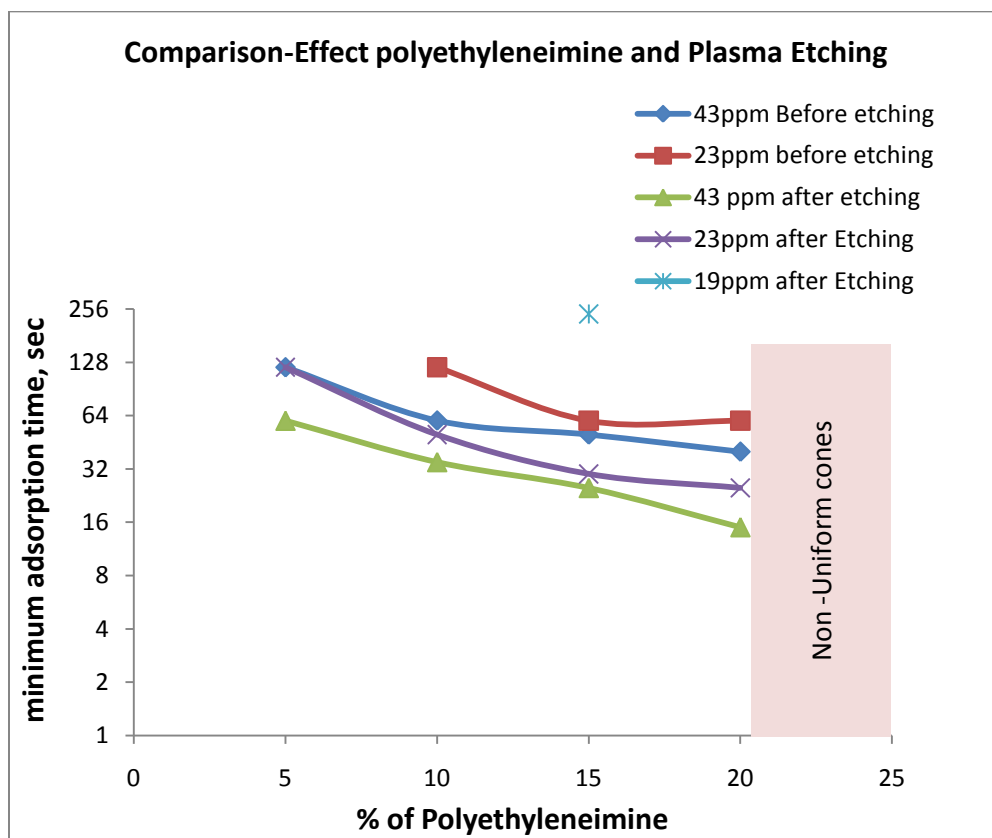


Figure 4-20. Polyethyleneimine amount vs adsorption time of sensors at different concentration.

CHAPTER 5

CONCLUSION

In general, during trace explosive detection a sufficient amount of sample should be collected and provided to analyzer for identification. The amount of sample collected for the analyzer affects the sensitivity of the analyzer. Experiments in this project proved that the newly developed nano coated sensor can be used to collect a mock explosive sample in a gas mixture.

Several tests were conducted to improve the ability of the sensor to selectively collect the vapors of a mock explosive at low concentrations. It is observed that increasing the percentage composition of polyethyleneimine in the nano coating mixture improved the rate and sensitivity of the sensor. It was verified that increasing the amount of polyethyleneimine in the nano coating mixture improved the adsorption speed of the sensor. Comparing the adsorption rate of a plasma etched sensor with one which is not plasma etched, it was found that the plasma etched one is found to be 1.7 to 2.6 times faster depending on the amount of polyethyleneimine in the mixture.

Moreover, the sensitivity of a sensor can be improved by optimizing the amount of polyethyleneimine in the mixture. It was shown that the sensitivity could be improved from 43 ppm to 23 ppm by simply varying the amount of polyethyleneimine. However there is a maximum limit of the percentage of polyethyleneimine for this effect. More than 15% polyethyleneimine has an adverse effect on the formation of pattern cones. It decreases the number of cones and causes the cone pattern to be non uniform. This, inturn, decreases the adsorption speed and sensitivity of the sensor.

The combination of the use of polyethyleneimine and plasma etching using argon gas improved the sensitivity of the nano coated sensor. This improved the limit of detection from 23 ppm to 19 ppm. Experiments in this project showed the best composition for consistent and reliable adsorption to be 80% ferrofluid, 15% polyethyleneimine and 5% binder.

In conclusion, the research performed in this study has shown that the nano coated sensor developed based on the concepts presented work reasonably well. The trends in this study indicate that there is a great potential that further research can lead to this sensor concept being able to capture trace explosive particles on a much lower level.

REFERENCES

LIST OF REFERENCES

1. Tiffany Miller “Raman Spectroscopy” tmiller@coe.drexel.edu;
<http://www.coe.drexel.edu/RET/personalsites/2007/Sullivan/Raman.html>.
2. “Raman Spectroscopy”, Power Technology Inc tel 501.407.0712, P. O. Box 191117
Little Rock, AR 72219-1117.
3. Larry Senesac and Thomas Thundat “Explosive vapor Detection Using Microcantilever
Sensor”, oak Ridge TN, 2007.
4. Thomas G. Thundat Jun “Microcantilever detector for explosives”, US Patent number
5918263, 29 1999.
5. G.Murahdharan, A. Wig, L.A. Pinnaduwege, D.Hedden, T.Thundat, Richard T.Lareau,
“Adsorption-desorption characteristics of explosive vapors investigated with
microcantilevers,” Oak Ridge National Laboratory, Life sciences division, Oak Ridge
TN; Federal Aviation administration, Atlantic City NJ, 2002.
6. “ Nanosensors for trace explosive detection”, Material today volume 11 issue 3, March 3
2008.
7. Bill Drafts, Acoustic Wave Technology Sensors magazine October 1, 2000, Microsensor
Systems Inc.
8. Sarah J. Toal and William C. Trogler, “Polymer sensors for nitroaromatic explosives
detection”, April 2006.
9. G.K.Kannan, A.T Nimal, U.Mittal, R.D.S Yadava, J.C. Kapoor “Adsorption studies of
carbowax coated surface acoustic wave (SAW) sensor for of 2,4 dinitro toluene (DNT)
vapor detection,” Center for fire, explosive and Environment Safety (CFEES), Defense R

- and D Organization (DRDO), Delhi India, 2004.
10. Christine J Hicks, "SERS Surface Enhanced Raman Spectroscopy", Spring 2001 MSU CEM 924.
 11. Colin Cumming, Mark Fisher and John Sikes, "Amplifying Fluorescent Polymer Arrays for Chemical Detection of Explosives", 2004.
 12. Lisa Thiesan, David Hannum, Dale W. Murray, John Parmeter, "Survey of Commercially Available Explosive detection Technologies and Equipment" 2004, presented to department of Justice .
 13. Eric Kirleis, "understanding Ion mobility and differential ion mobility Spectroscopy", On site Trace chemical detection part 1, Sensors magazine Jan 1 2008, Sionix Corp.
 14. Gary A. Eiceman, Hartwig Schmidt and Avi A. Cagan, "Explosive detection Using Differential Mobility Spectrometry", department of Chemistry and BioChemistry, New Mexico State University. (collected in a book "counterterrorist Detection Techniques of Explosives).
 15. Charles L. Rhykerd, David W. Hannum, Dale W. Murray, Dr. John E. Parmeter, "Guide for the Selection of Commercial Explosives Detection Systems for Law Enforcement Applications" September 1999.
 16. Eric Kirleis, "IMS and DMS Working Together", On-Site Trace Chemical Detection, Part 2, Sensors magazine Feb 1 2008, by, Sionix Corp.
 17. GE security, 2006.
 18. Sameer Singh, Manesha Singh, "explosive detection system (EDS) for aviation security", Jan 2002.

19. “microAnalyzer Gas Chromatography and Differential Mobility Spectrometry for Ultra Trace Detection”, Sionex Corporation.
20. Fuqiang An, Baojiao Gao, Xiaoqin Feng, “Adsorption of 2,4,6 Trinitrotoluene on a novel adsorption material PEI/SiO₂”, Department of Chemistry, North University of China, peoples Republic of China.
21. G.K.Kannan, J.C. Kappor, 2005. “Adsorption studies of carbowax and poly dimethyl siloxane to use as chemical array for nitro aromatic vapour sensing,” Center for fire, explosive and Environment Safety (CFEES), Deffence R and D Organization (DRDO), Delhi India, 2005.
22. E. Bentes, H.L.Gomes, P.Stallinga and L. Moura “Detection of explosive vapors using organic thin-film transistors” Faculty of Sciences and Technology, University of Algarve, Faro, Portugal.
23. Byung-Su Joo Jeung-Soo Huhb, Duk-Dong Lee “Fabrication of polymer SAW sensor array to classify chemical warfare agents” School of Electrical Engineering and Computer Science, Kyungpook National University, 1370 Sankyudong, Bukgu, Daegu, Republic of Korea, Department of Materials Science and Metallurgy, Kyungpook National University, 1370 Sankyudong, Bukgu, Daegu, Republic of Korea, 2006

VITA

Daniel Woldemichael Yebo, son of Woldemichael Yebo and Birke Desta, was born in Kaffa, Ethiopia. He attended the Faculty of Technology at Addis Ababa University, Ethiopia. He received a Bachelor of Science in Mechanical Engineering in August, 2001. Before he enrolled to the University of Mississippi in June 2009, he has been working as a design engineer in Houston TX. He attended graduate school, and obtained his Master of Science in Mechanical Engineering degree from University of Mississippi in May 2011.